

ACTIVATED CARBONS  
FOR  
ENVIRONMENTAL APPLICATIONS

*A Thesis submitted to Goa University for the  
degree of*

DOCTOR OF PHILOSOPHY  
in  
CHEMISTRY

By  
*Sabina Martins*

*Department of Chemistry*

*Goa University*

*Taleigao Plateau*

*Goa 403204*

INDIA



September 2008

433

## STATEMENT

*I hereby state that the thesis entitled 'Activated carbons for environmental Applications' is my original work and it has not previously formed basis for the award of any degree, diploma, associateship, fellowship or any other similar title to the best of my knowledge.*

*S. Martins*

Sabina Martins  
(Candidate)

*hereby certified that all the suggested corrections are incorporated into the thesis &*

*J.B.F.*

Prof. Julio B. Fernandes  
(Research Guide)



*Examined*

*John*

Dr. P. A. Doy  
20/10/2009

*Examined*  
*J.B.F.*

(Prof. J. B. Fernandes)  
30/10/2009

## CERTIFICATE

As required under the University Ordinance, I hereby certify that the thesis entitled '*Activated carbons for environmental applications*' submitted by Sabina Martins for the award of Doctor of Philosophy in Chemistry is a record of research done by the candidate during the period of study under my guidance and that it has not formed the basis for award to the candidate of any degree, diploma, associateship or other similar titles.



Prof. Julio B. Fernandes  
Research Guide  
Department of Chemistry  
Goa University

# ACKNOWLEDGEMENT

I owe my gratitude to Prof J. B. Fernandes who has been my teacher in chemistry right through Higher Secondary, Graduation, Post graduation level, to being my Research Guide for Ph.D. Analytical thinking, perfecting experimental techniques, deducing and testing hypothesis, how to persevere in what one does, despite the ups and downs, are some of the many valuable learnings I garnered with his guidance.

I am grateful to Dr. Salkar for being the subject expert and the teaching faculty of the Department of Chemistry for the assistance given whenever needed.

My sincere thanks to

- P Indra Neel from Indian Institute of Technology, Madras for all the effort he has put in, so as to enable me to get Surface area, Porosity, Pore volume, XRD, ESR data.
- Dr Anuradha Gandhe and Ms Bala from Indian Institute of Technology, Bombay, for the BET surface area measurements.
- Dr P Rao, Dr Shiv Prasad, Dr Naqvi, from National Institute of Oceanography for their help in providing XRD, SEM, EDS data. Arif Sardar and Vijay Khedekar for the SEM images. I would like to place on record my sincere appreciation of NIO staff for assisting me in so many small ways which made a big difference to my work.
- Dr. D'Sa from Department of Physics, Goa University for the use of planetary ball and mill grinder.

My thanks to the office staff, laboratory attendants, staff from instrumentation section and other non teaching staff for their assistance and cooperation.

The research team from the Physical Chemistry section, present and past, comprising of Aditi, Jeannette, Sachin, Purnakala, Sajo and Priyanka, for being there and assisting in their areas of competence whenever needed. I am fortunate to be part of this camaraderie.

The warm and friendly research colleagues and M Sc students from all sections of the Chemistry department. I would like to especially acknowledge the help rendered by Pranay, Rohan, Lactina, Narendra, Santosh, Ratan, Sidhali, Satish during the course of practical work. I would like to thank Nandkishore from Sharada Mandir for his cooperation and help.

Multi tasking as a working woman, social activist, home maker, while doing my Ph.D work was possible because of the support of my family and friends, who encouraged me to be what I am. Especially my husband, sisters, in laws, colleagues at Sharada Mandir, activists from Bailancho Saad and other organizations, who took on additional responsibilities so as to facilitate my work.

My very sincere appreciation of my friends Nisha, Sharmila, Deidre, Anshu, Shalini, my stress busters, who ensured that it was not 'all work and no play', at the same time egging me on to complete my work soon.

I am deeply touched with all that Subhas, my husband, has done for me to make it possible to complete my thesis. I remember my late parents whose blessings are always with me.

**Sabina Martins**

# CONTENTS

	<u>INDEX</u>	<u>PAGE NO.</u>
<i>Table of Catalyst Code</i>		
<i>Synopsis</i>		
<i>Chapter I – Introduction and Literature Review</i>		
<b>1.1</b>	<b>Introduction</b>	<b>1</b>
<b>1.2</b>	<b>Literature Review</b>	
1.2.2	<i>Classification of activated carbons</i>	6
1.2.3	<i>Precursors</i>	8
1.2.4	<i>Synthesis</i>	11
1.2.5	<i>Methods for surface modification</i>	14
1.2.6	<i>Physical activation methods</i>	16
1.2.7	<i>Chemical activation</i>	19
1.2.7.1	<i>Acid Treatment</i>	19
1.2.7.2	<i>Other Modification Methods</i>	22
1.2.8	<i>Heat Treatment Methods</i>	25
1.2.9	<i>Porosity</i>	27
1.2.10	<i>Characterisation of physical properties</i>	28
1.2.11	<i>Characterisation of Chemical properties</i>	30
1.2.12	<i>Applications</i>	33
	<b>References</b>	<b>36</b>
<i>Chapter II – Experimental</i>		
<b>2.1</b>	<b>Introduction</b>	<b>41</b>

<b>2.2</b>	<b>Preparation of carbon from sodium salt of carboxyl methyl cellulose (CMC)</b>	<b>43</b>
2.2.1	<i>Preparation of carbons</i>	44
2.2.2	<i>Ascertaining Porosity</i>	44
2.2.3	<i>Surface area</i>	46
2.2.4	<i>Identification of surface functional groups by IR</i>	47
2.2.5	<i>Porosity enhancement</i>	49
2.2.6	<i>SEM images at 10000 magnification</i>	49
2.2.7	<i>Activated carbon from carboxyl methyl cellulose</i>	51
2.2.8	<i>Conclusions</i>	52
<b>2.3</b>	<b>Characterisation of carbons</b>	<b>53</b>
2.3.1	<i>XRD</i>	54
2.3.2	<i>EPR</i>	54
2.3.3	<i>BET-SORPTOMETRY</i>	54
2.3.4	<i>SEM</i>	54
2.3.5	<i>TG</i>	55
2.3.6	<i>IR</i>	55
2.3.7	<i>EDS</i>	55
2.3.8	<i>Acid base titration</i>	55
2.3.9	<i>pH measurements</i>	56
2.3.10	<i>TPD</i>	56
2.3.11	<i>Decomposition of hydrogen peroxide</i>	56
<b>2.4</b>	<b>Results and Discussions</b>	
2.4.1	<i>XRD</i>	57
2.4.2	<i>EPR</i>	59

2.4.3	<i>Surface area and Porosity</i>	62
2.4.4	<i>SEM</i>	67
2.4.5	<i>Thermo gravimetric analysis</i>	71
2.4.6	<i>Infra Red Spectroscopic analysis</i>	75
2.4.7	<i>Energy Diffraction Spectra.</i>	78
2.4.8	<i>Acidity and Basicity titrations</i>	82
2.4.9	<i>pH</i>	83
2.4.10	<i>TPD of ammonia</i>	83
2.4.11	<i>Decomposition of hydrogen peroxide.</i>	85
2.4.12	<i>Conclusions</i>	86
	<b>References</b>	87
 <b>Chapter III – Adsorption Studies</b>		
<b>3.1</b>	<b>Adsorption of methylene blue</b>	
3.1.1	<i>Introduction</i>	88
3.1.2	<i>Experimental</i>	89
3.1.3	<i>Results and Discussions</i>	90
3.1.3.1	<i>Equilibration time for methylene blue</i>	90
3.1.3.2	<i>Comparative study of methylene blue adsorption by different carbons for a fixed weight of sample and a fixed time period</i>	91
3.1.3.3	<i>Langmuir’s adsorption isotherms</i>	92
3.1.3.4	<i>Freundlich Adsorption Isotherm</i>	94
<b>3.2</b>	<b>Adsorption of metal ions: Mn<sup>2+</sup>, Cu<sup>2+</sup></b>	
3.2.1	<i>Introduction</i>	98
3.2.2	<i>Experimental</i>	100

3.2.3	<i>Results and Discussions</i>	102
<b>3.3</b>	<b>Comparative study of adsorption on functionalised and non functionalised carbons</b>	
3.3.1	<i>Introduction</i>	106
3.3.2	<i>IR of functionalised and non functionalised carbon</i>	107
3.3.3	<i>Hydrogen peroxide decomposition</i>	111
3.3.4	<i>Methylene Blue adsorption</i>	113
3.3.5	<i>Adsorption of metal ions: Mn<sup>2+</sup> and Cu<sup>2+</sup> ions</i>	115
<b>3.4</b>	<b>Conclusions</b>	<b>117</b>
	<b>References</b>	<b>118</b>
 <i>Chapter IV – Adsorption on C-TiO<sub>2</sub> and photocatalysis</i>		
<b>4.1</b>	<b>Introduction</b>	<b>121</b>
<b>4.2</b>	<b>Phases of TiO<sub>2</sub></b>	<b>122</b>
<b>4.3</b>	<b>Mechanism of photodegradation</b>	<b>124</b>
<b>4.4</b>	<b>Synthesis of pure and suggested TiO<sub>2</sub> literature status</b>	<b>126</b>
<b>4.5</b>	<b>TiO<sub>2</sub> on Supports</b>	<b>128</b>
<b>4.6</b>	<b>Experimental</b>	<b>130</b>
4.6.1	<i>Synthesis of TiO<sub>2</sub>/C</i>	130
4.6.2	<i>Photocatalytic Degradation of Methylene Blue</i>	132
<b>4.7</b>	<b>Results and Discussion</b>	<b>133</b>
4.7.1	<i>Comparative study of adsorption of dyes</i>	133
4.7.2	<i>Comparative study of adsorption of methylene blue</i> <i>Methylene blue + C, methylene blue +TiO<sub>2</sub>.</i>	134
4.7.3	<i>Photocatalytic degradation of methylene blue.</i>	135

4.7.4	<i>Comparative study of anatase and rutile phase on the degradation of methylene blue</i>	136
4.7.5	<i>Comparative study of percentage loading of TiO<sub>2</sub> on Carbon</i>	139
4.7.6	<i>Comparative study of Carbon and Silicon dioxide as supports for TiO<sub>2</sub></i>	140
<b>4.8</b>	<b>Conclusions</b>	<b>141</b>
	<b>References</b>	<b>142</b>
 <b>Chapter V – Electrochemical and catalytic properties of carbons and carbon supported Mn (IV) oxide</b>		
<b>5.1</b>	<b>Electrochemical properties of activated carbon, MnO<sub>2</sub>/C</b>	
5.1.1	<i>Capacitors</i>	145
5.1.2	<i>Modification of Porous Carbon for Electrode Materials</i>	148
5.1.3	<i>MnO<sub>2</sub> supported carbons</i>	150
5.1.4	<i>Cyclic voltametry as an electro analytical technique</i>	150
5.1.5	<i>Experimental</i>	152
5.1.6	<i>Results and Discussion</i>	154
<b>5.2</b>	<b>Electrocatalysis</b>	
5.2.1	<i>Introduction</i>	163
5.2.2	<i>Electrocatalysis using porous carbon supports.</i>	163
5.2.3	<i>Electrocatalysis by Manganese Oxides</i>	165
5.2.4	<i>Hydrogen evolution reaction</i>	165
5.2.5	<i>Oxygen evolution</i>	167
5.2.6	<i>Tafel relationship</i>	168

5.2.7	<i>Experimental</i>	170
5.2.8	<i>Results and Discussion</i>	171
<b>5.3</b>	<b>Catalytic reactions of carbons and MnO<sub>2</sub>/C</b>	
5.3.1	<i>Introduction</i>	172
5.3.2	<i>Decomposition of potassium chlorate</i>	173
5.3.3	<i>Phase change of sodium sulphide</i>	174
5.3.4	<i>Catalytic gasification of carbon</i>	175
5.3.5	<i>Experimental</i>	176
5.3.6	<i>Results and Discussions</i>	177
5.3.7	<i>Conclusions</i>	183
	<b>References</b>	<b>184</b>
	<b>Summary and Conclusions</b>	<b>191</b>
	<b>Achievement</b>	<b>193</b>

# LIST OF SCHEMES, FIGURES AND TABLES

	<u>SCHEMES</u>	<u>PAGE NO.</u>
<i>Scheme 1.1</i>	<i>Diagrammatic representation of the form of activated carbon</i>	5
<i>Scheme 2.1</i>	<i>Synthesis of activated carbon from carboxyl methyl cellulose.</i>	43
<i>Scheme 4.1</i>	<i>Mechanism for the TiO<sub>2</sub>/UV process</i>	125

	<u>FIGURES</u>	<u>PAGE NO.</u>
<i>Fig 1.1</i>	<i>Some allotropes of carbon a) diamond; b) graphite; c) lonsdaleite; d-f) fullerenes (C<sub>60</sub>, C<sub>540</sub>, C<sub>70</sub>); g) amorphous carbon; h) carbon nanotube.</i>	3
<i>Fig 1.2</i>	<i>Surface functional groups containing Oxygen</i>	15
<i>Fig 1.3</i>	<i>Nitrogen containing functional groups when heated in nitrogen, ammonia, nitric acid</i>	15
<i>Fig 2.1</i>	<i>SEM images of carbons obtained after heating CMC at 400<sup>o</sup>C in nitrogen for 3hrs.</i>	44
<i>Fig 2.2</i>	<i>SEM images of carbons obtained after heating cellulose at 400<sup>o</sup>C in nitrogen for 3hrs.</i>	45
<i>Fig 2.3</i>	<i>SEM images of carbons obtained after heating starch at 400<sup>o</sup>C in nitrogen for 3hrs.</i>	45
<i>Fig 2.4</i>	<i>SEM images of carbons obtained after heating sucrose at 400<sup>o</sup>C in nitrogen for 3hrs.</i>	46
<i>Fig 2.5</i>	<i>IR of carbon prepared from CMC</i>	47
<i>Fig 2.6</i>	<i>IR of carbon prepared from cellulose</i>	47
<i>Fig 2.7</i>	<i>IR of carbon prepared from starch</i>	48
<i>Fig 2.8</i>	<i>IR of carbon prepared from sucrose</i>	49
<i>Fig 2.9</i>	<i>SEM images of CMC carbon after activation by quenching</i>	50
<i>Fig 2.10</i>	<i>SEM images of carbon from Cellulose after activation by quenching</i>	50
<i>Fig 2.11</i>	<i>SEM image of carbon from CMC, having high porosity, obtained as per the new synthesis method developed</i>	51
<i>Fig 2.12</i>	<i>XRD profiles of the activated carbon obtained from CMC</i>	57
<i>Fig 2.13</i>	<i>XRD profile of commercial activated carbon C1</i>	58
<i>Fig 2.14</i>	<i>XRD profile of commercial activated carbon C2</i>	58
<i>Fig 2.15</i>	<i>EPR spectrum for DPPH reference</i>	60
<i>Fig 2.16</i>	<i>EPR spectrum for activated carbon CMC-N</i>	60
<i>Fig 2.17</i>	<i>EPR spectrum for commercial activated carbon C1</i>	61
<i>Fig 2.18</i>	<i>EPR spectrum for commercial activated carbon C2</i>	61
<i>Fig 2.19</i>	<i>BJH isotherms for the nitrogen adsorption desorption in relation to pore size distribution for CMC-N</i>	63
<i>Fig 2.20</i>	<i>BJH isotherms for the nitrogen adsorption desorption in relation to pore size distribution for activated carbon C1</i>	64

Fig 2.21	<i>BJH isotherms for the nitrogen adsorption desorption in relation to pore size distribution for activated carbon C2</i>	65
Fig 2.22	<i>BJH isotherms for the nitrogen adsorption desorption in relation to pore size distribution for activated carbon C2</i>	66
Fig 2.23	<i>SEM images of carbon from CMC after carbonisation and before activation showing the aromatised sheets as well as pores.</i>	68
Fig 2.24	<i>SEM images of carbon from CMC after activation by quenching indicating the surface burn off.</i>	68
Fig 2.25	<i>SEM images of carbon from CMC after activation by quenching showing smaller pores within the pores.</i>	69
Fig 2.26	<i>SEM images of commercial activated carbon C1</i>	69
Fig 2.27	<i>SEM images of commercial activated carbon C2</i>	70
Fig 2.28	<i>Thermogravimetric analysis of sodium carboxyl methyl cellulose in nitrogen</i>	71
Fig 2.29	<i>Thermo gravimetric analysis of carbon synthesised from CMC-N in nitrogen</i>	74
Fig 2.30	<i>IR of activated carbon CMC-N</i>	76
Fig 2.31	<i>IR of activated carbon C1</i>	76
Fig 2.32	<i>IR of activated carbon C2</i>	77
Fig 2.33	<i>Energy diffraction spectra of activated carbon from CMC</i>	79
Fig 2.34	<i>Energy diffraction spectra of commercial activated carbon C1</i>	80
Fig 2.35	<i>Energy diffraction spectra of commercial activated carbon from C2</i>	81
Fig 2.36	<i>Temperature Programmed Desorption of activated carbon CMC-N using ammonia as probe molecule</i>	83
Fig 2.37	<i>Temperature Programmed Desorption of activated carbon C1 using ammonia as probe molecule</i>	84
Fig 2.38	<i>Temperature Programmed Desorption of carbon C2 using ammonia as probe molecule</i>	84
Fig 2.39	<i>Volume of oxygen evolved on decomposition of hydrogen peroxide using CMC-N and C1, C2</i>	85
Fig 3.1	<i>Equilibration time for methylene blue adsorption by activated carbons C1, C2 and CMC- N</i>	90
Fig 3.2	<i>Comparative study of methylene blue adsorption by different carbons for a fixed weight of sample and a fixed time period</i>	91
Fig 3.3	<i>Langmuir's adsorption isotherms for Methylene Blue adsorption by commercial carbon C1</i>	92
Fig 3.4	<i>Langmuir's adsorption isotherms for Methylene Blue adsorption by commercial activated carbon from IGCL, Kerala (C2).</i>	93
Fig 3.5	<i>Langmuir's adsorption isotherms for Methylene Blue adsorption by carbon synthesized from carboxyl methyl cellulose (CMC-N).</i>	93
Fig 3.6	<i>Freundlich adsorption isotherms for Methylene Blue adsorption by commercial activated carbon (C1).</i>	95

Fig 3.7	<i>Freundlich adsorption isotherms for Methylene Blue adsorption by commercial activated carbon from IGCL, Kerala, (C2)</i>	95
Fig 3.8	<i>Freundlich adsorption isotherms for Methylene Blue adsorption by activated carbon synthesized from CMC (CMC-N)</i>	96
Fig 3.9	<i>Comparative study of Cu<sup>2+</sup> adsorption by activated carbons C, C2, CMC-N</i>	
Fig 3.10	<i>Comparative study of Mn<sup>2+</sup> adsorption by activated carbons C, C2, CMC-N</i>	102
Fig 3.11	<i>Langmuir's adsorption isotherms for Mn<sup>2+</sup> ion adsorption by CMC-N carbon</i>	102
Fig 3.12	<i>Langmuir's adsorption isotherms for Cu<sup>2+</sup> ion adsorption by activated carbon CMC-N</i>	102
Fig 3.13	<i>IR of activated carbon C1 and nitric acid functionalized C1</i>	107
Fig 3.14	<i>IR of activated carbon C2 and nitric acid functionalized C2</i>	108
Fig 3.15	<i>IR of activated carbon CP and nitric acid functionalized CP</i>	109
Fig 3.16	<i>IR of activated carbon CMC-N and nitric acid functionalized CMC-N</i>	110
Fig 3.17	<i>Volume of oxygen evolved on H<sub>2</sub>O<sub>2</sub> decomposition by activated carbon C1 and nitric acid functionalized C1</i>	111
Fig 3.18	<i>Volume of oxygen evolved on H<sub>2</sub>O<sub>2</sub> decomposition by activated carbon C2 and nitric acid functionalized C2</i>	111
Fig 3.19	<i>Volume of oxygen evolved on H<sub>2</sub>O<sub>2</sub> decomposition by activated carbon CP1 and nitric acid functionalized CP</i>	112
Fig 3.20	<i>Volume of oxygen evolved on H<sub>2</sub>O<sub>2</sub> decomposition by activated carbon CMC-N and nitric acid functionalized CMC-N</i>	112
Fig 3.21	<i>gives the equilibration time for methylene blue adsorption by activated carbons and nitric acid treated carbons</i>	113
Fig 3.22	<i>Comparative study of adsorption of Mn<sup>2+</sup> ions by nitric acid functionalized and non functionalized activated carbons</i>	115
Fig 3.23	<i>Comparative study of adsorption of Cu<sup>2+</sup> ions by nitric acid functionalized and non functionalized activated carbons</i>	115
Fig 4.1	<i>XRD profiles of Anatase (A) and rutile (R) phase of TiO<sub>2</sub></i>	122
Fig 4.2	<i>Mechanism of photocatalytic degradation of a dye molecule</i>	124
Fig 4.3	<i>Comparative optical density of congo red, methylene blue and methyl orange with and without activated carbons.</i>	133
Fig 4.4	<i>Comparative optical density of methylene blue, MB and TiO<sub>2</sub>, MB and C2 when in dark and in light</i>	134
Fig 4.5	<i>Graph of optical density v/s time indicating photocatalytic degradation of 0.012 g/L methylene blue by various catalysts</i>	135

Fig 4.6	Graph of optical density v/s time indicating photocatalytic degradation of 0.012g/L methylene blue by 10% TiO <sub>2</sub> A2/C2, 10% TiO <sub>2</sub> R2/C2.	136
Fig 4.7	XRD images of A2 (anatase ) and R2 (rutile ) phases	137
Fig 4.8	Graph of optical density v/s time indicating photocatalytic degradation of methylene blue by, 10% TiO <sub>2</sub> R2/C2 and 30% TiO <sub>2</sub> R2/C2.	139
Fig 4.9	Comparative study of TiO <sub>2</sub> /SiO <sub>2</sub> and TiO <sub>2</sub> /C on the photodegradation of methylene blue.	140
Fig 5.1	Cyclic voltagram of TiC and ZrC Carbide Derived carbons .	151
Fig 5.2	Cyclic Voltagrams of activated carbons C1 and C1 with OMS-2	154
Fig 5.3	Cyclic Voltagrams of activated carbon C2 and C2 with OMS-2	155
Fig 5.4	Cyclic Voltammogram of CMC carbon (CMC-N) and CMC-N with OMS-2	156
Fig 5.5	Cyclic Voltagrams of polymer carbons ( CP) and CP with OMS-2	157
Fig 5.6	Cyclic Voltagrams of manganese dioxide supported carbons ( MnO <sub>2</sub> /C 1) and MnO <sub>2</sub> /C 1 with OMS	158
Fig 5.7	Cyclic Voltagram of OMS-2	159
Fig 5.8	Cyclic Voltagram of Carbon nano tube	159
Fig 5.9	Comparative cyclic voltagram of activated carbon C1 with OMS-2, CMC-N with OMS -2 and OMS-2	162
Fig 5.10	(a) OMS-2 (b) OMS-1	165
Fig 5.11	Illustration of excess potential E <sub>i</sub> needed during electrolysis, over the equilibrium potential.	166
Fig 5.12	Electrochemical cell set up for Tafel plot	168
Fig 5.13	Tafel graph of $\eta$ v/s log i	169
Fig 5.14	Experimental set up for Tafel measurements	170
Fig 5.15	Tafel plot of electrooxidation of sulphuric acid acidified water.	171
Fig 5.16	Thermogravimetric analysis of potassium chlorate	173
Fig 5.17	TG of KClO <sub>3</sub> , MnO <sub>2</sub> and KClO <sub>3</sub> + MnO <sub>2</sub> in argon atmosphere.	177
Fig 5.18	TG of C1 and CMC in oxygen atmosphere and TG of C1K and CMCK in argon atmosphere.	178
Fig 5.19	TG profiles of mixtures of MnO <sub>2</sub> + KClO <sub>3</sub> , Mn O <sub>2</sub> /C1+ KClO <sub>3</sub> , C1+ KClO <sub>3</sub> in argon atmosphere.	180
Fig 5.20	TG profiles of mixtures of CMC + KClO <sub>3</sub> + Na <sub>2</sub> S and C1 + KClO <sub>3</sub> + Na <sub>2</sub> S in argon atmosphere.	181
Fig 5.21	TG profiles of CMC+ Na <sub>2</sub> S, MnO <sub>2</sub> /C1+Na <sub>2</sub> S, C1+ Na <sub>2</sub> S, Na <sub>2</sub> S in argon atmosphere.	181

**TABLES****PAGE NO.**

Table 1.1	Density of some forms of carbons	
Table 1.2	Properties of carbons from different precursors and its applications	4
Table 1.3	List of the impregnating chemical and the application of the impregnated carbon.	10
Table 2.1	BET surface area of carbons prepared from CMC, Cellulose, Starch and Sucrose when heated for 3 hrs in nitrogen at 400 <sup>0</sup> C.	34
Table 2.2	g values of activated carbons CMC-N, C1, C2 obtained by EPR spectra analysis using DPPH as reference.	47
Table 2.3	Comparison of specific surface area, pore specific volume, density of CMC-N, C1, C2 and CMC N	59
Table 2.4	Surface area and pore volume data of CMC carbons with oxidation but no quenching (CMC-A) and with oxidation and quenching (CMC-N).	62
Table 2.5	Percentage of volatiles at T1 and T2 and percentage of residue at 400 <sup>0</sup> C and 900 <sup>0</sup> C	67
Table 2.6	Assignment of bands in I R to surface functional groups.	75
Table 2.7	Acidity and Basicity of carbons in milimoles g <sup>-1</sup>	82
Table 2.8	pH of carbons in solution	
Table 2.9	Temperature programmed Desorption profiles of C, C1, C2, CMC-N using ammonia as probe molecule	82
Table 3. 1	Linear Regression and max amount adsorbed for Langmuir's adsorption isotherms for Methylene Blue adsorption by the activated carbons C1, C2, CMC-N	94
Table 3.2	Linear Regression and Freundlich adsorption constant for Methylene Blue adsorption by activated carbons C1, C2, CMC-N	96
Table 3.3	Linear Regression constant and the maximum amount of Cu <sup>2+</sup> and Mn <sup>2+</sup> ions adsorbed X <sub>m</sub> calculated from Langmuir adsorption isotherm for adsorption by CMC-N carbon	104
Table 3.4	Equilibration time for activated carbon and nitric acid treated carbons for methylene blue adsorption	114
Table 4.1	Characteristic peaks of rutile and anatase TiO <sub>2</sub>	123
Table 4.2	Characteristic peaks of A2 (anatase) and R2 (rutile) TiO <sub>2</sub>	138
Table 5.1	Current I (A) at 0.5V for carbons with and without OMS-2	160
Table 5.2	Current density of carbons C1, C2, CP, CMC-N with OMS-2, MnO <sub>2</sub> supported carbons with OMS-2, OMS-2 and Carbon nano tube.	161
Table 5.3	List of the impregnating chemical and the application of the impregnated carbon.	173
Table 5.4	List of the Decomposition temperature of KClO <sub>3</sub> , MnO <sub>2</sub> and KClO <sub>3</sub> + MnO <sub>2</sub>	177

## LIST OF CATALYST CODES

1. C1: activated carbon was obtained from SD Fine Chemicals
2. C2: activated carbon from coconut shell from IGCL, Kerala
3. CMC-N: activated carbon from CMC
4. FC1: activated carbon obtained from SD-Fine chemicals Ltd treated with nitric acid.
5. FC2: activated carbon from coconut shell IGCL treated with nitric acid.
6. F CP: meso porous carbon from polymer treated with nitric acid
7. FCMC-N: activated carbon from CMC treated with nitric acid
8.  $\text{MnO}_2/\text{C}$ :  $\text{MnO}_2$  was supported on carbon by calcining Manganese Nitrate and carbon C1 in the furnace at  $400^\circ\text{C}$  to obtain C- $\text{MnO}_2$ .
9. OMS-2 as synthesized in [79]
10. Carbon nanotubes
11. C1O: C1+OMS2
12. C2O: C2+OMS2
13. CPO: C3+OMS2
14. CMC NO: CMC-N+OMS2
15.  $\text{MnO}_2/\text{C O}$ :  $\text{MnO}_2/\text{C}$ +OMS2
16.  $\text{MnO}_2/\text{C1}$ : manganese dioxide supported on C1 by calcining manganese nitrate.

17.  $\text{MnO}_2$ : synthesized by calcining manganese nitrate.
18.  $\text{KClO}_3$ : obtained from Loba Chemicals
19. MK: prepared by mixing  $\text{KClO}_3 + \text{MnO}_2$  in the ratio 1:1
20. C1K: prepared by mixing C1 and  $\text{KClO}_3$
21. CMCK: prepared by mixing CMC and  $\text{KClO}_3$
22. MC1K: prepared by mixing  $\text{MnO}_2/\text{C1}$  and  $\text{KClO}_3$
23. NS: fused sodium sulphide obtained from Loba chemicals
24. C1NS: prepared by mixing C1 and fused sodium sulphide.
25. CMC NS: prepared by mixing CMC and  $\text{Na}_2\text{S}$
26. MC1NS: prepared by mixing  $\text{MnO}_2/\text{C1}$  and  $\text{Na}_2\text{S}$
27. C1KNS: prepared by mixing C1,  $\text{KClO}_3$ ,  $\text{Na}_2\text{S}$
28. CMCKNS: prepared by mixing CMC,  $\text{KClO}_3$ ,  $\text{Na}_2\text{S}$

# **SYNOPSIS**

## **CHAPTER I: INTRODUCTION AND LITERATURE REVIEW**

Activated carbons are carbonaceous substances having adsorbent properties. The high surface area due to porosity and the surface functional groups on the carbons are responsible for physical and chemisorption of adsorbate.

The nature of the activated carbons depends on many factors such as the precursors, temperature, rate of heating, method of carbonisation and activation agents.

The precursors generally used are biomass, nut shells, fruit seeds, husks, cellulose and their derivatives, coal, charcoal, sludge, synthetic polymers have been used.

Carbon possesses allotropes such as graphite, diamond and fullerenes. They may be powdered or granular. Spherical, fibre, planar sheets, crystalline articles, nano tubes are some identifiable shapes.

Preparation of activated carbons involves a two step process, namely, carbonisation and activation. This creates porosity and develops surface functional groups. It can be achieved by physical and chemical methods.

Carbonisation is achieved by heating the precursor in the absence of air and then activation is done by heating it at high temperatures of 800<sup>0</sup>C by passing air or carbon dioxide or steam. In the chemical methods, activating agents like zinc chloride, potassium hydroxide, phosphoric acid are used and the carbonisation and activation is done simultaneously.

During the carbonisation process, first dehydration takes place and the inorganics get removed as volatiles and ash. Restructuring of carbons takes place within with the formation of aromatic sheets. The escaping gases produce pores. During activation the oxygen combines with the carbon giving rise to newer functional groups. Some of these surface oxides get removed during heating leaving behind surface valencies which help in the adsorption process.

Certain functional groups can be introduced by surface modification by various treatments like concentrated nitric acid and sulphuric acid, amination with ammonia, treatment with ozone or just air oxidation.

The activated carbons so formed can be characterized by various methods to ascertain its properties. Some of the characterization tools used are BET surface area measurements, SEM, TG, IR, TPD, pH, decomposition of hydrogen peroxide.

Historically these carbons have been used in food industry, medicine, water purification, recovery of metals, gas masks, room purifiers etc. Carbons are used as supports for catalysis. Elements and compounds can be supported on carbons to achieve higher degree of efficiency in catalytic reactions. Titanium oxide supported on carbons doubles photocatalysis. Manganese dioxide on carbon can enhance electrochemical reactions.

The wide application of activated carbons has generated a lot of interest in preparing carbons with varied surface modifications as per the need of desired properties.

This thesis on “Activated carbons for environmental applications” is one such compilation of work done. Activated carbons have been prepared from sodium salt of carboxyl methyl cellulose by a green process, at low temperatures, having high surface area, having multiple applications. The carbon has been characterized and various applications like adsorption of dyes, metal ions of Cu and Mn, decomposition of hydrogen peroxide, carbon as support for titanium dioxide for photocatalysis, support for manganese dioxide for electrochemical applications have been studied.

## ***CHAPTER II: EXPERIMENTAL***

### **A] PREPARATION AND FUNCTIONALISATION**

#### **Preparation**

The carbon was prepared by dehydrating the precursor (sodium salt of carboxymethyl cellulose) at 170<sup>0</sup> C for one hour. It was then heated for 3 hours in an atmosphere of nitrogen at 400<sup>0</sup>C. The carbonized material was then removed, oxidized by air, and then quenched in double distilled water. The carbon was then washed, dried and ground in the planetary ball mill grinder. It was labeled as CMC-N.

Carbons were also prepared from cellulose, starch, sucrose and glucose by a similar process. The carbons were labeled as cel, sta, suc, glu.

### **Functionalisation**

Carbon prepared from carboxymethyl cellulose was functionalized with 5M concentrated nitric acid for three hours using the soxhlet apparatus. Three other carbons obtained from other sources were also functionalized by a similar process. C1, C2, CP and CMC-N. The functionalized carbons were labeled as FC1, FC2, FCP and FCMC-N.

## **B] CHARACTERISATION**

### **i) TG:**

From the thermo gravimetric analysis of the precursors, the percentage loss of water and volatiles and the amount of carbon left was calculated.

### **ii) SEM**

The images of carbons provided by scanning electron microscope provided the information about the surface morphology of the carbons. The CMC-N carbons showed graphitic sheets and pores.

### **iii) BET surface area measurements**

The surface area was found out by BET. The pore volume was also obtained. The surface area of the CMC-N was  $1025 \text{ m}^2/\text{g}$  which was higher than the commercial carbons. The pore volume was  $0.057 \text{ cm}^3$  which was also higher than the other carbons.

### **iv) XRD**

The XRD showed typical peaks at 2 theta values corresponding to regular hexagonal carbons at 12.5 and a broad peak at 24 of graphitic carbon.

### **v) IR**

The surface functional groups were identified from IR. The data showed the presence of carboxyl groups and lactones.

vi) TPD

The temperature programmed desorption with ammonia provided relative strengths of acid sites.

vii) Acidity and Basicity measurements by titration

Activated carbons show both acidic as well as basic sites. CMC-N carbons had more basic sites as compared to acidic sites.

viii) pH

pH of the carbons was found out. CMC-N carbon was most basic

ix ) Decomposition of hydrogen peroxide.

Decomposition of hydrogen peroxide depended on the acidic sites of carbon. It was found that the CMC N carbon which was more basic showed lesser degree of decomposition of hydrogen peroxide.

### ***CHAPTER III: ADSORPTION STUDIES***

#### **A] ADSORPTION OF METHYLENE BLUE**

Dyes are used in several industries like textiles, leather, food, paper etc. Dye pollutants in water have been a major concern. While several techniques like chemical oxidation, coagulation, electrochemical have been used, adsorption technique is the most preferred one for removal of dyes.

Various adsorbents such as alumina, silica, metal hydroxides have been used; however, activated carbons are widely used for commercial applications. Activated carbons have been modified with treatment and efficacy of methylene blue adsorption has been tested.

The activated carbon prepared from CMC-N was used as adsorbent to remove methylene blue dye and compared with two other commercial carbons.

CMC-N showed methylene blue adsorption. Methylene Blue is a cationic dye. The commercial carbons had more acidic sites as compared to CMC-N, hence the adsorption of the dye was more by C1 and C2. The carbons obeyed Langmuir and Freundlich adsorption isotherms.

The equilibration time was also calculated. The commercial carbons showed higher equilibration time of 72 hours as compared to 24 hrs for CMC-N.

#### BJ ADSORPTION OF METAL IONS $\text{Cu}^{2+}$ , $\text{Mn}^{2+}$

Activated Carbons have been used to remove metal ions. The contamination of ground water with high concentration of Cu ions in the vicinity of the industrial area of Cu processing units has been a concern. Similarly contamination of water bodies with Fe and Mn ions in the mining areas is a serious environmental threat.

There are several reported methods on the removal of gold, mercury, arsenic, ferrous and ferric, manganese, copper, cadmium ions from solutions prepared using chemically treated carbons.

CMC-N carbon showed high percentage of removal of  $\text{Cu}^{2+}$ . The amount of copper removed was estimated by the EDTA method.

The equilibration time for the carbons was found out. The equilibration time for CMC-N carbon was 2 hours. Adsorption isotherms were plotted for the carbons.

It has been reported that lactone group on carbon assist in copper and nickel adsorption.

The adsorption can be attributed to the basic nature of the carbons. Due to the concentration of  $\text{OH}^-$  ions on the carbons, Cu is removed as copper hydroxide by chemisorption on the carbon.

CMC-N carbon also showed a high percentage of removal of  $\text{Mn}^{2+}$ . The amount of manganese removed was estimated by EDTA method. The equilibration time for the carbons was found out. The equilibration time for CMC-N carbon was 2 hours. Adsorption isotherms were plotted for the carbons.

## C] COMPARATIVE STUDY OF FUNCTIONALISED AND NON FUNCTIONALISED CARBON

A comparative study was done of unfunctionalized and functionalized carbons. Four carbons prepared from different precursors were treated with concentrated nitric acid.

Their activity in the following applications were studied

- a) Decomposition of hydrogen peroxide.
  - b) Adsorption of methylene blue
  - c) Adsorption of  $\text{Cu}^{2+}$  and  $\text{Mn}^{2+}$
- It was observed that the decomposition of hydrogen peroxide decreased for functionalized carbons but remained constant for CMC-N carbon
  - There was a decrease in the equilibration time of methylene blue.
  - The adsorption of  $\text{Cu}^{2+}$  and  $\text{Mn}^{2+}$  ions decreased

Functionalisation with nitric acid leads to the introduction of oxygen groups leading to the decrease in adsorption.

### ***CHAPTER IV: ADSORPTION ON C-TiO<sub>2</sub> AND PHOTOCATALYSIS***

TiO<sub>2</sub> is a known photocatalyst. Its properties can be enhanced when supported on activated carbons.

TiO<sub>2</sub> was supported on carbon. Two methods were employed. In the first method C and TiO<sub>2</sub> were mechanically mixed and calcined. In the second method, insitu preparation of TiO<sub>2</sub> was done from TiCl<sub>3</sub>.

The C-TiO<sub>2</sub> was used to test photocatalytic degradation of methylene blue dye. It was found that the insitu preparation of C-TiO<sub>2</sub> showed better photocatalytic activity.

Photocatalytic activity was also tested for the anatase and rutile phase of TiO<sub>2</sub>. It was observed that the anatase phase gave better results.

Effect of percentage loading of  $\text{TiO}_2$  on carbon was studied. It was observed that 10% loading showed better photocatalytic activity as compared to 5% and 30% loading.

#### ***CHAPTER V: ELECTROCHEMICAL AND CATALYTIC PROPERTIES OF CARBONS AND CARBON SUPPORTED Mn (IV) OXIDE***

Carbons have been used as electrode material. The capacitance of the carbon electrodes increases with increase in functional groups on them, if it is an inorganic electrolyte. The pore size also influences the capacitance.

$\text{MnO}_2$  is known for its electrochemical properties. If supported on carbons, these properties get enhanced.

$\text{MnO}_2$  was supported on carbon by calcining manganese nitrate and carbon. Capacitance studies were done for various carbons and compared with C- $\text{MnO}_2$ , OMS-2 (which is a form of manganese dioxide having octahedral molecular sieve structure) and carbon nanotubes. It was observed that carbons showed comparable capacitance to C- $\text{MnO}_2$ , OMS and carbon nanotubes.

The current density increased on addition of OMS-2 for all carbons but decreased for CMC-N and was maximum for carbon C2.

A comparative study was done of Pt and Pt/C electrodes on electrolysis of water. It was found that the use Pt/C electrode resulted in higher evolution of oxygen as compared to Pt at the same overpotential.

Catalytic activity of carbons was tested for  $\text{KClO}_3$  decomposition and sodium sulphide oxidation. CMC-N and C1 carbons decreased the decomposition temperature of  $\text{KClO}_3$ . Manganese dioxide supported on carbon C1 was more effective in  $\text{Na}_2\text{S}$  oxidation. It was observed that  $\text{KClO}_3$  catalysed the gasification of carbons.

*CHAPTER I*

**INTRODUCTION AND LITERATURE**

**REVIEW**

## 1.1 INTRODUCTION

Activated carbons are generally defined [1] as amorphous carbon having high porosity and inter particulate surface area, obtained from carbonaceous materials. These carbons have high degree of surface reactivity, which increases their adsorption capacity. Activated carbons whether granular or powdered find wide application in the domestic as well in the industrial sector. These are used for water purification, removing odours and toxins, recovering metals from solutions, treating bacteria related ailments, as catalysts, catalyst supports and electrode materials. Hence it generates a lot of economic interest.

Traditionally, coconut and coconut chars have been used in Goan households to remove excess vinegar, odour, tenderize meat during cooking. Powdered charred coconut mixed in coconut oil is used to decolourise skin after a burn injury.

The use of activated carbons to purify water collected in the mining pits of Goa has been recommended by Tata Energy Research Institute in its report 'Area wide quality management plan for the mining belt of Goa State'. This AEQEM report, was commissioned by the Government of Goa and published by the Directorate of Planning, Statistics and Evaluation in 1997 [2].

The system of Granular Activated Carbons having carbon contactors and reactivation of spent carbon has been proposed. The recommendation was made to augment water supply to the mining villages facing acute shortage of water. There is only one factory in the Cuncolim Industrial Estate which manufactures activated carbons from coconut shell. Though Goa is known as the land of swaying coconut palms, the raw material is brought from outside the state. Viable water purification plant is urgently required to ameliorate the sufferings, especially of women who have to walk long distances,

queue up for tanker water, get up at odd hours for tap water and do the drudgery of water collection.

The leaching of manganese and ferrous ions into water bodies needs to be addressed.

One of the aims of the present investigation is to prepare activated carbons from renewable sources, by a green process to remove metal ions such as  $Mn^{2+}$  and  $Cu^{2+}$ .

The other aspects of investigation include removal of dyes by adsorption and photocatalytic degradation, catalyst and catalyst supports for chemical reactions, applications in electrocatalysis and capacitance.

In the ensuing pages of this chapter, an attempt has been made to review the literature available on the various methods of preparation of activated carbons, their modifications, characterization and applications.

## 1.2 LITERATURE REVIEW

The versatile use of activated carbons stems from the fact that it is a good adsorbent. Its highly porous structure gives it an extended surface area for adsorption. Changing pore size or linking the carbon with surface groups or impregnating it with metals can alter the surface chemistry and surface characteristics. The raw material, the method of preparation also determines its properties.

### 1.2.1 Forms of carbon

Carbon has several allotropes. These include diamond, graphite, lonsdaleite, fullerenes, amorphous carbons and carbon nanotubes. The structure of these is illustrated in Fig 1.1.

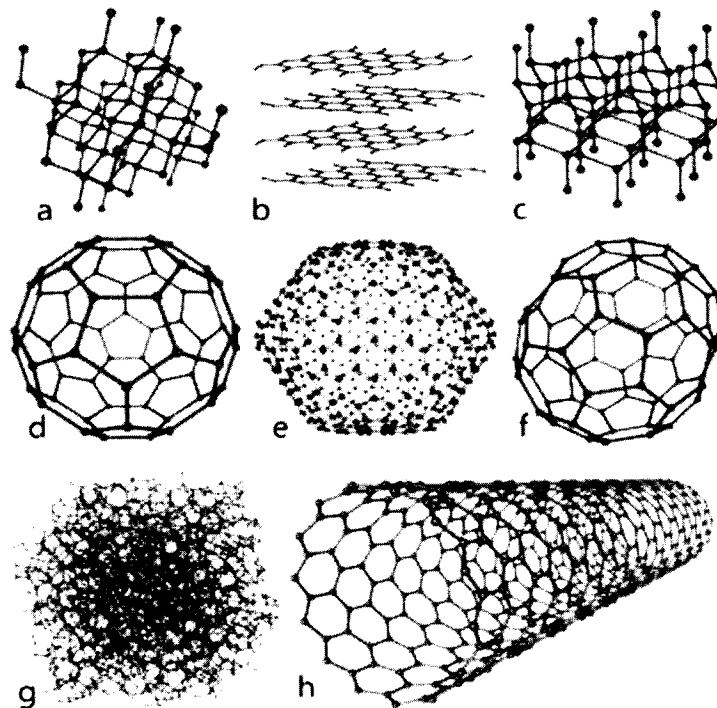


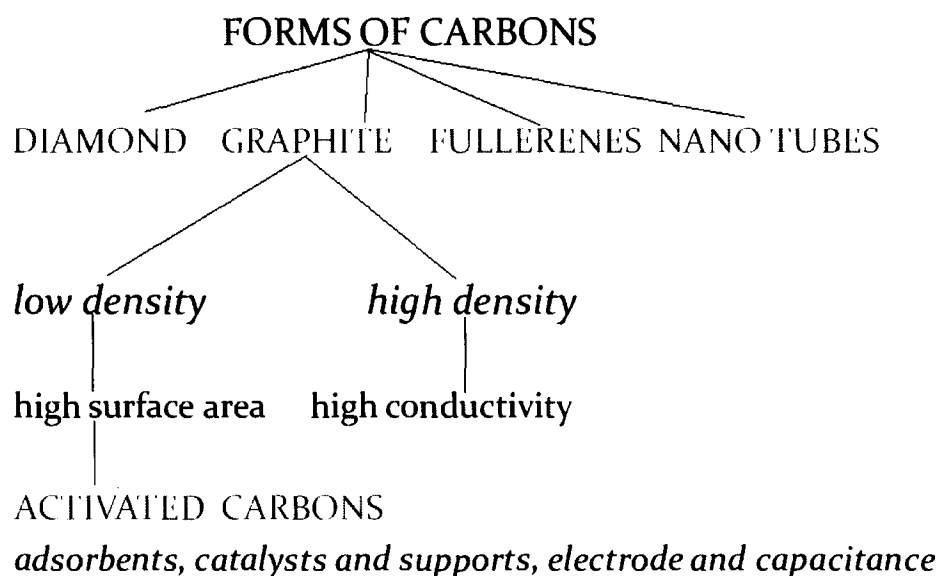
*Fig 1.1: Some allotropes of carbon a) diamond; b) graphite; c) lonsdaleite; d-f) fullerenes (C60, C540, C70); g) amorphous carbon; h) carbon nanotube.*

The amorphous and crystalline forms of carbons have different densities as is given in Table 1.1. Between the crystalline and amorphous stage, carbons can be modified for various applications.

<b>Form of Carbon</b>	<b>Density (grams/cubic centimeter)</b>
Amorphous carbon	1.8 - 2.1
Buckminsterfullerene C <sub>60</sub>	1.69
Graphite	1.9 - 2.3
Diamond	3.50 - 3.53

*Table 1.1 Density of some forms of carbons*

Of these various forms, activated carbons are generally of low density and graphitic in nature. The structure of activated carbon has been considered to be microcrystalline and compared with that of carbon. With the advent of Transmission Electron Microscopy, the perspective has changed. Active carbons are now visualized as stacks of flat aromatic sheets cross linked in a random manner.



***Scheme 1.1 Diagrammatic representation of the form of activated carbon***

Electron spin resonance studies have shown that aromatic sheets in active carbons contain free radicals structures or structures with unpaired electrons. These unpaired electrons are resonance stabilized and are trapped during carbonization process as a result of breaking up of the bonds at the edges of the aromatic sheets thus creating edge carbon atoms. These edge atoms have unsatisfied valencies and can thus interact with hetero atoms such as oxygen, hydrogen, nitrogen and sulphur giving rise to different types of surface functional groups.[3]

The elemental analysis of a typical activated carbon was found to be 88% C, 0.5% H, 0.5% N, 1% S and 6.7% O the balance representing ash content. The content of the oxygen can vary between 1-25% depending upon the raw material and the conditions of activation process.

The activation process significantly influences the nature of the carbon-oxygen surface complex. At low temperature these complexes are less stable and at high temperature the functional groups formed are more stable.

### *1.2.2 Classification of activated carbons*

Activated carbons are difficult to classify based on their behavior, surface characteristics and other properties. Therefore, they are often classified on the basis of their particle size and particle shapes.

#### Powdered activated carbon

They have a fine granulometry less than 100um with average diameter of 15-25 um. They present a large external surface and a small diffusion distance. The rate of adsorption is very high. They are therefore preferably used for adsorption from solutions. The carbon is added to the solution directly, agitated, left in contact for a short time, 5-30 minutes and then filtered. These groups of carbons are used for decolourisation and in medicines. They are generally prepared by chemical activation methods from sawdust.

#### Granulated Activated Carbon

Granulated carbon are prepared from bituminous and lignite coals [4, 5], petroleum oil and heavy residues [6], synthetic and natural fibre [7] and pyrolysis of waste rubber tyres [8].

They have a relatively larger size of carbon particles in the granules as compared to carbon powders and consequently smaller external surface. These carbons are preferred for the adsorption of gases and vapours as their rate of diffusion is faster. The size of the carbon particles is important as it should not be carried away with the gaseous stream. The greater the height of the bed used, larger is the size of the granules. Granulated carbons are also used for water treatment and sometimes for decolourisation and separation of components of the flow system.

### Spherical Activated Carbons

Katori et al [9] and Nagai et al [10] developed a process for the preparation of spherical carbon from pitch. The pitch is melted in the presence of naphthalene or tetralin and converted into spheres. These spheres are contacted with solvent naphtha, which extracts naphthalene and creates a pore structure. Spherical activated carbons in the form of hollow spheres [11] and spherical pellets [12] have also been obtained.

### Impregnated carbons

Several types of carbons impregnated with inorganics such as iodine [13], silver [14], cations such as aluminum, manganese, zinc, iron, lithium and calcium [15]. Organics impregnates such as pyridines [16], ketones [17] and tertiary amines [18] have also been prepared.

## Polymer coated carbon

Fennimore [19] described a process by which a porous carbon can be coated with a biocompatible polymer to give a thin, smooth and permeable coating without blocking the pores. The resulting substance is useful for haemofusion.

### *1.2.3 Precursors*

Carbon is called 'Activated carbon', when it is processed from precursors to make it extremely porous and thus to have a very large surface area available for adsorption or chemical reactions. Surface modifications are also done to introduce functionalities for facilitating adsorption or chemical reactions of specific substances.

The conventional sources of activated carbons are bituminous coal, peat, lignite, petroleum, coke, wood and nutshells. [20]. The non conventional sources of raw materials include rice husk, viscose rayon, coir pith, banana pith, orange peel, peanut hull, tamarind shell, cashew nut sheath, sunflower seed, palm seed coat, castor seed, moringa seed, guava seed, barley straw. Sugarcane baggase, pulp of fruit have been used.

Carbons are generally obtained from biomass which has high carbon content and low inorganics. Soft wood like pine, scrapings of wood, sawdust, husk, nutshells, fruit seeds have been used as precursors. Carbon fibres have been produced from polymers. Cellulosic compounds are also used.

The criterion for producing carbons profitably on a commercial scale depends upon the easy availability of cheap raw materials, which can be stored and handled with ease. The volume of raw material with respect to carbon obtained will factor in the cost for handling and storage. The uses of activated carbons are directly linked to the properties of the raw material. Less amount of inorganic keeps the ash content low, however large amount of volatiles help in increasing the pore volume when the gases escape.

The raw material has to be of high density where carbons with high structural strength are required, especially in gas vapor adsorption. Low density raw materials, with large amount of volatiles produce low density carbons having large pore volume.

Raw material	Carbon %	Volatile %	Density Kg/L	Ash %	Texture of carbon	Application of activated carbons
Soft wood	40-45	55-60	0.4-0.5	0.3-1.1	Soft, large pore volume	Aqueous phase adsorption
Hard wood	40-42	55-60	0.55-0.80	0.3-1.2	Soft, large pore volume	Aqueous phase adsorption
Lignin	35-40	58-60	0.3-0.4	-	Soft, large pore volume	Aqueous phase adsorption
Nutshells	40-45	55-60	1.4	0.5-0.6	hard, large micropore volume	Aqueous phase adsorption
Lignite	55-70	25-40	1.00-1.35	5-6	Hard, small pore volume	Wastewater treatment
Soft coal	65-80	20-30	1.25-1.50	2-12	Medium hard, medium micropore volume	Liquid and vapour phase adsorption
Petroleum coke	70-85	15-20	1.35	0.5-0.7	Medium hard, medium pore volume	Wastewater treatment
Semi hard coal	70-75	10-15	1.45	5-15	hard, large pore volume	Gas vapour adsorption
Hard coal	85-95	5-10	1.5-1.8	2-15	hard, large pore volume	Gas vapour adsorption

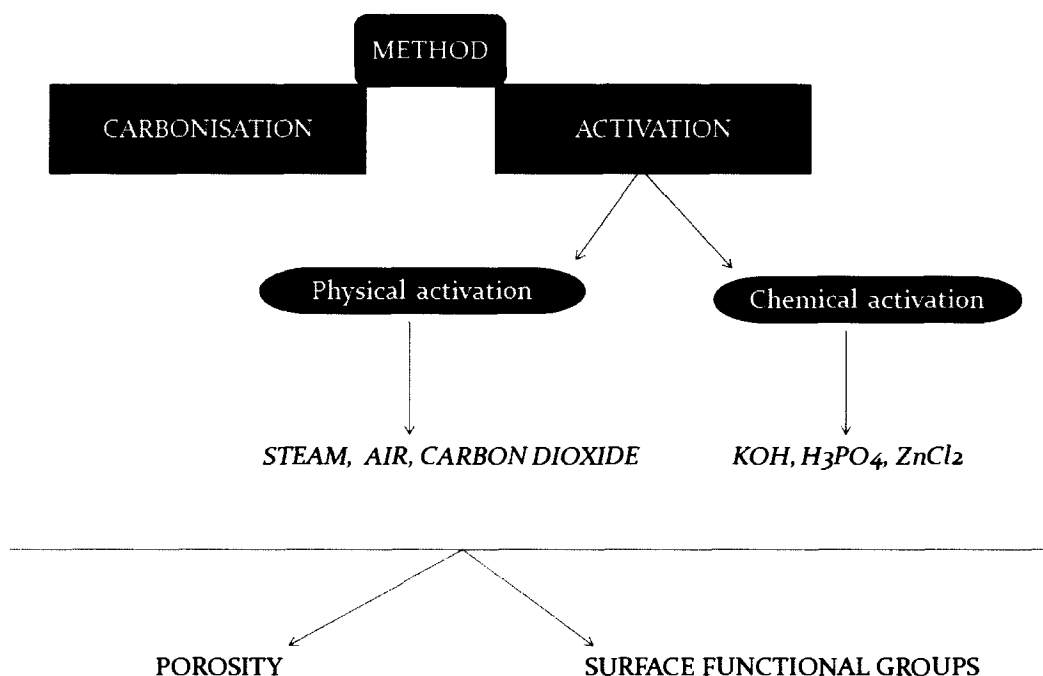
***Table 1.2 Properties of carbons from different precursors and its applications***

The above table gives the properties of carbons from different precursors and its applications.

### 1.2.4 Synthesis

Carboxyl methyl cellulose (sodium salt) has been used during the preparation of activated carbons to make carbons of higher density [8]. The approach is to attain product mechanical strength and water stability by cross linking rather than high temperature heat treatment. The cross linking reaction occurs at temperatures below 270<sup>0</sup> C. In addition, this new binder technology produces shaped carbon bodies having key properties beyond the best level that has been accomplished with other binders.

Carboxyl methyl cellulose a soluble derivative of cellulose, which produces solutions of high viscosity in water, is used extensively as a binder. This binding property of CMC obtained from renewable sources, opens up avenues for preparation of activated carbons. McEnancy and Devaston prepared a series of microporous carbons from cellulose triacetate [7].



***Scheme 1.2 Method of preparation of activated carbon***

It is well known that the manufacture of activated carbons involves two processes namely carbonization and activation (Scheme 1.2).

#### **a) Carbonization**

During the carbonization process, at first dehydration takes place and the inorganic components get removed as volatiles and ash.

Low heating rate results in higher volatilization [21] because of increased dehydration and better stabilization of the polymeric component. Restructuring of carbons take place with the formation of aromatic sheets. The escaping gases produce pores. During activation, the oxygen or nitrogen combines with the carbon giving rise to newer functional groups. Some of these surface oxides get removed during heating leaving behind unpaired electrons. These unpaired electrons are resonance stabilized and are trapped during the carbonization process as a result of breaking up of the bonds at the edges of the aromatic sheets thus creating edge carbons [3]. These edge carbon atoms have unsatisfied valencies and thus react with hetero atoms like oxygen, hydrogen or nitrogen

#### **(b) Activation**

To enhance porosity, activation has to be carried out so that the surface area increases due to the increase in the number and size of the pores. Activation is an oxidation reaction which is done either by physical methods or chemical methods.

*Physical methods* involve heating with steam, carbon dioxide or air at elevated temperatures above 800°C. *Chemical methods* involve use of chemicals for dehydration and oxidation in a one step carbonization and activation process using chemicals such as phosphoric acid, potassium hydroxide and zinc chloride [22]. Generally chemical activation is carried out between 400<sup>0</sup> to 800<sup>0</sup> C in the absence of air. These temperatures are lower than those used in physical activation.

The pore structure of chemical carbons is determined by the degree of impregnation of the chemical, larger the impregnation of the carbon larger is the pore size.

The impregnated chemical on calcination causes dehydration and aromatization of the carbon skeleton creating a porous structure. After calcination the carbon is cooled and washed to remove the impregnated material. This can be recycled. The yield of char is more in case of chemical carbons as chemicals inhibit tar, methanol, acetic acid and other product formation.

During activation, the micropores formed during the carbonization period are developed. Widening of pores takes place and new porosity is developed. This is done by initially burning off the disorganized carbons which opens blocked pores. As the contact of the activating agent increases, the burn off of walls between the pores occurs resulting in widening of pores. This results in the formation of mesopores or macro pores, decreasing the number of micro pores.

Activated carbons can be produced by combining both chemical and physical activation. Thus, guava seeds have been dried, milled and activated, by pyrolysis at temperature 700 °C using zinc chloride as chemical activation agent. Pyrolysis alone showed poor adsorption due to blockage of pores by decomposition products of lignocellulosic materials. Optimum adsorption capacity was obtained when the samples were subjected to chemical activation followed by pyrolysis at 700°C.

The pore volume, surface area, mean pore diameter, surface functional groups, besides depending on precursors, depend upon rate of heating during carbonization, final temperature, activating agents and duration of activation period.

Activated carbons prepared by chemical activation are called chemical carbons and the one obtained by physical methods as physical carbons. Activated carbons are generally amphoteric in nature as they have both acidic and basic functional groups. However, depending upon their adsorption of acids and bases they have been classified as acidic or basic carbons.

#### *1.2.5 Methods for surface modification*

Surface functionalization can be brought about by a) acids b) bases c) salts d) gases. Various methods such as heat treatments, microwave and plasma have been used.

Figueiredo [23] proposed that the following functional groups are present on carbons. They get suitably altered depending on the reacting substance and the method.

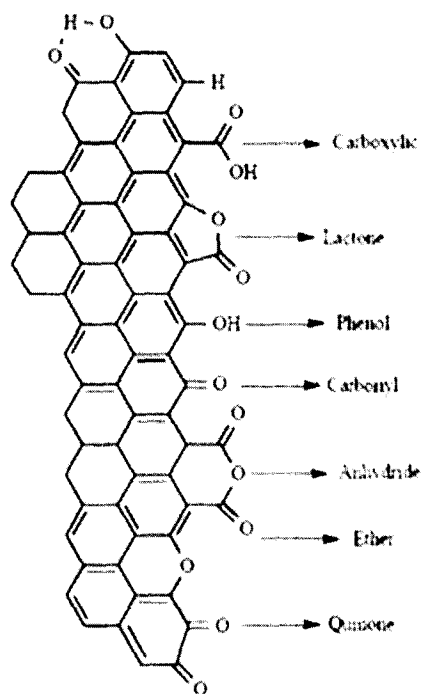


**Fig 1.2 Surface functional groups containing Oxygen [23]**

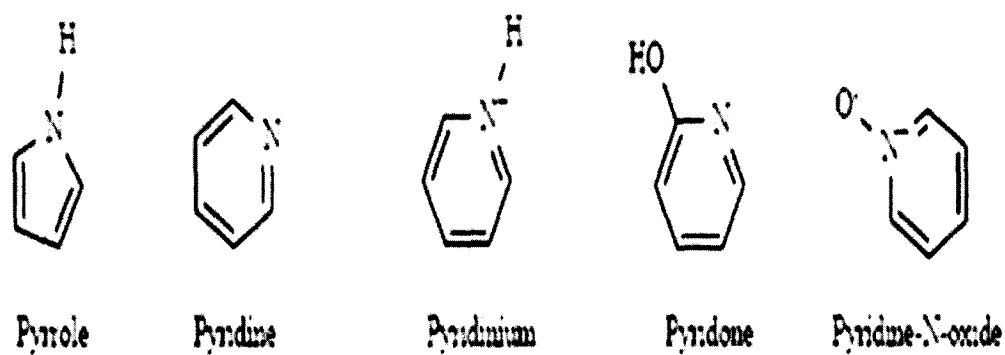


**Fig 1.3 Nitrogen containing functional groups when heated in nitrogen,  
ammonia, nitric acid**

The nature and concentration of surface functional groups might be modified by suitable thermal or chemical post-treatments. Oxidation in the gas or liquid phase could be used to increase the concentration of surface oxygen groups while heating under inert atmosphere might be used to selectively remove some of these functions. It was shown that gas phase oxidation of the carbon mainly increased the concentration of hydroxyl and carbonyl surface groups, while oxidations in the liquid phase increased especially the concentration of carboxylic acids [23]. Carboxyl, carbonyl, phenol, quinone and lactone groups on carbon surfaces were shown in Fig 1.2 [24]. While, the ammonization could introduce the basic groups, such as, C-H, C=N groups, amino, cyclic amides, nitrile groups, pyrrole-like structure [25], which were shown in Fig. 1.3 [26].

#### *1.2.6 Physical activation methods*

##### *Physical methods involve activation with air, steam or carbon dioxide*

Activation with carbon dioxide promotes external oxidation and development of larger pores compared to activation with steam. The relative amount of external and internal oxidation depends on how well developed the pores are in the carbonized material. The activation of chars with no developed pore structure only results in decrease in the carbon granule size.

- Kalback et al. [27] reacted cylinders of a very pure graphitized porous carbon with carbon dioxide at 1030°C resulting in 10-30% burnoff and measured their pore size distributions as a function of the burnoff. These workers observed that the major part of early pore development occurred by preferential burning of the single aromatic sheets, which constitute the active carbon structure, and yielded pores of approximately the same size as the

original carbon sheets. The pore development in this region reached a maximum and then ceased probably because the exposed properly oriented sheets were exhausted. This was followed by the burning away of the walls of the layer planes, resulting into the formation of larger pores.

- Marsh and Rand [28], while reacting a polyfurfuryl alcohol carbon with carbon dioxide, observed that the activation caused opening of previously inaccessible pores and widening of existing pores.
- McEnancy and Dovaston [29] prepared a series of microporous carbons from cellulose triacetate by heat treatment in the temperature range 1230-1275 K and activated them with carbon dioxide to 30% burnoff. The changes in porosity were measured by nitrogen adsorption and mercury density measurements. The activation at lower temperatures predominated in the development of mesopores and macropores. Heat treatment in the temperature range 1500-1700 K converted open porosity into closed porosity.
- Tourkow et al. (30) studied the activation of two brown coals carbonized at 900°C with water vapor, carbon dioxide, and oxygen and observed that each activation produced a different distribution of porosity. All the three activating agents at low weight loss (burnoff) produced solely micropores and their volume was the highest with oxygen activation. With water vapor activation there was an indication that the activation resulted in the development of mesoporosity to a higher extent than with either carbon dioxide or oxygen.

At higher burnoffs the differences in porosity created by the different activating agents become more pronounced. Activation with water vapor resulted in a progressive development and widening of all sized pores until at a burnoff of 70%, the activated product contained a well-developed porous system with a wide pore size distribution in which almost all pore sizes were represented. Activation between 50% and 70% burnoff, caused an increase in the total adsorption volume from 0.6 to 0.83 cm<sup>3</sup>/g. But, as this was associated mainly with widening of the pores, the surface area was not affected and for both burnoffs it was almost the same (920 m<sup>2</sup>/g).

Activation with carbon dioxide produces a more uniform porosity. The activated carbons produced by carbon dioxide activation had lower total pore volume than those of the corresponding sample obtained by activation with steam.

The activation with oxygen showed a different behaviour. A very low burnoff resulted in the development of strong microporosity, which changed very little with further burnoff, which clearly indicated that micropores were being converted into mesopores and macropores during activation by water vapor. However, no such decrease in microporosity was observed at higher burnoffs in the case of activation by carbon dioxide. Thus, in the case of activation by oxygen, the activation occurs only in the initial stages of the process. In the latter stages of activation, the micropores are blocked by the surface oxygen structures formed at their entrances causing the interior of the micropores to be inaccessible for further activation. In addition, burning of the outer parts can take place. Thus the oxygen-activated carbon at 70% burnoff has the lowest total adsorption volume

A detailed study of the activation of carbonized pure wood char with water vapor at 950°C was done following the activation as a function of weight loss (degree of gasification) [30]. It is seen that the adsorption capacity of the activated carbon for all molecules increases as the weight loss increases. Thus the most important factor in obtaining, from the same carbonized material different qualities of activated carbon is the level of burnoff, i.e., the duration of activation and the time it stays in the oven. Thus for industrial-scale production of activated carbons a compromise has to be found between the capacity of production and the quality of the material produced.

### *1.2.7 Chemical activation*

#### *1.2.7.1 Acid Treatment*

Acid treatment was generally used to oxidize the porous carbon surface; it enhanced the acidic property, removed the mineral elements and improved the hydrophilic nature of the surface. The acid used in this case should be oxidising in nature; nitric acid and sulfuric acid were the most selected.

- Liu *et al.* [31] reported that coconut-based activated carbon was modified by nitric acid and sodium hydroxide; it showed excellent adsorption performance for Cr (VI) .
- Shim *et al.* [32] also modified the pitch-based activated carbon fibers with nitric acid and sodium hydroxide. The specific surface area of the activated carbon fibers decreased after oxidation with 1M nitric acid, but the total acidity increased three times compared to the untreated activated carbon fibers, resulting in an improved ion-exchange capacity of the activated carbon fibers. The carboxyl groups of activated carbon fibers decreased, while the lactone and ketone groups increased after the sodium hydroxide treatment. The adsorption

capacity of copper and nickel ions is mainly influenced by the lactone groups on the carbon surface, pH and by the total acidic groups.

- Coal-based activated carbons were modified by chemical treatment with nitric acid and thermal treatment under nitrogen flow [33]. The treatment with nitric acid caused the introduction of a significant number of oxygenated acidic surface groups onto the carbon surface, while the heat treatment increased the basicity of carbon.
- The coconut-based activated carbon was pretreated with different concentrations of nitric acid (from 0.5 to 67%) and was selected as palladium catalyst support [34], the result showed that the amount of oxygen-containing groups and the total acidity on the activated carbons, the Pd particle size and catalytic activity of Pd/C catalysts are highly dependent upon the nitric acid concentration used in the pretreatment. The pretreatment of activated carbon with a low concentration of nitric acid could increase the structure parameters due to removal of the impurities, would be beneficial to create an appropriate density of total acidity environment, and would further improve the Pd dispersion and the catalytic activity of Pd/C catalysts.
- Peach stone shells were pretreated by  $H_3PO_4$  and pyrolysed at  $500^\circ C$  for 2 h and different carbons were prepared by changing the gas atmosphere during thermal treatment (nitrogen, carbon dioxide, steam and air) [35]. High uptake of *p*-nitrophenol appears, affected to low extent with gaseous atmosphere except steam which raises adsorption considerably. The removal of lead ions was considerably enhanced by running air during thermal treatment (two-fold increase) due to the formation of acidic oxygen functionalities.

- The activated carbon derived from a polymer source was treated with  $\text{HNO}_3/\text{H}_2\text{SO}_4$  solutions followed by heat-treatment in argon [37]. Acid-treatment increased the adsorption of methyl mercaptan compared with the original activated carbon, and the adsorbed amounts increased with ratio of  $\text{H}_2\text{SO}_4$  in  $\text{HNO}_3/\text{H}_2\text{SO}_4$  solutions. Hydrogen bonding between acidic groups formed by acid-treatment and thiol groups played a crucial role in adsorption of methyl mercaptan on activated carbon.
- Hasenberg *et al.* showed a process with a catalyst blend for selectively producing mercaptans and sulfides from alcohols [38]. Surface modification of a coal-based activated carbon was performed using thermal and chemical methods [39]. Nitric acid oxidation of the conventional sample produced samples with weakly acidic functional groups. There was a significant loss in microporosity of the oxidized samples which was caused by humic substances that were formed as a by-product during the oxidation process.
- Calvo *et al.* reported that the surface chemistry of commercial activated carbon was one of the factors determining the metallic dispersion and the resistance to sintering, being relevant to the role of surface oxygen groups [41]. The surface oxygen groups were considered to act as anchoring sites that interacted with metallic precursors and metals increasing the dispersion, with CO-evolving complexes significantly implied in this effect. On the other hand, CO<sub>2</sub>-evolving complexes, mainly carboxylic groups, seemed to decrease the hydrophobicity of the support improving the accessibility of the metal precursor during the impregnation step. The treatment of activated carbons with nitric acid led to a higher content in oxygen surface groups, whereas the porous structure was only

slightly modified. As result of oxidation, the dispersion of Pd on the surface of activated carbon was improved.

- Santiago *et al.* compared several activated carbons for the catalytic wet air oxidation of phenol solutions [42]. Two commercial activated carbons were modified by HNO<sub>3</sub>, (NH<sub>4</sub>)<sub>2</sub>S<sub>2</sub>O<sub>8</sub>, or H<sub>2</sub>O<sub>2</sub> and by demineralisation with HCl. The treatments increased the acidic sites, mostly creating lactones and carboxyl, though some phenolic and carbonyl groups were also generated. Characterisation of the used activated carbon evidenced that chemisorbed phenolic polymers formed through oxidative coupling and oxygen radicals played a major role in the catalytic wet air oxidation over activated carbon.
- Also, citric acid was used to modify a commercially available activated carbon to improve copper ion adsorption from aqueous solutions [43]. It was found that the surface modification by citric acid reduced the specific surface area by 34% and point of zero charge (pH) of the carbon by 0.5 units. But the modification did not change both external diffusion and intra particle diffusion.

#### *1.2.7.2 Other Modification Methods*

It was well known, that nitrogen-containing surface groups, gave to activated carbons increased ability to adsorb acidic gases [44]. Practically, nitrogen was introduced into structure of activated carbon according to several procedures including treatment with ammonia or preparation of the adsorbent from nitrogen-containing polymers (Acrylic textile, polyaryamide or Nomex aramid fibers) [45-47]. Heating of phenol-formaldehyde-based activated carbon fiber in the atmosphere of dry ammonia at several temperatures ranged from 500°C to 800°C resulted in a formation of new

nitrogen-containing groups in the structure of the fiber including C-N and C=N groups, cyclic amides, nitrile groups (C -N) [48], and pyrrole-like surface structures with N-H groups [49]. As is reported, extensive heat treatment with gaseous ammonia might cause changes in the relative amounts of macropore, mesopore and micropores of commercial activated carbon [42].

The commercial activated carbons were treated by gaseous NH<sub>3</sub> ranging from 400°C to 800°C for 2 h [50]. The C-H and C-N groups appeared after NH<sub>3</sub> treatment. A series of activated carbon fibers were produced by treatment with ammonia to yield a basic surface [49]. Commercial activated carbon and activated carbon fiber were modified by high temperature helium or ammonia treatment, or iron impregnation followed by high temperature ammonia treatment [51]. Iron-impregnated and ammonia-treated activated carbons showed significantly higher dissolved organic matter uptakes than the virgin activated carbon. A commercial raw granular activated carbon was modified by polyaniline to improve arsenate adsorption [52].

Ozone as a strong oxidizing agent was widely applied in organic degradation; it could also oxidize the carbon material surface to introduce oxygen-containing groups. The ozone dose and oxidation time affected the oxygen containing groups and the oxygen concentration on the carbon surface. The result of bituminous origin-based activated carbon oxidised with ozone showed that the higher the ozone dose, the higher was the oxidation of the carbon and the greater was the number of acid groups present on the carbon surface, especially carboxylic groups, whereas the pH of the point of zero charge decreased [55].

The surface area, micropore volume, and methylene blue adsorption all reduced with higher doses. These results were explained by the ozone attack on the carbon and the fixation of oxygen groups on its surface. Jackson introduced a method for supercritical ozone treatment of a substrate [56].

The impact of ozonation on textural and chemical surface characteristics of two coal-based activated carbons and their ability to adsorb phenol, *p*-nitrophenol, and *p*-chlorophenol from aqueous solutions had been investigated by Alvarez *et al.* [57]. The porous structure of the ozone-treated carbons remained practically unchanged with regard to the virgin activated carbon. At 25°C primarily carboxylic acids were formed while a more homogeneous distribution of carboxylic, lactonic, hydroxyl, and carbonyl groups was obtained at 100°C.

Lin *et al.* provided a method for deposition of polyaniline onto microporous activated carbon fibres that could enhance the capacitance of the carbon which could then be used as electrodes for electrochemical capacitors [54].

When the commercial activated carbon was loaded with sodium and potassium, it could efficiently remove NO and SO<sub>2</sub> from waste gases by adsorption [58]. Activated carbon from coconut shell was modified by sodium acetate; its adsorption for copper ion could be increased 2.2 times, after it was regenerated with NaOH, the adsorption

capacity increased 3 times [59]. Pitch-based ordered carbon could be fluorinated at room temperature or moderately elevated temperature, which has great potential for applications in electrochemistry or batteries [60]. When the rayon activated carbon fiber was modified by chlorine or bromine, its surface hydrophilic property was increased and the adsorption capacity for dimethyl sulfide was increased [61]. Rayon activated carbon fiber prepared by nitrocellulose combustion, showed excellent adsorption for amines and carbon disulfide [62]. Tannic acid was employed in the modification of the surface properties of granulated commercial activated carbon [63]. Tannic acid was found effective to enhance the metal adsorption capacity of activated carbon surfaces. The surface of activated carbon was modified with KOH, its adsorption and desorption behaviors for NO<sub>x</sub> and the accompanied surface reaction mechanism as well as the distribution of molecular ions on the surface were illustrated [64].

#### *1.2.8 Heat Treatment Methods*

Thermal treatments had been used to produce activated carbons with basic character and such carbons were effective in the treatment of some organic hydrocarbons [65]. Heat treatment of carbons under inert atmospheres (nitrogen or argon) could increase carbon hydrophobicity by removing hydrophilic surface functionalities, particularly various acidic groups [66-69]. It has also been shown that H<sub>2</sub> could be more effective than inert atmospheres because it could also effectively stabilize the carbon surface by deactivation of active sites (i.e., forming stable C-H bonds and/or gasification of unstable and reactive carbon atoms) found at the edges of the crystallites. H<sub>2</sub> treatment at 900°C could produce highly stable and basic carbons [64-67]. The presence of a platinum catalyst could considerably lower the treatment temperature

used [68]. The wood, coal-based activated carbons and a commercial activated carbon fiber with different physicochemical characteristics were subjected to heat treatment at 900°C under vacuum or hydrogen flow [70]. Different precursors resulted in various elemental compositions and imposed diverse influence upon surface functionalities after heat treatment. The surface of heat treated activated carbon fibers became more graphitic and hydrophobic. Polyacrylonitrile and rayon-based activated carbon fibers were subjected to heat treatments to obtain porous carbons [71].

Thermal treatment of polyacrylonitrile activated carbon fibers had been carried out using a microwave device [72-73] Microwave treatment affected the porosity of the activated carbon fibers, causing a reduction in micropore volume and micropore size. Moreover, the microwave treatment was a very effective method for modifying the surface chemistry of the activated carbon fibers with the production of pyrone groups. As a result very basic carbons, with points of zero charge approximately equal to 11, were obtained. Microwave heating offered apparent advantages for activated carbon regeneration, including rapid and precise temperature control, small space requirements and greater efficiency in intermittent use [74]. Quan *et al.* investigated the adsorption property of acid orange 7 by microwave regeneration of coconut-based activated carbons [75].

The plasma treatment was regarded as a promising technique to modify the surface chemical property of porous carbon since it produced chemically active species affecting the adsorbability. It was possible to create any ambience for oxidative, reductive, or inactive reaction by changing the plasma gas [76]. Plasma could

introduce basic and acidic functional groups that were determined by the gaseous resource [77]. Some experimental efforts had been reported on activated carbon treatment with oxygen-included plasmas. The negative charge of activated carbon was brought after the plasma treatment was due to dissociation of newly formed acidic groups. The hydrophilicity of plasma-treated carbons did not change significantly. The oxygen plasma appeared not to reach the smallest micropores of the carbon, indicating that the reaction took place only near the external surfaces of the particles [78, 79]. The surface area of activated carbon that was treated by oxygen non-thermal plasma was decreased, and the concentrations of acidic functional groups at the surface were increased and the saturated adsorption amount of copper and zinc ions was considerably increased [81-84]. Oxygen species produced during the discharge react on the activated carbon surface resulting in the creation of weakly acidic functional groups that played an important role in adsorbing metal cations. Improvement in the adsorbability was attributed to the change in the surface chemical structure of the commercial activated carbon rather than the modification of the surface physical structure [85]. Several works are reported on plasma treatment [86-95].

### *1.2.9 Porosity*

The degree of burn off in a carbon determines whether the carbon will be micro porous, meso porous or macro porous. Carbons are classified as micro porous when the diameter of the pore is less than 2 micron, between 2 and 50 microns as meso porous and above 50 microns as macro porous. In case the burn off is less than 50%, then micro porosity is produced. If the burn off is more than 75%, macro porosity is produced. Between 50 to 75% mixed pores are produced [96].

The carbons may be in powdered, granular or in the form of fibers. They may be shaped suitably into pellets, spherical, cylindrical or other forms as per need. The pores contribute to the surface area. It is mostly the microporous carbon below 2 nm that contribute to the surface area. Macroporous carbons with pore size above 50 nm do not contribute to the surface area, but act as conduits to reach micro and mesopores where adsorption takes place.

Carbons having surface area as high as 4000 m<sup>2</sup>/g have been made. However, the most often used carbons, have surface areas in the range of 800m<sup>2</sup>/g to 1500m<sup>2</sup>/g for commercial applications [97].

The pore size distribution and density of the carbon depends on the type of raw material used as well as the method of preparation employed.

#### *1.2.10 Characterisation of physical properties*

The characterisation of activated carbons is carried out on the basis of several physical and chemical properties, commonly including their surface area, pore size distribution, impact hardness, ability to absorb several selected substances such as benzene, carbon tetrachloride, nitrogen from the gaseous phase as well as iodine, molasses, phenol, and methylene blue from the aqueous phase. The nitrogen BET value, for example, expresses the surface that can be covered by nitrogen in a monomolecular layer. Typical nitrogen BET surface area values are found to be

between 400 and 1500 m<sup>2</sup>/g, the former representing low-activity carbons and the latter, high activity carbons. However, surface area measurements alone are not sufficient to characterize a carbon product since the nitrogen molecule is very small and can penetrate into pores which are not available for larger molecules. The accessibility of larger molecules that are involved in the actual use of activated carbons may be small compared to adsorption of nitrogen. Furthermore, the adsorption of nitrogen being carried out at very low temperature (-195°C), the nitrogen adsorption cannot measure some of the extremely ultrafine microcapillary pores. Thus the BET surface area should be used with caution [97].

Thermogravimetric analysis gives the decomposition temperatures. Weight loss as a function of time helps to deduce the amount of water and other components lost. Data on endothermic and exothermic reactions can be obtained from DSC. Van Driel carried out thermogravimetric analysis of activated carbon and analysed the gases evolved using a gas chromatograph. The adsorption products were mainly CO<sub>2</sub> and CO. The desorption spectra of CO<sub>2</sub> showed two maxima and that of CO also showed two. These results were attributed to the existence of different structures with varying stability [98].

XRD data enables to ascertain a substance through its characteristic 2 theta peaks.

The Scanning Electron Microscope provided images of high magnification to enable the researcher observe surface characteristics. Pore size measurements, particle size and surface morphology data can be obtained [99].

EPR analysis helps in knowing whether the element is paramagnetic [100].

### *1.2.11 Characterisation of Chemical property*

The acidic or basic character of the carbon is developed as a result of surface oxidation.

Acidic carbons are defined as those carbons that show acidic behavior and adsorb appreciable amounts of bases but very little acids. They are generally obtained when in inert atmosphere are exposed to oxygen between 200 and 700°C. The optimum temperature for the development of the maximum capacity to adsorb bases has been found to be around 400°C.

Various attempts have been made to identify and estimate the surface oxygen using several techniques such as neutralization of basic groups, desorption of oxide layer, potentiometric, thermometric and radiometric titrations, direct analysis of oxide layer by specific chemical reactions, polarography, IR spectroscopy and X Ray photoelectron spectroscopy. As a result of these investigations, the existence of carboxyls, phenols, lactones, aldehydes, ketones, quinones, hydroquinones, anhydrides and ethereal structures have been postulated. However, these results have not yielded comparable results and the entire amount of combined oxygen is not accounted for [101].

Titration with alkalis is one of the oldest methods of determining the acidic surface groups of carbons. However, the standard conditions under which comparable results can be obtained have been realized lately. It is now recognized that the base neutralization capacity of a carbon should be measured after it is degassed at about 150 °C so as to free it from adsorbed gases. The alkali solution should be sufficiently strong 0.1-0.2 N and the contact period long enough 24-72 hrs to obtain reproducible

neutralization values. The contact time can be reduced if the carbon and alkali is heated under reflux.

Various studies have been carried out to measure total acidity as well as to determine the acidic groups responsible for the acidity.

Bohem [102] differentiated various groups present on the carbon by selective neutralization techniques using bases of different strength. In this method carbon sample was agitated for 6 hours with 0.05N solutions of  $\text{NaHCO}_3$ ,  $\text{Na}_2\text{CO}_3$ ,  $\text{NaOH}$  and  $\text{C}_2\text{H}_5\text{ONa}$  (sodium ethoxide). The neutralization capacity of these 4 bases for most of the carbons was in the simple ratio of 1:2:3:4 which according to Bohem is not by chance but implies that four different groups of characteristic acidities occurred side by side on the carbon surface in equivalent amounts. This ratio was observed when the carbons were completely oxidized in an oxygen stream at 420-450°C after 5 hours when burn off was 25-50%. Another important factor was the slow cooling of the sample in oxygen.

The strongly acidic groups neutralized by  $\text{NaHCO}_3$  were postulated as  $\text{COOH}$  groups whereas those neutralized by  $\text{Na}_2\text{CO}_3$  were but not by  $\text{NaHCO}_3$  were lactones. The weakly acidic groups neutralized by  $\text{NaOH}$  but not by  $\text{Na}_2\text{CO}_3$  were postulated as phenols. The groups reacting with  $\text{C}_2\text{H}_5\text{ONa}$  but not with  $\text{NaOH}$  were suggested to be carbonyls.

However, Puri [103] questioned the validity of Boehm's postulates stating that the same acid group will neutralize different amounts of alkalis of varying strength. According to him titration with barium hydroxide alone can measure the total acidity. These methods have not been able to account for the entire combined oxygen.

Graphic representation of the data shows that different carbons are associated with different amounts of oxygen, the amount depending on source material and history of formation. Trembly [104] carried out linear programmed thermal desorption analysis to measure the energies of carbon-oxygen surface compounds. The desorption energies of these surface groups were a function of their coverage, indicating that the surface complex consisted of several types of functional groups which decomposed in different temperature range. Various studies have shown that the products of decomposition are carbon dioxide, carbon monoxide and water vapour. The total oxygen content thus obtained agreed fairly with the total of the oxygen obtained by ultimate analysis. Hence, thermal desorption methods are fairly accurate.

IR spectroscopy can provide the basic information of the surface functional groups and can provide basic spectra of the activated carbon for comparison with spectra of the same carbon containing adsorbed species. Spectral studies also provide information about the molecular forces involved in the adsorption process [105].

Carbons being black adsorb most of the radiation in the visible region but it can transmit radiation in the IR region, when examined using extremely thin sections. Activated carbons being hard are difficult to grind. Friedaël and Hofer [106] devised a technique by

which activated carbon and chars could be converted into finely ground state for making halide pellets for IR studies. The spectra showed definite bands at 1735, 1590 and 1215  $\text{cm}^{-1}$  which were attributed to carbonyl, aromatic structures or conjugated chelated carbonyl and C-O structures respectively. Several workers have done IR studies. Studebaker and Rnehart examined carbon black using KBr pellets. They used integrated intensities rather than absorbance at characteristic wavelengths, as the band position and shapes changed due to environmental effects.

### 1.2.12 Applications

Activated carbons have been extensively used as adsorbent for dye, for electrochemical applications such as capacitors and electrode materials which are discussed in the relevant chapters. It acts as a catalyst as well as a support for catalyst as is indicated by the Table 1.3 [107].

<b>Impregnation</b>	
<b>Chemicals</b>	<b>Examples for application</b>
Sulfuric acid	Ammonia, amine, mercury
Phosphoric acid	Ammonia, amine
Potassium Carbonate	Acid gases (HCL, HF, SO <sub>2</sub> , H <sub>2</sub> S, mercaptan,
Iron Oxide	H <sub>2</sub> S, mercaptan,
Potassium iodide	H <sub>2</sub> S, PH <sub>3</sub> , Hg, AsH <sub>3</sub> , Radioactive Gases/radioactive methyl iodide
Triethylene Diamine (TEDA)	Radioactive Gases/radioactive methyl iodide
Sulfur	Mercury

Potassium Permanganate	H <sub>2</sub> S from oxygen-lacking gases
Manganese IV Oxide	Aldehyde
Silver	Phosphine, arsine, domestic drinking water Filters (oligo dynamic effect)
Zinc oxide	Hydrogen cyanide
Chromium Copper-silver Salts	Civil and military gas protection Phosgene, chlorine, arsine Chloropicrin, sarin and other nerve gases
Mercury II Chloride	Vinyl chloride synthesis Vinyl fluoride synthesis
Zinc acetate	Vinyl acetate synthesis
Noble metals (palladium, platinum)	Organic synthesis, Hydrogenation.

***Table 1.3 List of the impregnating chemical and the application of the impregnated carbon [92]***

## REFERENCES

1. Bansal R. C, Donnet J. B, Stoecki F, Active Carbon, Marcel Decker Inc New York, 1988.
2. AEQM Plan for mining belt in Goa TERI Report no 93/EE/63, 1997.
3. Smisek M, Cerny S, Active Carbon, Elsevier, Amsterdam, 1970.
4. Johnson B, Sinha R. K, Urbanic J. E, U. S Patent 4,014,817, Mar. 29, 1977.
5. Murthy H. N, U. S Patent 4,032, 476, June 28, 1977.
6. Yokogawa A, Mitooka M and Shima K, U. S Patent 3,940, 344, Feb.24, 1976.
7. Devong G. J, U. S Patent 3, 886, 088, May 27, 1975.
8. Watanable Y and Miyajina T, U. S Patent 4,002,587, June 11, 1977.
9. Katori K, Nagai H and Shuki Z, U. S Patent 4,045,368, Aug.30, 1977.
10. Nagai H, Katori K, Shuki Z and Amagi Y, U. S Patent 3,909,449, Sept. 30, 1975.
11. Kobayashi K, Wateri S, Kato T, Shiraishi M and Kawana Y, U. S Patent 3,891,574, June 24, 1975.
12. Voet A and Lamond , U. S Patent 3,533,961, Oct. 31, 1970
13. Sterp K, Wirth H, Rottinger G and Hohmann V, U. S Patent 4,075,282, Feb. 21, 1978.
14. Piccione S, Urbanic J. E, U. S Patent 3, 294,572, Dec. 27, 1966.
15. Zall D. M, U. S Patent 3,876, 451, Apr. 8, 1975.

16. Dolian F. E and Hormats S, U. S Patent 2,963, 441, Dec. 6, 1960.
17. Urbanic J. E. and Sutt R. F, U. S Patent 3,778, 387, Dec. 11, 1973.
18. Dietz. V. R and Blachly C. H, U.S Patent 4, 040, 802, Aug. 9, 1977.
19. Fennimore J, Ruder G and Simmonite D, U.S Patent 4,076,892, Feb. 28, 1978.
20. Carron J. Private Communication,1985
21. Mackey D. M and Roberts P.V, Carbon, 20 (1982) 95-99
22. Dubinin M. M and Zaverina E. D, Dekl. Akad. Nauk. SSSR, 65 (1949) 295-301
23. Figueiredo J. L, Pereira M. F. R, Freitas M. M. A, Orfao J. J.M, Carbon, 37 (1999) 1379-1389
24. Yang RT. Adsorption, John Wiley & Sons Inc., Hoboken, New Jersey 2003
25. Abe M, Kawashima K, Kozawa K, Sakai H, Kaneko K. Langmuir, 16 (2000) 5059 -5063
26. Fels J. R, Kapteijn F, Moulijn JA, Zhu Q, Thomas KM. Carbon, 33 (1995) 1641-1653
27. Kalback W. M, Brown L. F and Wert R.E, Carbon, 8 (1970) 117-123
28. Marsh H and Rand B, Carbon, 9 (1971) 47-52.
29. McEnancy B and Dovaston N, Carbon, 13 (1975) 515-521
30. Tourkow K, Siemieniowska T, Czeckowski F and Gankowska , Fuel, 56 (1977) 121-127
31. Liu SX, Chen X, Chen XY, Liu ZF, Wang H. L, J Hazard Mater, 141 (2007) 315-319.
32. Shim J.W, Park S. J, Ryu S. K, Carbon, 39 (2001) 1635-1642.

33. Wibowo N, Setyadhi L, Wibowo D, Setiawan J, Ismadji S, *J Hazard Mater*, 146 (2007) 237-242.
34. Li J.Y, Ma L, Li X. N, Lu C.S, Liu H.Z, *Ind Eng Chem Res*, 44 (2005) 5478-5482.
35. Badie S. G, Amina A.A, Nady A. F, *J of Chem*, 67, (1996) 243-254
36. Li Li, Li W, US 20077205248 (2007).
37. Tamai H, Nagoya T, Shiono. *J Colloid Interf Sci*, 300 (2006) 814-817.
38. Hasenberg, D.M., Refvik, M.D.: WO 07070496 (2007).
39. Chingombe , Saha B, Wakeman R. J, *Carbon*,43 ( 2005) 3132-3143.
40. Vinke P, Eijk der van M, Verbree M, Voskamp AF, Bekkum H, *Carbon*, 32 (1994) 675-686.
41. Luisa C, Miguel AG, Jose AC, Angel FM, Juan JR. *Ind Eng Chem Res*, 44 (2005) 6661-6667.
42. Marta S, Frank S, Agust F, Azael F, Josep F, *Carbon*,43 ( 2005) 2134-2145.
43. Chen J. P, Wu S, Chong K. H, *Carbon*, 41 (2003) 1979-1986.
44. Li K. X, Ling L. C, Lu C. X, *et al.* *Carbon*, 39 (2001) 1803-1808.
45. Carrott P. J. M, Nabais J. M.V, Ribeiro-Carrott M. M. L, Pajares J. A, *Carbon*, 39 (2001) 1543-1555.
46. Stoeckli F, Centeno T. A, Fuertes A. B, Muniz J, *Carbon*, 34 ( 1996) 1201-1206.
47. Blanco Lopez M. C, Martínez-Alonso A, Tascon J. M. D, *Micropor Mesopor Mater*, 34 (2000) 171-179.
48. Mangun C. L, Benak K. R, Economy J, Foster K. L, *Carbon*, 39 (2001) 1809-1820.
49. Strelko V, Kuts V. S, Thrower P. A, *Carbon*, 38 (2000) 1499-1524.

50. Przepiorski J, *J Hazard Mater* 135 (2006) 453-456.
51. Cheng W, Dastghei S. A, Karanfil T, *Water Res* 39 (2005) 2281-2290.
52. Yang L, Wu S. N, Chen J. P, *Ind Eng Chem Res*, 46 (2007) 2133-2140.
53. Surface Chemical Modification of Porous Carbon Recent Patents on Chemical Engineering, 2008, Vol. 1, No. 131
54. Lin Y. R, Teng H. S, *Carbon*, 41 (2003) 2865-2871.
55. Valdes H, Sanchez-Polo M, Rivera-Utrilla J, Zaror C. A, *Langmuir*, 18 (2002) 2111-2116.
56. Jackson D. P, US 20077219677 (2007)
57. Alvarez P. M, García-Araya J. F, Beltrán F. J, Masa F. J, Medina F, *J Colloid Interf Sci* , 283 (2005) 503-512
58. Zhu J. L, Wang Y. H, Zhang J. C, Ma R. Y, *Energy Convers Manage*, 46 (2005) 2173-2184.
59. Mugisidi D, Ranaldo A, Soedarsono J. W, Hikam M, *Carbon* 45 (2007) 1081-1084.
60. Li Z. J, Del Cul G. D, Yan W. F, Liang C. D, Dai S. J, *Am Chem Soc* 126 (2004) 12782-12783.
61. Economy J, Foster K, Jung H, *Chemtech*, (1992) 597-603.
62. Shen W. Z, Wang H, Liu Y. H, Guo Q. J, Zhang Y. L. A, *Physicochemi Eng Aspects* 308 (2007) 20-24.
63. Ucer A, Uyan K. A, Cay S, Ozkan Y, *Sep Purif Technol* 44 (2005) 11-17.
64. Lee Y. W, Park J. W, Jun S. J, Choi D. K, Yie J. E, *Carbon* 42 (2004) 59-69.
65. Radovic L. R, Silva I. F, Ume J. I, Menendez J. A, Leony Leon C. A, Scaroni A. W, *Carbon* 35 (1997) 1339-1348.
66. Menendez J. A, Phillips J, Xia B, Radovic L. R, *Langmuir*, (1996) 14404-4410.

67. Menendez J. A, Illan-Gomez M. J, Leony Leon C. A, Radovic L. R, Carbon 33 (1995) 1655-1657.
68. Menendez J. A, Radovic L. R, Xia B, Phillips J, J Phys Chem,100 (1996) 17243-17248.
69. Shin S, Jang J, Yoon S. H, Mochida I, Carbon, 35 (1997) 1739-1743.
70. Seyed A. D, Karanfil T, J Colloid Interf Sci, 274 (2004) 1-8.
71. Chiang Y. C, Lee C. Y, Lee H. C, Mater Chem Phys, 101 (2007) 199-210.
72. Haque K. E, Int J Miner Process, 57 (1999) 1-24.
73. Nabais M. V, Carrott P. J. M, Carrott M. M. L. R, Menendez J. A, Carbon, 42 (2004) 1315-1320.
74. Van W. E. J, Bradshaw S. M, Swardt J. B .D, J Microwave Power Electromagn Energ, 33 (1998) 151-157.
75. Quan X, Liu X. T, Bo L. L, Chen S, Zhao Y. Z, Cui X. Y, Water Res, 38 (2004) 4484-4490.
76. Park S. J, Kim J, J Colloid Interf Sci, 244 (2001) 336-341.
77. Kodama S, Sekiguchi H, in: D'Agostino, Wertheimer, Favia, Oehr (Eds.), Willey-VCH, Weinheim (2005) 131.
78. Garcia A. B, Martinez-Alonso A, Leon C. A. L, Tascon J. M. D. Fuel, 77 (1998) 613-624.
79. Boudou J. P, Martinez-Alonzo A, Tascon J. M. D, Carbon, 38 (2000) 1021-1029.
80. Kodama S, Habaki H, Sekiguchi H, Kawasaki J. Thin Solid Films. 407 (2002) 151-155.
81. Domingo-Garcia M, Lopez-Garzon F. J, Perez-Mendoza M, J Colloid Interf Sci, 222 (2000) 233-240.

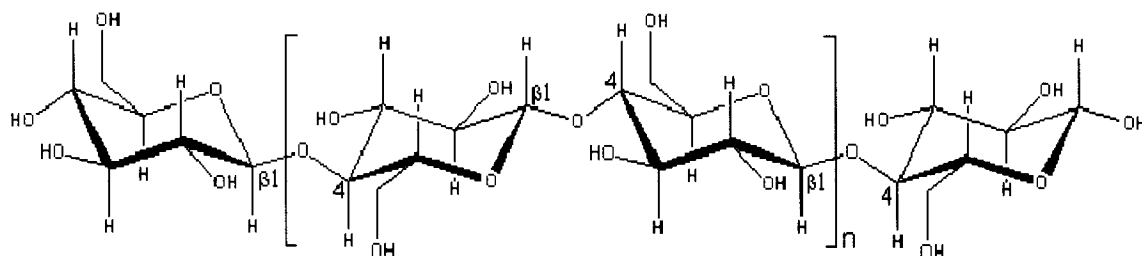
82. Wen H.C, Yang K, Ou KL, Wu WF, Chou CP, Luo RC, Chang, *Applied Surface Sc*, 253 (2007) 9248-9253
83. Wen H.C, Yang K, Ou KL, Wu WF, Chou CP, Luo RC, Chang, *Surf Coat Technol*, 200 (2006) 3166-3169.
84. Boudou J. P, Paredes J. I, Cuesta A, Martínez-Alonso A, Tascón J. M. D, *Carbon*, 41 (2003) 41-56.
85. Lee D. S, Hong S. H, Paek K. H, Ju W. T, *Surf Coat Technol* , 200 (2005) 2277-2282.
86. Pai Y. H, Ke J. H, Huang H. F, Lee C. M, Zen J. M, Shieu F. S. *J Power Sources*, 161 (2006) 275-281.
87. Eisenmenger-Sittner C, Schrank C, Neubauer E, Eiper E, Keckes J, *Appl Surf Sci* 252 (2006) 5343-5346.
88. Paredes J. I, Martinez-Alonso A, Tascon J. M. D, *Carbon*, 40 (2002) 1101-1108.
89. Brüser V, Heintze M, Brandl W, Marginean G, Bubert H, *Diamond Relat Mater*, 13 (2004) 1177-1181.
90. C Liu, Lu D. N, *Plasma Chem Plasma Process* 26 (2006) 119-126.
91. Zhu Q, Sun J, He C, Zhang J, Wang Q. *Macromol Sci Part A Pure Appl Chem*, 43 (2006) 431853-1865.
92. Miller J.R., Zhang, T.: WO 07040603 (2007)
93. Huang H. C, Ye D. Q, Huang B. C, *Surf Coat Technol*, 201 (2007) 9533-9540.
94. Tashima D, Kurosawatsu K, Sung Y. M, Otsubo M, Honda C, *Mater Chem Phys* 2007 ( 103: 158-161.
95. Tendero C, Tixier C, Tristant P, Desmaison J, Leprince P.A *Review Spectrochimica Acta Part B* 61 (2006) 2-30.

*CHAPTER II*

**EXPERIMENTAL**

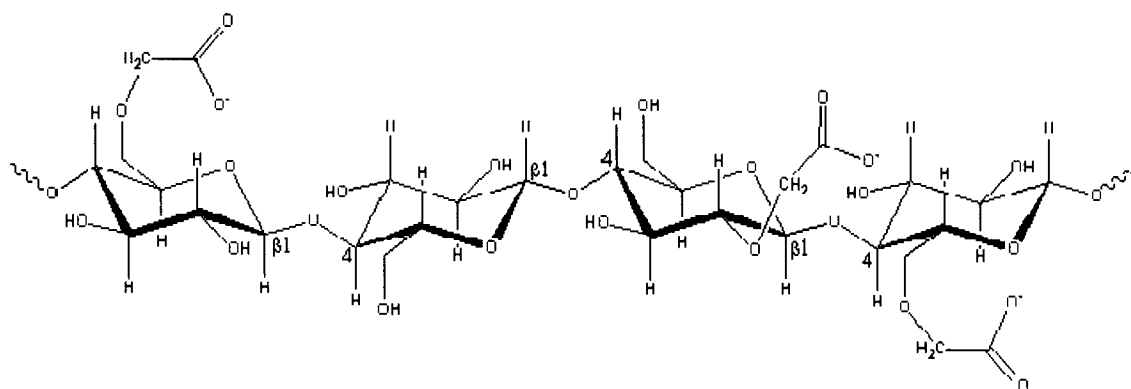
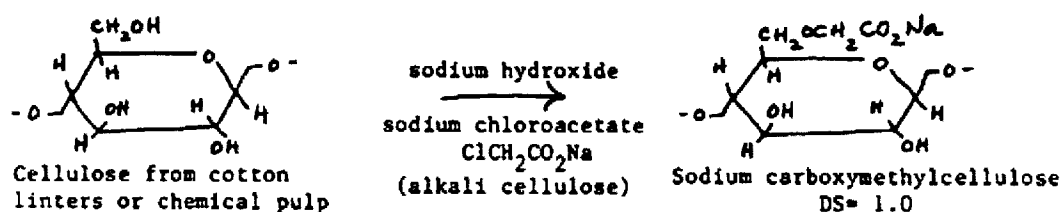
## 2.1 INTRODUCTION

Cellulose and its derivatives have since long been a renewable source of activated carbons.



*Structure of cellulose*

Sodium carboxyl methyl cellulose are cellulose ethers made from alkali cellulose which has been chemically altered so that a substitution of either  $-\text{CH}_3$  or  $-\text{CH}_2\text{COONa}$  is made for the proton (H) in the  $-\text{OH}$  hydroxyl groups on the glucose unit of the cellulose polymer.



*Structure of carboxyl methyl cellulose*

The molecular formula is  $\text{C}_8\text{H}_{16}\text{O}_8$  and molecular weight is 240.20[g/mol].

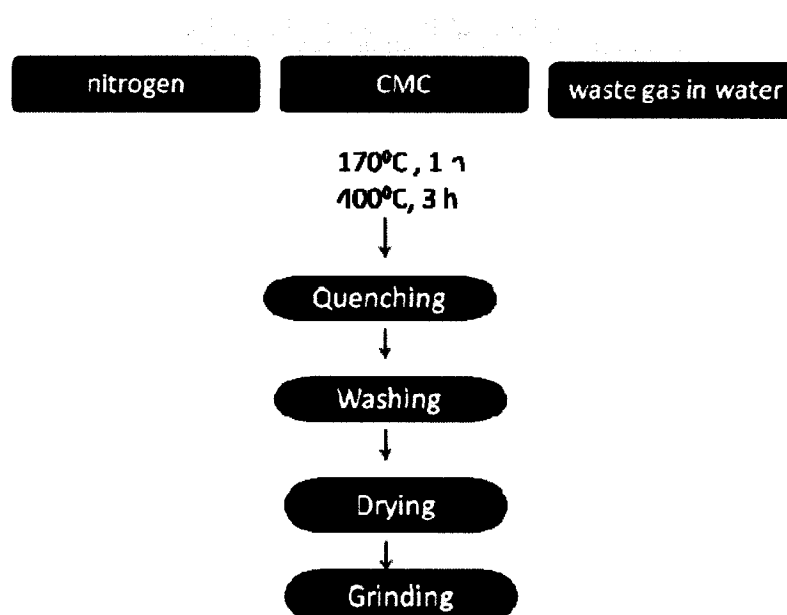
CMC molecules are most extended (rod-like) at low concentrations but at higher concentrations the molecules overlap and coil up and then, at high concentrations, entangle to become a thermoreversible gel. Increasing ionic strength and reducing pH both decrease the viscosity as they cause the polymer to become more coiled. At low pH, CMC may form cross-links through lactonization between carboxylic acid and free hydroxyl groups

They are used in products such as toothpaste, laxatives, or diet pills. Other products include ice cream, water-based paints, detergents and a variety of paper products to name but a few. Characteristics which make them useful are: high viscosity in low concentrations, defoaming abilities, surfactant, and bulking abilities. It has been used as a binder in the making of activated carbons [2].

*The objective of this study is to develop a simple method to prepare high surface area activated carbons from renewable sources such as cellulose and its derivative by low temperature physical methods.*

## 2.2 PREPARATION OF CARBON FROM SODIUM SALT OF CARBOXYL METHYL CELLULOSE (CMC)

The free flowing precursor was put in a glass column placed in a furnace having arrangement for gas flow. Sodium salt of carboxyl methylcellulose was first dehydrated at 170°C. The precursor was heated for three hours at 400°C, in an atmosphere of nitrogen. The rate of heating was 10°C per minute. The red hot carbonised material was then quenched in double distilled water maintained for 30 minutes. The carbon obtained was washed, dried and ground in a planetary ball mill grinder and labelled as CMC N



*Scheme 2.1 Synthesis of activated carbon from carboxyl methyl cellulose.*

This method for preparing activated carbons with high surface area was developed after systematically studying various parameters in the following manner.

### *2.2.1 Preparation of carbons using CMC, Cellulose, Starch and Sucrose precursors*

The precursor was taken in a horizontal furnace where there was provision for gas flow and heated in nitrogen at 400<sup>0</sup> C, in an atmosphere of nitrogen. The rate of heating was 10<sup>0</sup> C per minute. The carbon obtained was washed, dried, ground in a planetary ball mill grinder.

### *2.2.2 Ascertaining Porosity*

*SEM images of all the carbons were taken*

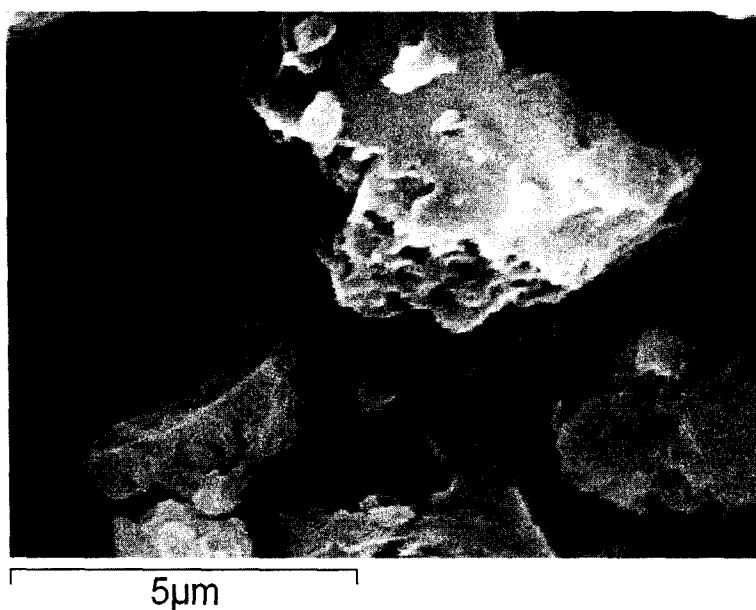


*Fig 2.1 SEM images of carbons obtained after heating CMC at 400<sup>0</sup>C in nitrogen for 3hrs.*



*Fig 2.2 SEM images of carbons obtained after heating cellulose at 400<sup>o</sup>C in nitrogen for 3hrs.*

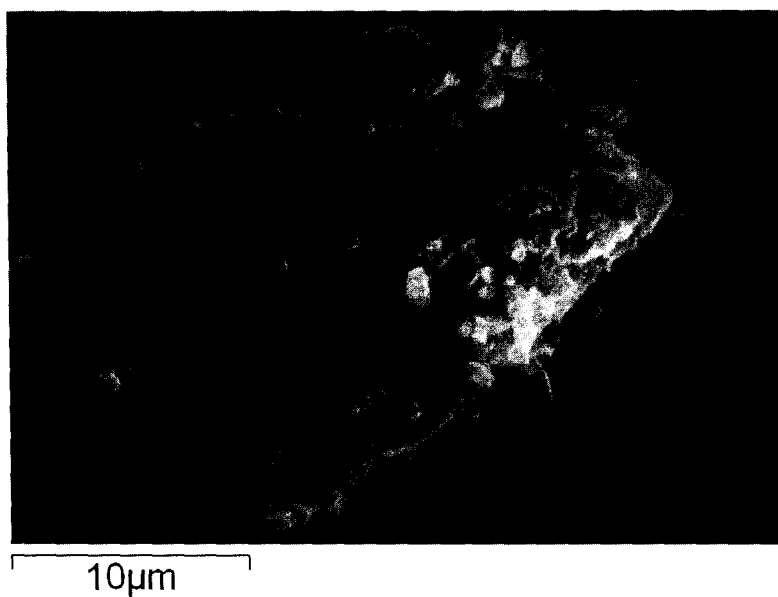


*Fig 2.3 SEM images of carbons obtained after heating starch at 400<sup>o</sup>C in nitrogen for 3hrs.*

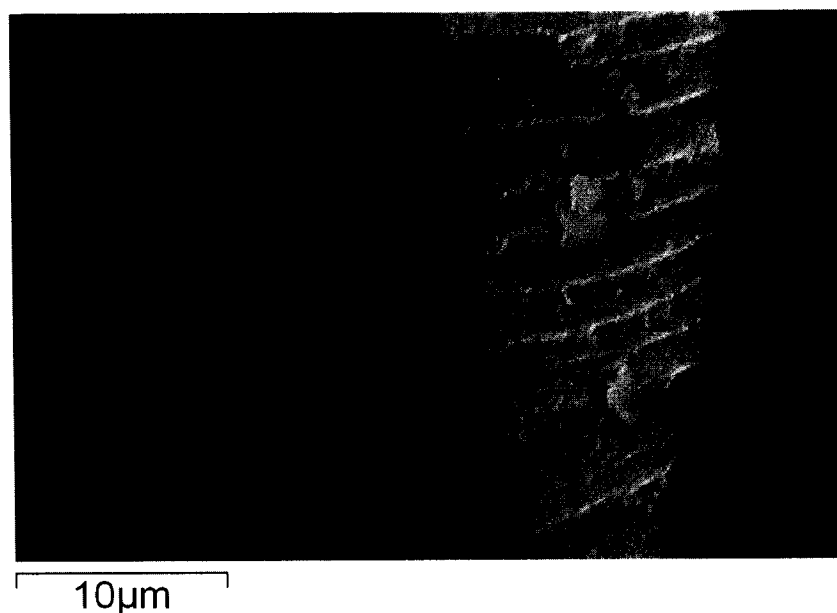


*Fig 2.4 SEM images of carbons obtained after heating sucrose at 400<sup>o</sup>C in nitrogen for 3hrs.*

Carbon prepared from CMC showed sheets and pores, whereas carbon from cellulose did not show any as observed in the SEM images at magnification 10,000. Carbon from starch showed sheets whereas etching was observed on carbon prepared from sucrose at 2,500 magnification.

### *2.2.3 Surface area*

The BET surface area measurements showed that the carbons had poor surface area in case of CMC and Cellulose carbon, whereas, carbon from starch and sucrose showed surface area less than 2 m<sup>2</sup>/ g.

Carbon from different precursors	BET surface area m <sup>2</sup> /g
CMC	3
Cellulose	2
Starch	-
Sucrose	-

*Table 2.1 BET surface area of carbons prepared from CMC, Cellulose, Starch and Sucrose when heated for 3 hrs in nitrogen at 400 °C.*

*2.2.4 Identification of surface functional groups by IR*

*IR of carbons prepared from different precursors were studied*

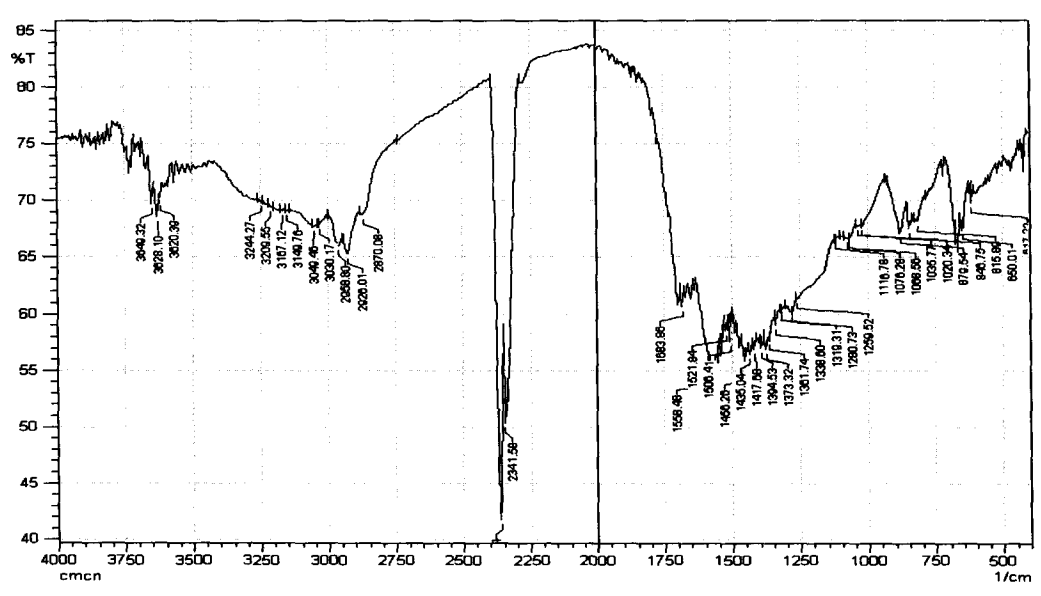


*Fig 2.5 IR of carbon prepared from CMC*

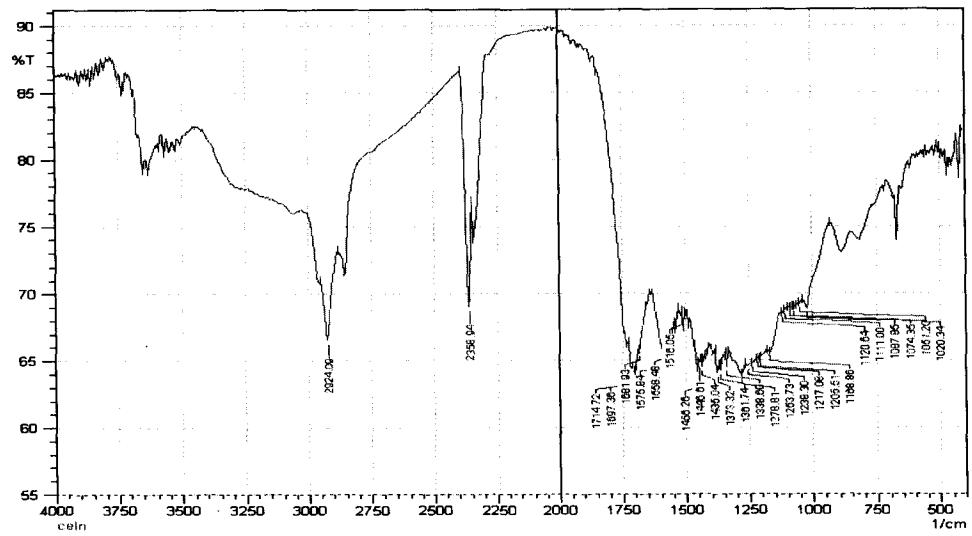


*Fig 2.6 IR of carbon prepared from cellulose*

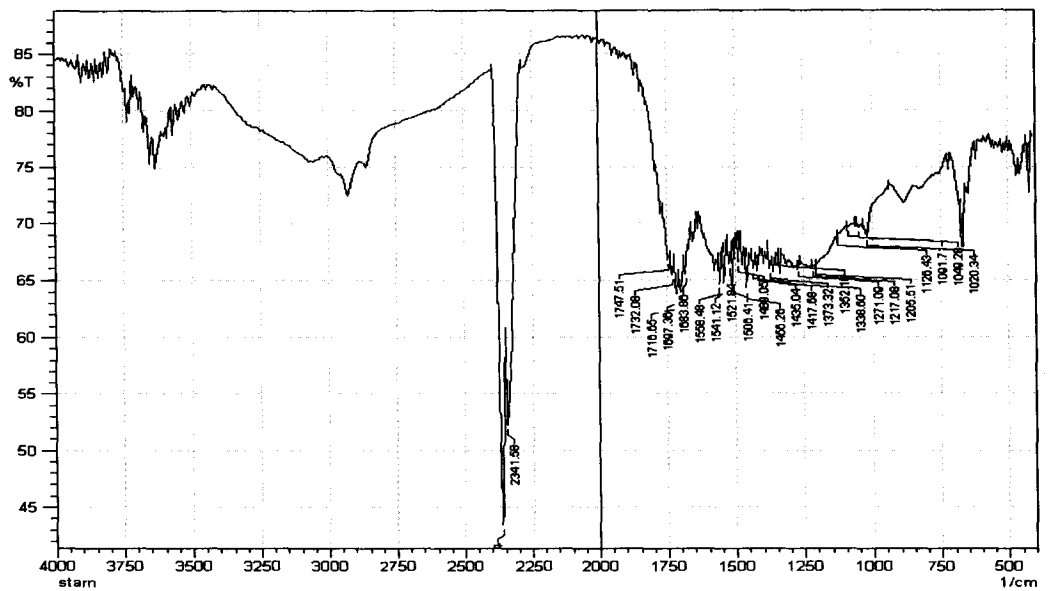


*Fig 2.7 IR of carbon prepared from starch*

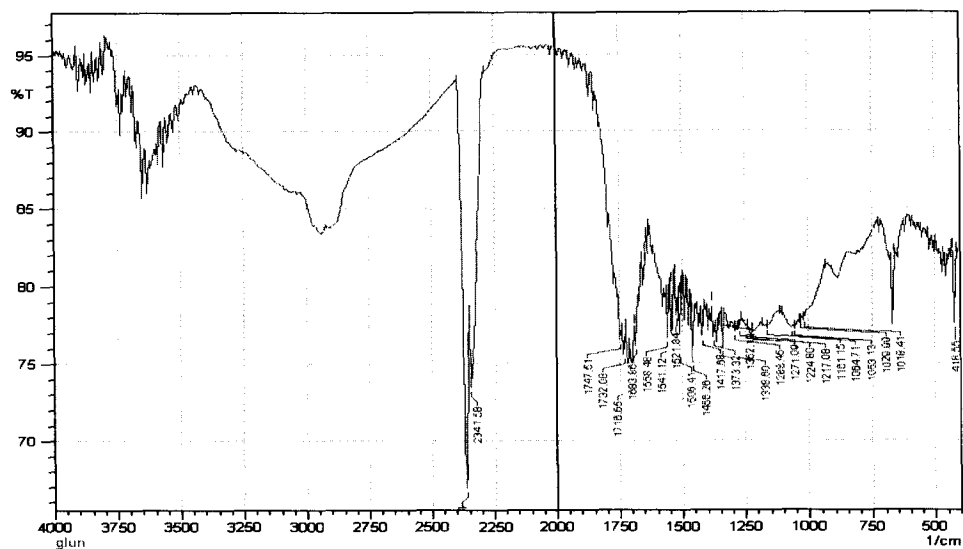


**Fig 2.8 IR of carbon prepared from sucrose**

All the carbons showed the presence of functional groups but porosity was shown only by CMC and Cellulose carbons.

### 2.2.5 Porosity enhancement

To enhance the porosity shown in carbons from CMC and cellulose, after heating in nitrogen at 400 °C for 3hrs, the red hot carbon was then quenched in water.

### 2.2.6 SEM images

SEM images showed that porosity was enhanced in case of CMC carbon whereas there were no new porosity developed in case of cellulose carbon

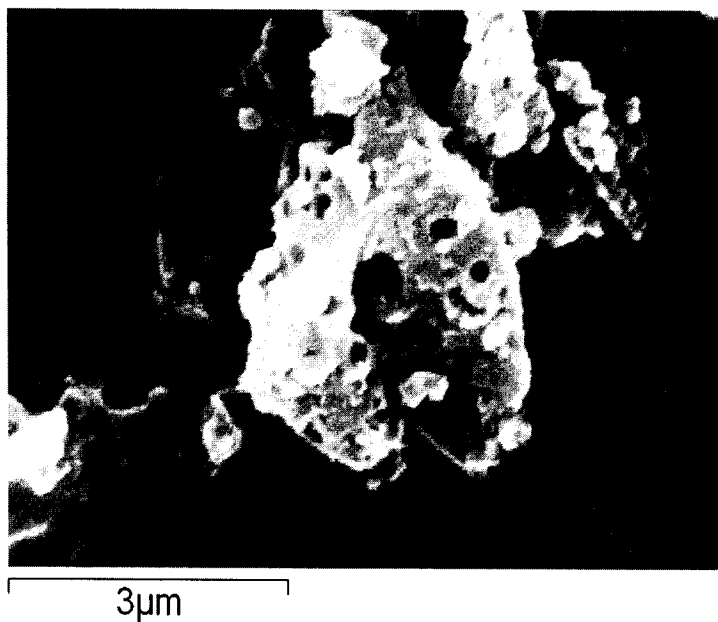


*Fig 2.9 SEM images of CMC carbon after activation by quenching*

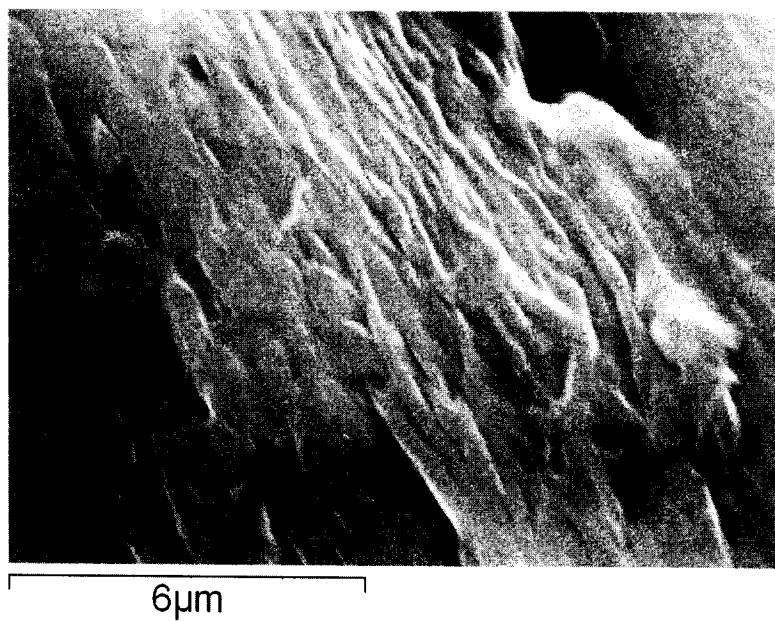


*Fig 2.10 SEM images of carbon from Cellulose after activation by quenching*

The CMC carbon showed development of pores whereas there was no marked visibility of the pores on the carbon from cellulose.

#### *2.2.7 Activated carbon from carboxyl methyl cellulose*

CMC was dehydrated for an hour at 170 °C, prior to carbonization and activation as stated above. It was observed that when the red hot carbon was quenched, the porosity was enhanced as indicated in the SEM image.

The end product was a highly porous activated carbon from carboxyl methyl cellulose

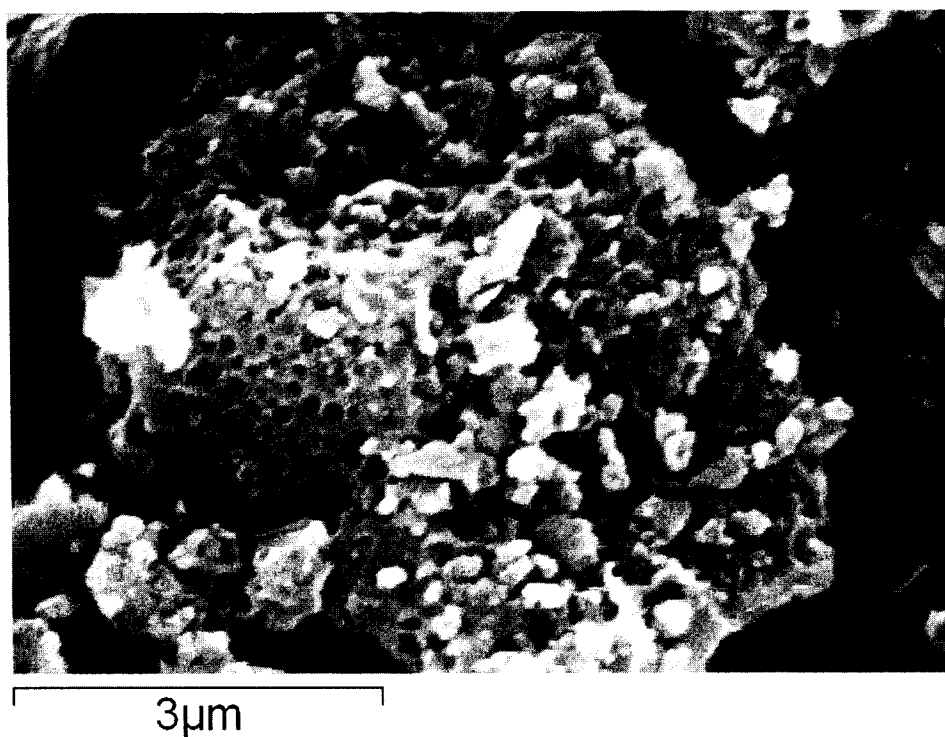


*Fig 2.11 SEM image of carbon from CMC having high porosity, obtained as per the new Synthesis method developed (Scheme 2. 1)*

### 2.2.8 Conclusions

- *A new simple method has been developed to prepare activated carbons from carboxyl methyl cellulose by low temperature, physical activation.*
- *The CMC-N carbon showed both porosity and surface functional groups.*
- *Carbons prepared from cellulose showed poor porosity whereas those prepared from starch and sucrose showed none.*
- *All the carbons showed the presence of surface functional groups.*

## **2.3 CHARACTERISATION OF CARBONS**

The CMC N carbon prepared from CMC as per Scheme 2.1 was taken up for study and compared with two other commercial carbons namely C1 and C2.

a) C1 –activated carbon obtained from SD -Fine Chemicals Ltd

b) C2- activated carbon from coconut shell, IGCL, Kerala.

**Carbons were characterized by**

- **XRD**
- **ESR**
- **BET surface area**
- **SEM**
- **TG**
- **IR**
- **EDS**
- **pH measurements**
- **Acid base titrations**
- **TPD**
- **Decomposition of hydrogen peroxide**

### *2.3.1 XRD*

XRD diffraction patterns of carbon materials were recorded using a Rigaku Miniflex II desk top X-ray diffractometer operating at a scanning rate of  $0.05^{\circ}$  with  $\text{CuK}\alpha$  and a Ni filter. Diffraction profiles were obtained in the  $2\theta$  range of  $5\text{-}70^{\circ}$ .

### *2.3.2 EPR*

The EPR spectra were recorded on Varian E-112 X band EPR spectrometer at 77 K (liquid nitrogen temperature) operated at a frequency of 9.2 GHz and a microwave power of 10mW.

### *2.3.3 BET-SORPTOMETRY*

BET–Sorptometry studies were carried out to find out the surface area and pore volume. Nitrogen sorption isotherms were recorded using Sorptomatic 1990 Carlo Erba instrument at  $-196^{\circ}\text{C}$  on carbon materials. Prior to the measurements, samples were degassed overnight at  $250^{\circ}\text{C}$  under vacuum. Nitrogen of high purity was used as adsorbate.

### *2.3.4 SEM*

SEM images were taken using Jeol JSM-5800LV Scanning electron microscope. The samples were coated with a thin film of gold to prevent charging and to protect the material from thermal damage by the beam.

### *2.3.5 TG*

Thermogravimetric analysis of the precursor and the final product were carried out in nitrogen atmosphere from ambient temperature to 900<sup>0</sup>C at a heating rate of 10<sup>0</sup>C/min using Netzsch instrument.

### *2.3.6 IR*

The infrared spectrum was recorded in KBr pellets between 400cm<sup>-1</sup> and 4000cm<sup>-1</sup> using IR Prestige 21 Shimadzu instrument to study the surface functional groups.

### *2.3.7 EDS*

To analyse the elemental composition, EDS measurement was carried out using Jeol JSM-5800LV Scanning electron microscope. The sample was coated with a thin film of gold to prevent charging and to protect the material from thermal damage by the beam.

### *2.3.8 Acid base titration*

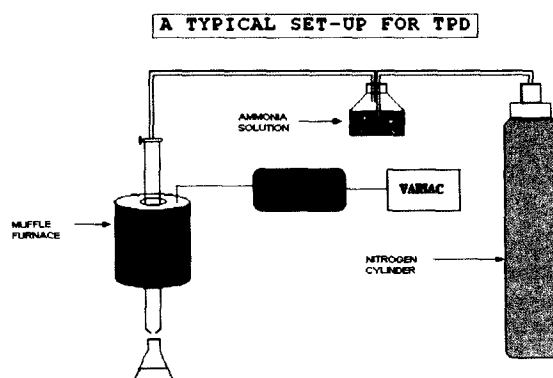
The acidic and basic sites were found out by the titration method. In a typical experiment 0.30g of each carbon was added to four separate flasks containing 60 ml of 0.01 M HNO<sub>3</sub>. The solution was stirred for 48 hours, filtered and titrated against 0.01 M NaOH using phenolphthalein as indicator.

### *2.3.9 pH measurements*

The pH of the carbons in solution was determined by the pH meter by equilibrating 0.50 g of the carbons in 50 ml of double distilled water, stirring for 24 hours. The solution was filtered and measurements taken.

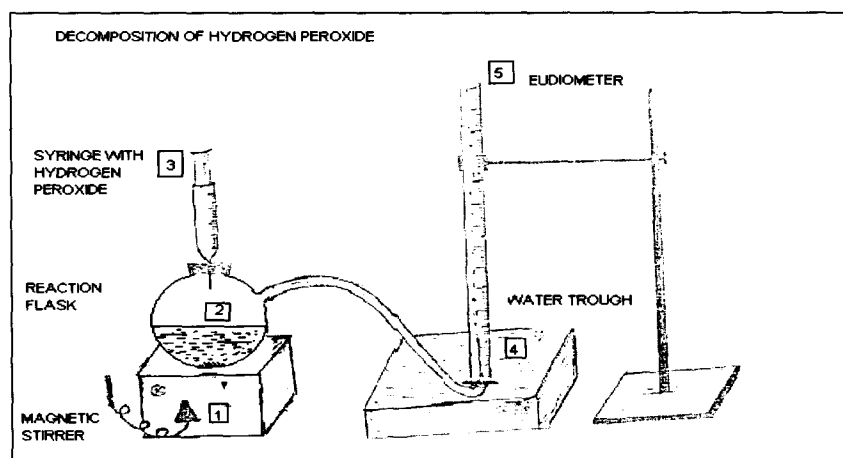
### 2.3.10 TPD

The strength of the surface acidic groups was done by Temperature Programmed Desorption using ammonia. 0.50g of CMC- N was heated at 150<sup>0</sup> C for 1 hour by passing air and then cooled to room temperature. Ammonia was then passed for 45 minutes. The desorption of ammonia was carried out up to 500<sup>0</sup>C as per the typical set up for TPD.



### 2.3.11 Decomposition of hydrogen peroxide

The activity of the carbon was tested for decomposition of hydrogen peroxide in alkaline medium. In a typical run 0.25 g of the carbon was added to H<sub>2</sub>O<sub>2</sub> taken in a double necked flask, with 25 mL of 0.1 M KOH and the activity was measured from the volume of oxygen liberated as per the set up shown below.



## 2.4 RESULTS AND DISCUSSIONS

### 2.4.1 XRD

Fig 2.1, 2.2, 2.3 gives the XRD profiles of the CMC carbon along with C1 and C2. The aromatisation was evident from the XRD data. All the three carbons CMC-N, C1 and C2 showed diffraction peaks characteristic of ordered hexagonal carbons as indicated by the diffraction peak at 2 theta value of 12.5 and graphitic nature as evidenced by the broad intense diffraction peak at 2 theta value of 24. The scanning rate was of  $0.05^\circ$  with  $\text{CuK}\alpha$  radiation and a Ni filter as described in 2.3.1

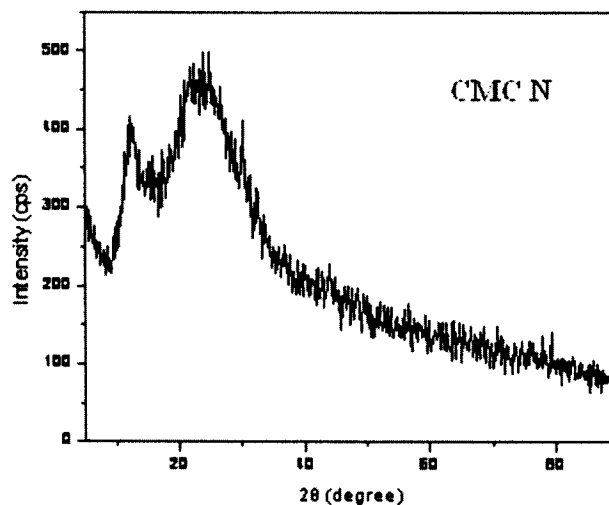


*Fig 2.12 XRD profiles of the activated carbon obtained from CMC*

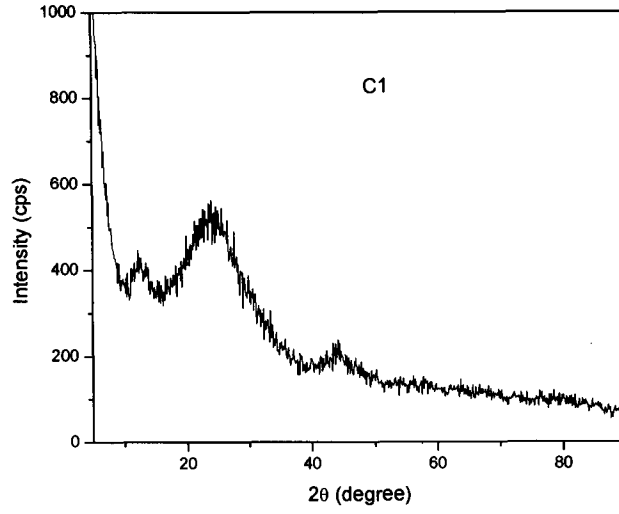


***Fig 2.13 XRD profile commercial of activated carbon C1***

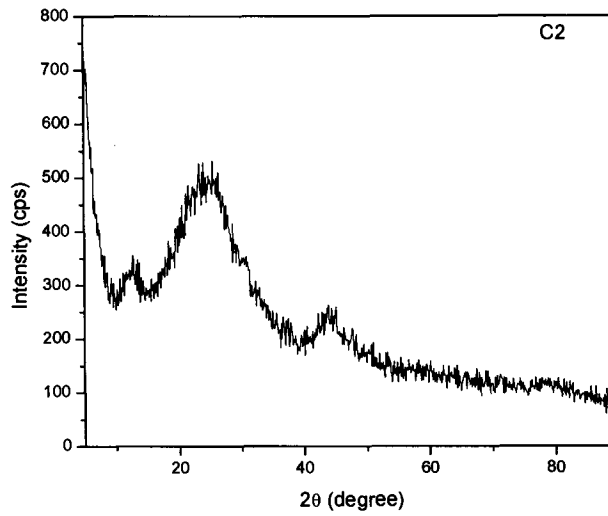


***Fig 2.14 XRD profile commercial of activated carbon C2***

#### 2.4.2 EPR

Diphenyl picryl hydrazyl radical is used as standard or reference. The g values were calculated for all the carbon samples which are close to the g value of DPPH indicating the presence of free electron in the carbon materials. The carbon materials are therefore paramagnetic in nature. The g values are given in Table 2.2

The experimental g-value is determined by substituting the measured values of H and  $\nu$  into the following equation.

$$h\nu = g\beta H,$$

where  $h$  = Planck Constant =  $6.626 \times 10^{-27}$  erg sec

$\beta_e$  = Bohr Magnetron of electron =  $9.274 \times 10^{-21}$  erg. Gauss<sup>-1</sup>

H = Magnetic field strength

$\nu$  = Microwave frequency

Sr no	Sample	H (in Gauss)	V(G Hz)	g value
1	CMC N	3373	9.49	2.00998
2	C1	3392	9.49	1.99470
3	C2	3374	9.49	2.00998
4	DPPH	3370	9.49	2.009960

**Table 2.2 g values of activated carbons CMC N, C1, C2 obtained by EPR spectra analysis using DPPH as reference.**

**Fig 2. Shows EPR spectrum for DPPH reference CMC-N, C1 and C2**

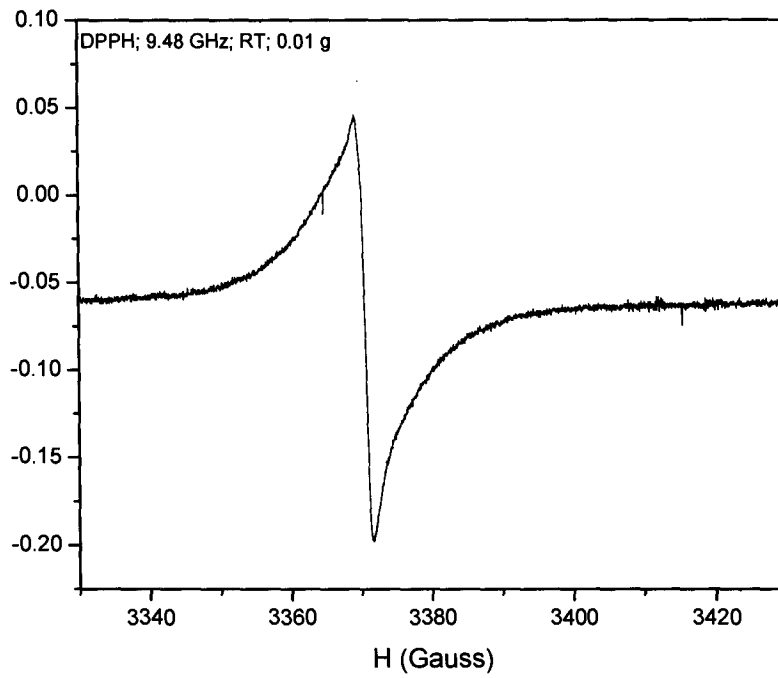


**Fig 2.15 EPR spectrum for DPPH reference**

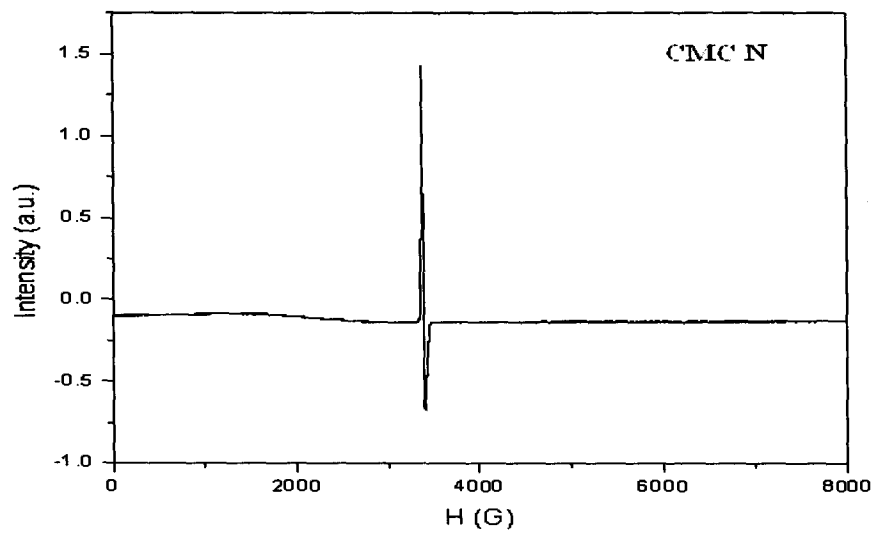


**Fig 2.16 EPR spectrum for activated carbon CMC-N**

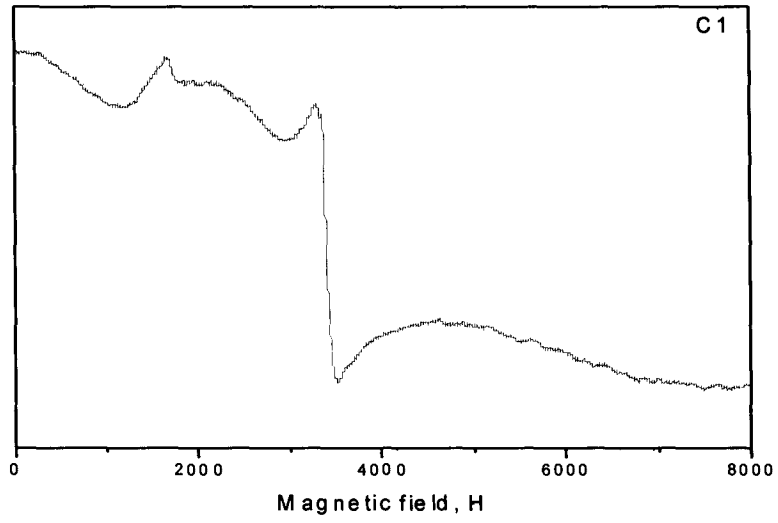


***Fig 2.17 EPR spectrum for commercial activated carbon C1***

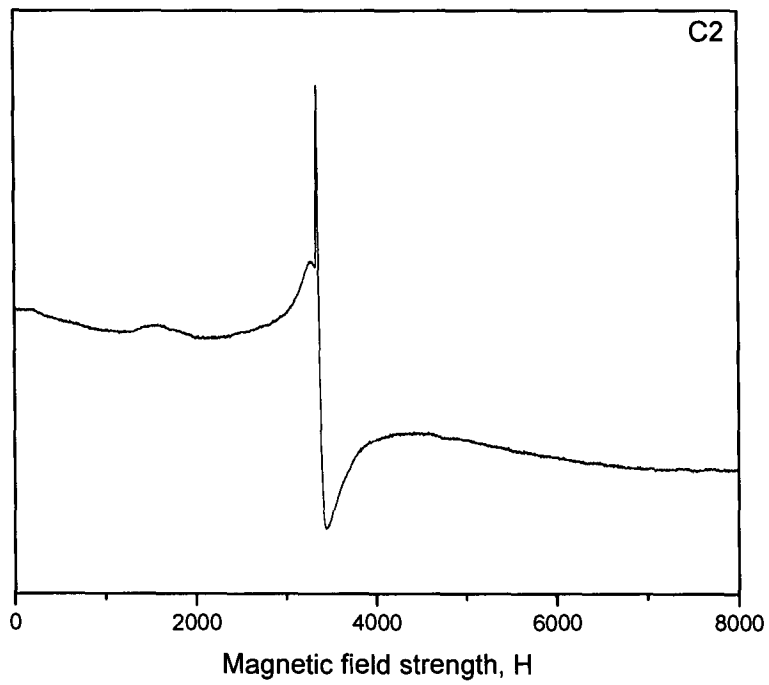


***Fig 2.18 EPR spectrum for commercial activated carbon C2***

### 2.4.3 Surface area and porosity

Surface area, porosity measurements and density of the carbons were found out for all the three carbons as listed in Table 2.3. It can be seen from Table 2.3 that the CMC N carbon possessed higher specific surface area and pore volume as compared to the commercial carbons which had relatively low density.

It is known that low density materials like wood and lignin which contains a high amount of volatile content produce activated carbon with large pore volume and low density. In the present work the precursor NaCMC was of low density and in the powdered state resulted in low density carbons. Further the large pore volume is attributed to the formation of pores during the discharge of large amount of volatiles during the thermal treatments which are further developed during air oxidation and quenching.

	CMC-N	C1	C2
Specific surface area	1025 m <sup>2</sup> /g	873 m <sup>2</sup> /g	988 m <sup>2</sup> /g
Pore specific volume	0.57 cm <sup>3</sup> /g	0.4722 cm <sup>3</sup> /g	0.45 cm <sup>3</sup> /g
Density	0.36g/cc	0.41g/cc	0.62g/cc

**Table 2.3 Comparison of specific surface area, pore specific volume, density of CMC N, C1 and C2**

Figures 2.19 - 2.22 gives the BJH analysis for the nitrogen adsorption-desorption isotherms in relation to pore size distribution for the various activated carbons.

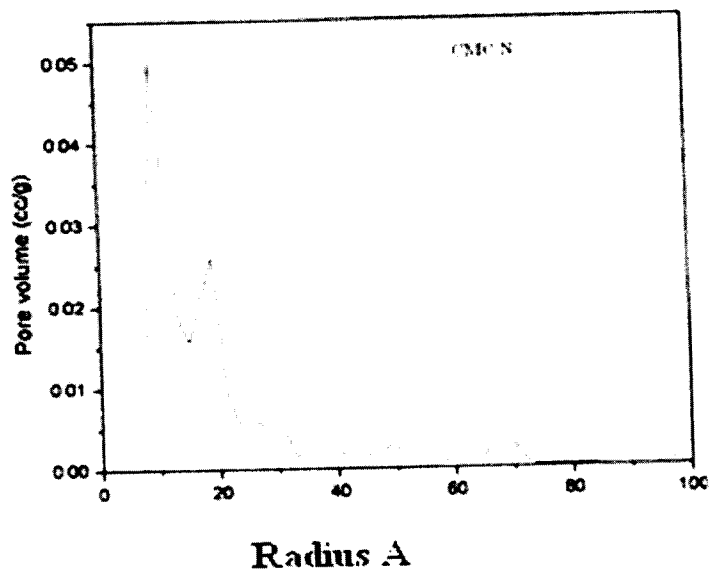
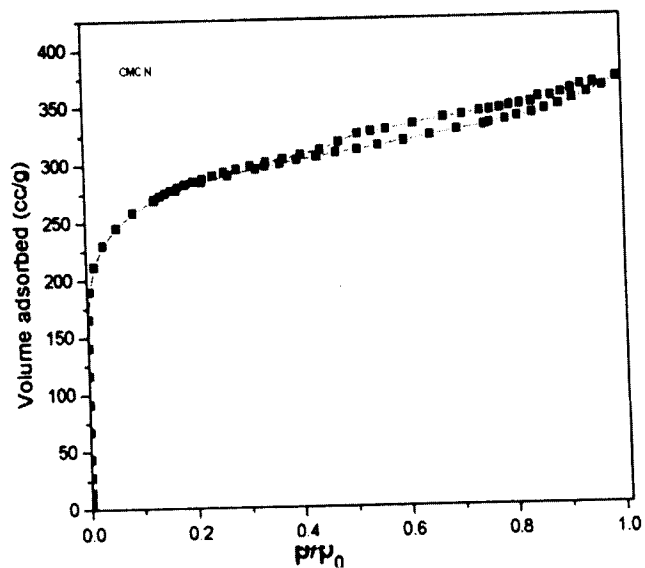


*Fig 2.19 Nitrogen adsorption desorption in relation to pore size distribution (BJH analysis) for CMC N*

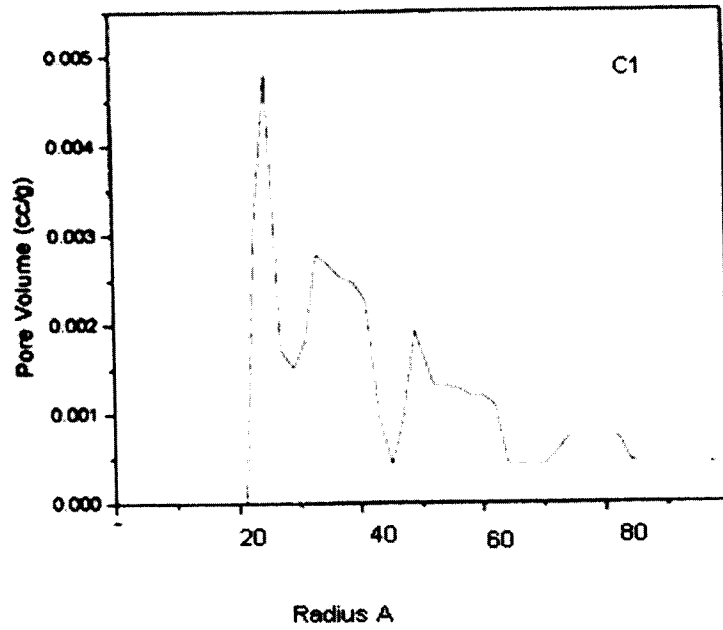
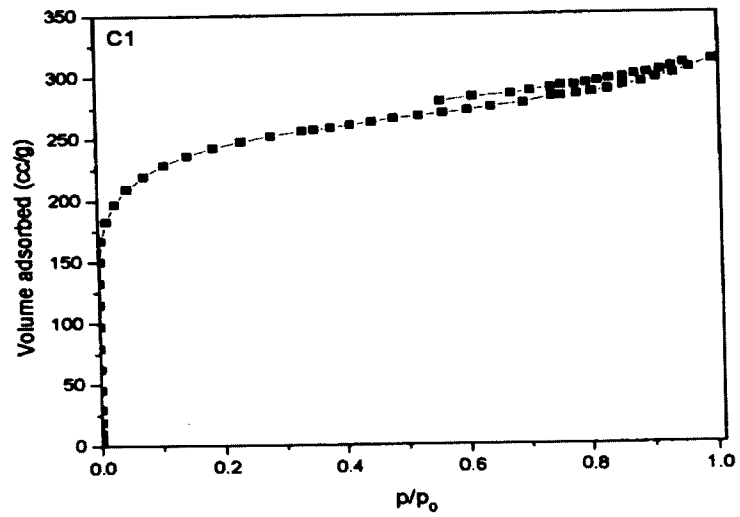


*Fig 2.20 Nitrogen adsorption desorption in relation to pore size distribution for activated carbon C1*

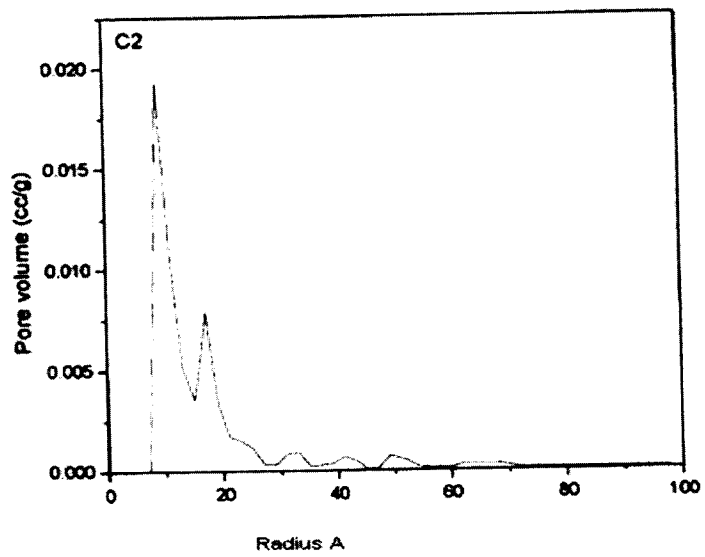
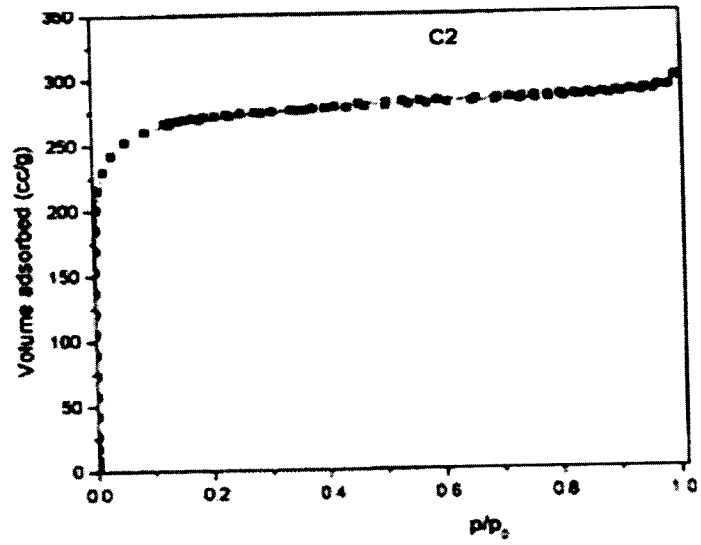


*Fig 2.21 Nitrogen adsorption desorption in relation to pore size distribution for activated carbon C2*

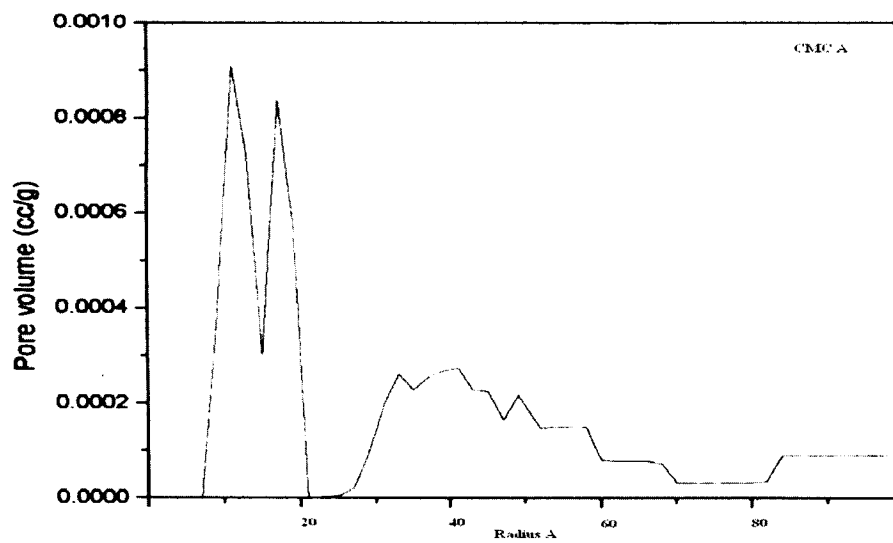
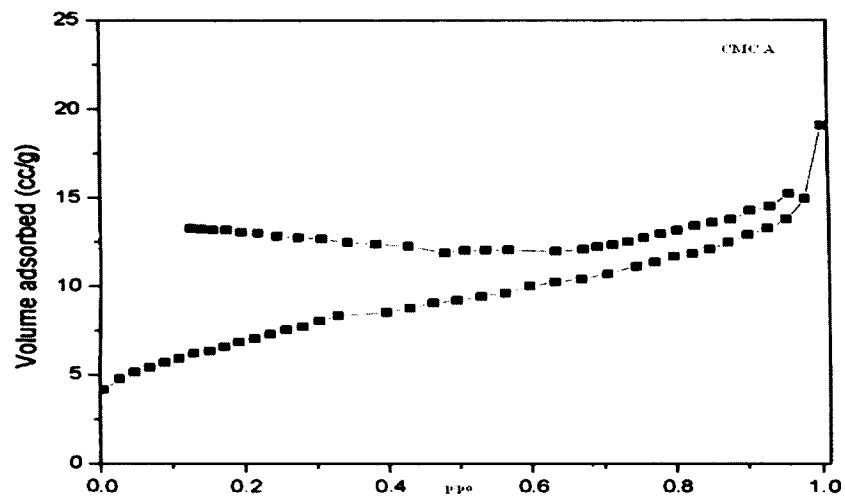


*Fig 2.22 Nitrogen adsorption desorption in relation to pore size distribution for activated carbon CMC-A(air oxidised instead of N<sub>2</sub>)*

A comparative study between the surface area, porosity measurements of CMC-N carbon before and after quenching was done. It can be seen from Table 2.4 that the CMC-N carbon possessed higher specific surface area and pore volume as compared to the carbon which was not quenched (CMC- A )

	CMC-A	CMC-N
Surface area m <sup>2</sup> /g	0.24	1025
Pore volume cm <sup>3</sup> /g	0.02	0.57

***Table 2.4 Surface area and pore volume data of CMC carbons with oxidation but no quenching (CMC-A) and with oxidation and quenching (CMC-N).***

It can be concluded that the surface area of CMC carbon was comparable to that of the commercial carbons. In fact CMC-N carbon had significantly higher surface area, although it had less density.

#### **2.4.4 SEM**

SEM images of carbons before and after the quenching step indicate that the porosity was partly developed during the carbonisation stage and was greatly enhanced after quenching. During the carbonisation period the escaping volatiles produced the pores as in Fig 2.23. These pores were enlarged due to the burn off that resulted after the carbon was removed from the furnace at 400<sup>0</sup>C due to atmospheric oxidation shown in Fig 2.24. The red hot carbon was then quenched in water which generated a lot of steam. The steam helped in removing the tarry matter produced during carbonisation that had blocked the pores within the pores indicated by Fig 2.25.

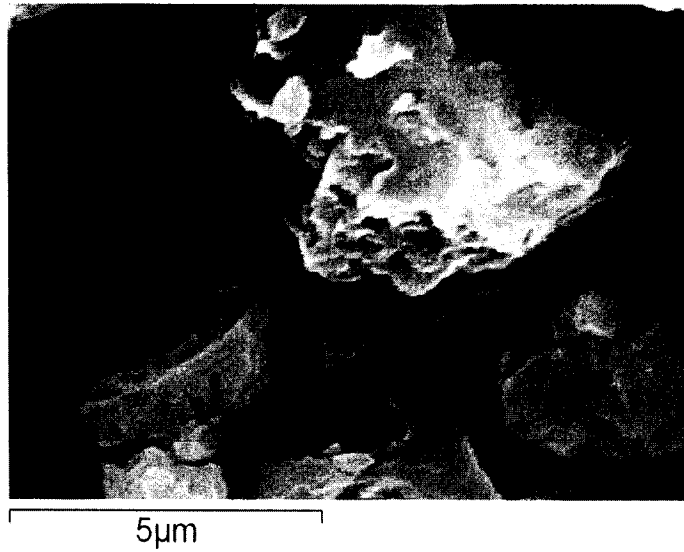


*Fig 2.23 SEM images of carbon from CMCN after carbonisation and before activation showing the aromatised sheets as well as pores.*

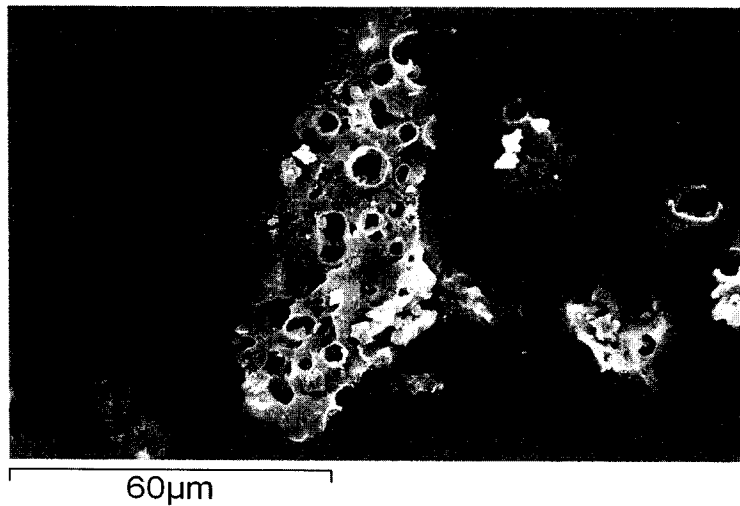


*Fig 2.24 SEM images of carbon from CMC after activation by quenching indicating the surface burn off.*

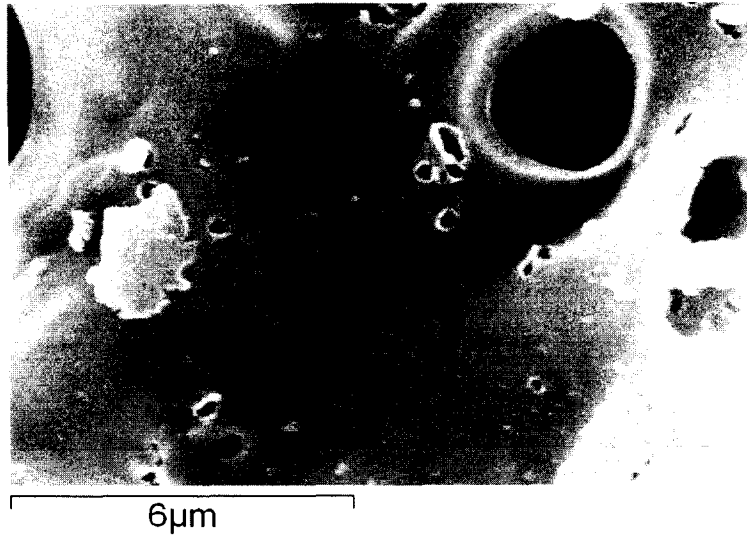


*Fig 2.25 SEM images of carbon from CMC after activation by quenching showing smaller pores within the pores.*

The SEM images of commercial carbons C1 showed micropores whereas C2 showed a mix of micro and macro pores.

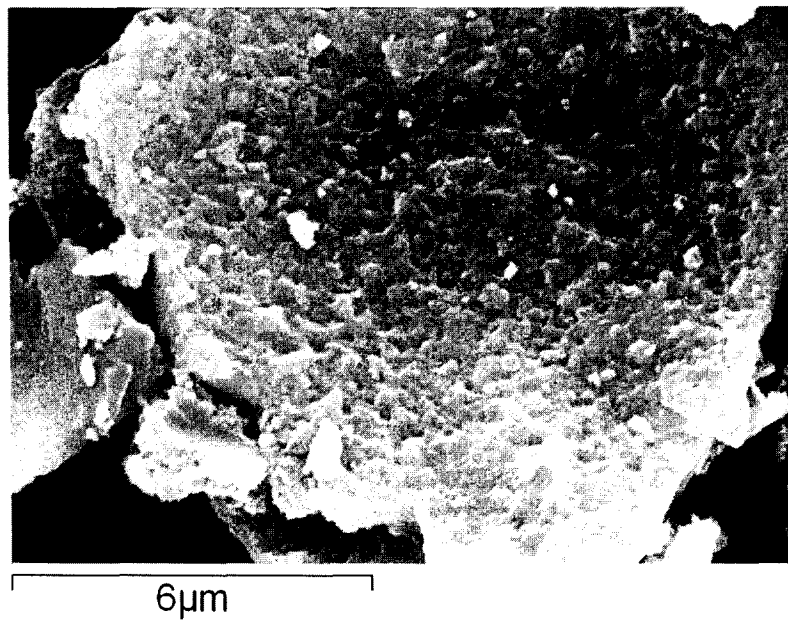


*Fig 2.26 SEM images of commercial activated carbon C1*

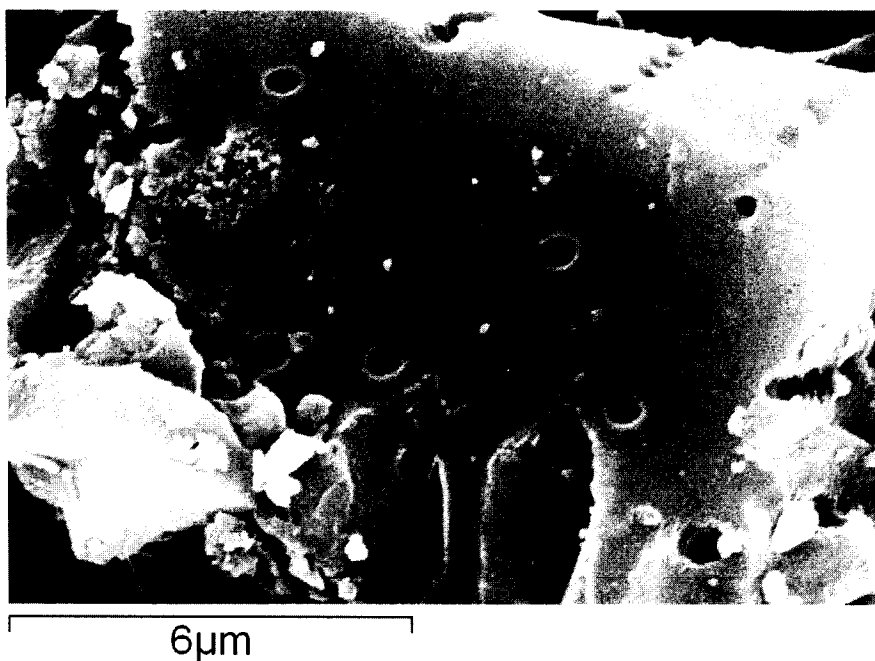


*Fig 2.27 SEM images of commercial activated carbon C2*

2.4.5 *Thermo gravimetric analysis* from the thermo gravimetric analysis of Na CMC, the percentage loss of water and volatiles evolved at T1 and T2 temperature and the amount of carbon left was calculated.

Sample	T1 °C	T2 °C	%residue at 400°C	% residue at 900°C
CMC	288.7	595.2	29.88	2.25

*Table 2.5 Percentage of volatiles at T1 and T2 and percentage of residue at 400°C and 900°C*

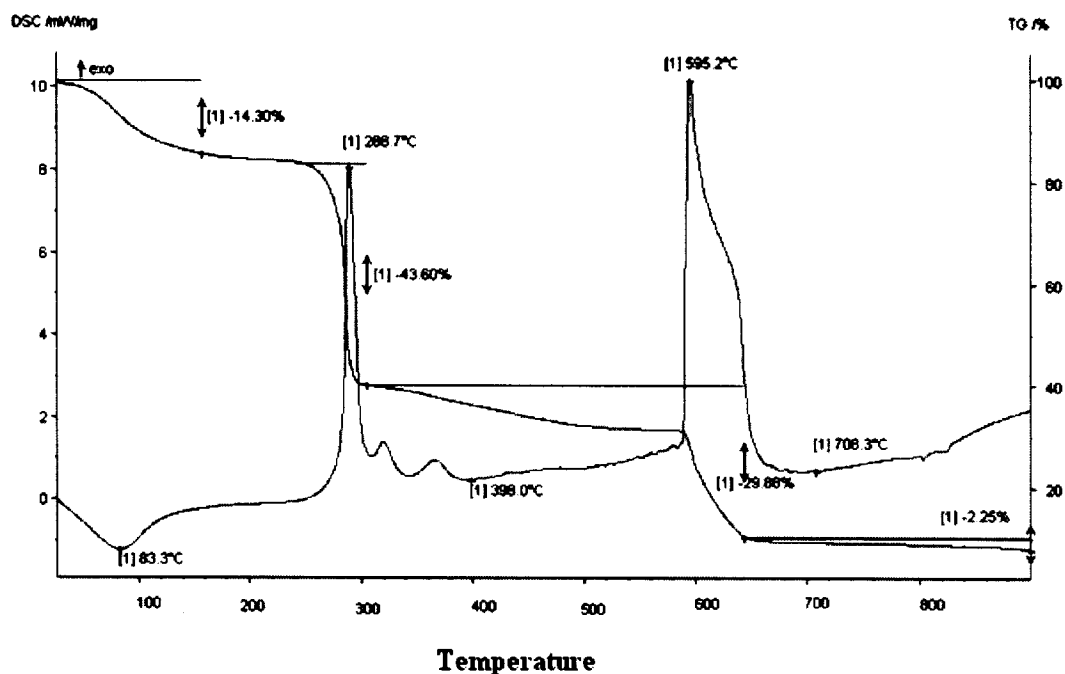


**Fig 2.28 Thermogravimetric analysis of sodium carboxyl methyl cellulose in nitrogen**

The moisture was lost by NaCMC was in the temperature range upto 150°C. Softening of the material takes place and the precursor becomes viscous. At 285°C, the evolution of gases begin and then soon becomes vigorous indicating exothermic decomposition. Reddish brown fumes and clouds of white gases are evolved.

During carbonisation oxygen gets removed as CO and CO<sub>2</sub>. The oxygen from the precursor also combines with the nitrogen atmosphere used for carbonisation, to form reddish brown gas. The reddish brown gas could be of nitrogen dioxide as a result of catalytic reaction occurring during carbonisation.

The evolution of gases continues from 285<sup>0</sup>C-380<sup>0</sup>C. The carbonised char is heated at 400<sup>0</sup>C for 3 hours. This leads to the stabilisation and reorganisation of the carbon atoms. The amount of char produced is 29.8% at 400<sup>0</sup>C.

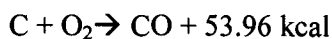
In case of wood carbonisation dehydration takes place at 170<sup>0</sup>C. The partial degradation of material begins above this temperature where CO<sub>2</sub>, CO and C<sub>2</sub>H<sub>4</sub>O<sub>2</sub> is formed. When the temperature reaches 270-280<sup>0</sup>C the exothermal decomposition takes over and a large amount of tar and other substances are released. The carbonisation is almost complete at 400<sup>0</sup>C [3].

Lower rate of heating during carbonization, results in lower amount of volatiles and hence more char because of increased dehydration and stabilization of aromatic sheets. The rate of pyrolysis is affected by the moisture content and the temperature of carbonization [4].

Activation has been reported with CO<sub>2</sub> and CO at higher temperatures as activating agents. A mixture of these gases has been shown to produce micropores [5]. These gases which are evolved during decomposition of NaCMC contribute towards the development of pore.

Tourkou et al [6] studied the activation of brown coal carbonised at 900 <sup>0</sup>C with water vapour, carbon dioxide and oxygen. All the three activating agents at low burn offs produced micropores and their volume was highest for oxygen activation. With water vapour activation it resulted in the development of mesoporosity to a higher extent as compared to carbon dioxide or oxygen.

The red hot carbonised char of CMC, when in contact with air resulted in the surface carbon being burnt off and evolution of carbon oxides.



This led to the widening of pores and development of new pores. Since the contact time of the hot carbonised material and air was 10 minutes, the burnoff was less.

The red hot carbonised material was then dropped in hot water 100°C which resulted in the production of steam. The steam helped in the clearing of blocked pores and further oxidation of carbon, thus activating it. The solution was boiled for half an hour to wash the carbon.



Since the reaction with carbon and steam is endothermic, the exothermic burning of carbon and the boiling water provided the external heating to drive the above reaction.

The large pore volume is due the large number of mesopores of radius 10 - 50 Å, and very few macropores of radius 50 – 80 Å

The TG of NaCMC showed that the volatiles were given out at 288.7 °C and 595.2 °C. Since the carbonisation step was restricted upto 400°C, the surface functional groups that would have evolved gases upto 595.2°C were still present in the CMC-N carbon.

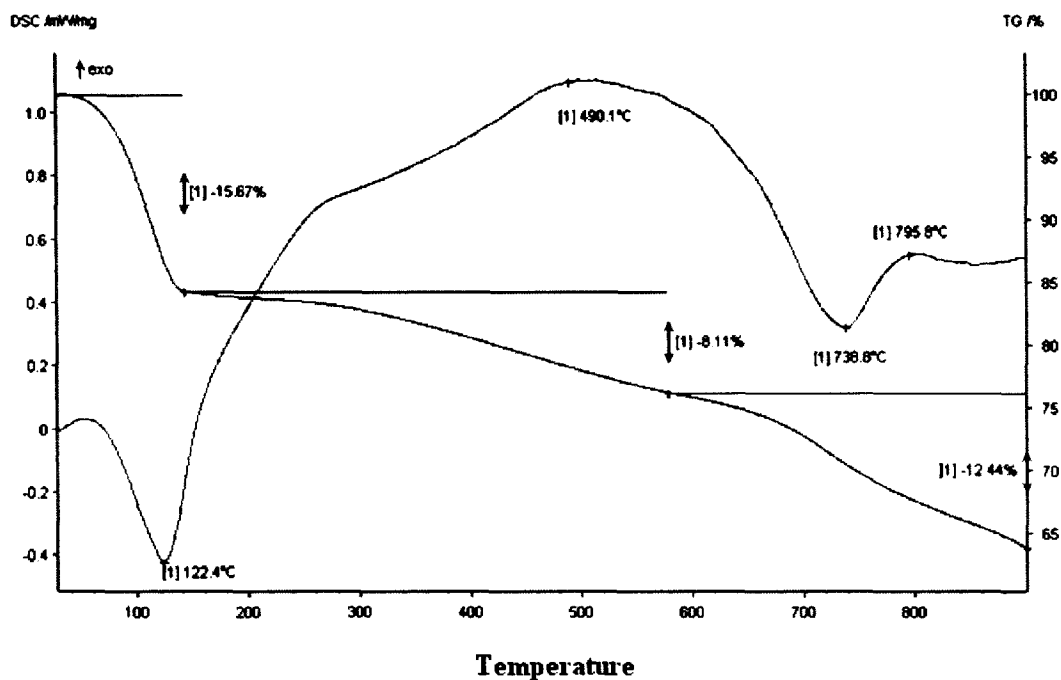


**Fig 2.29 Thermo gravimetric analysis of carbon synthesised from CMC N in nitrogen**

TG of the CMC N carbon showed exothermic and endothermic peaks at 490.1°C and 738.8°C respectively, indicating that the surface functional groups gave out volatiles at two different temperatures. Therefore it can be concluded that the carbon has different functional groups

After the reorganisation and stabilising of the carbon the nature of functional groups changed. The exothermic peak at 490.1°C and endothermic peak at 738.8°C indicate that there are distinct functional groups.

#### 2.4.6 Infra Red Spectroscopic analysis

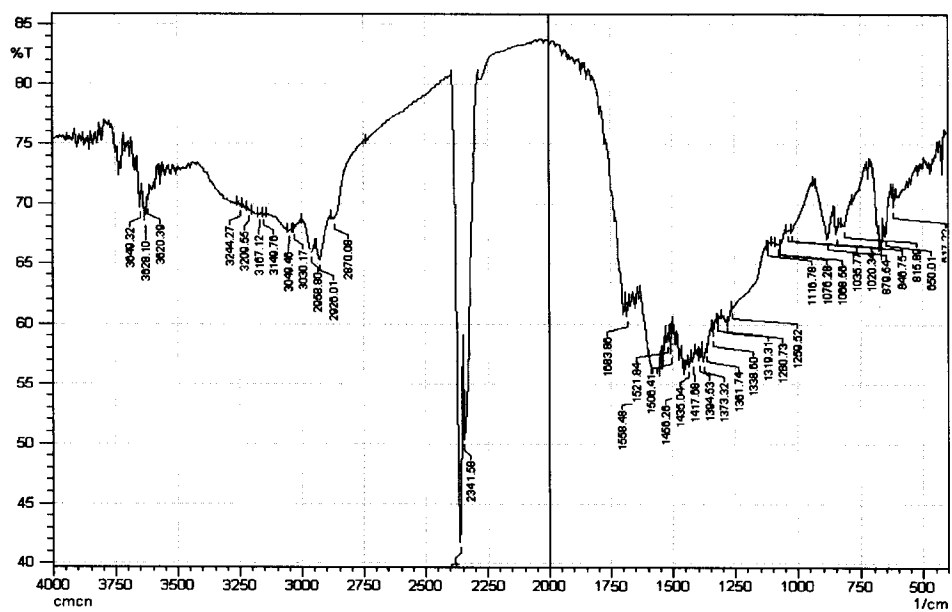
Surface functional groups play an important role along with porosity. A detailed IR investigation to identify the surface functional groups on activated carbon has been carried out.

Group or functionality	Assignment region: (cm <sup>-1</sup> )	Group or functionality	Assignment region: (cm <sup>-1</sup> )
C-O in ethers (stretching)	1000-1300	N-H, C=N	1550-1570
Alcohol:	1040-1176, 3200-3640	Cyclic amides:	646, 1461, 1546, 1685
Phenolic group:		C-N aromatic ring	1000, 1250, 1355
-C-OH (stretching)	1000-1220	C-N	1190
O-H	1160-1200, 2500-3620	C=C=N	2070-2040
Carbonates; carboxyl-carbonate:	1100-1300, 1590-1600	N-O	1300-1000
-C-C aromatic (stretching)	1585-1800		
Quinones:	1550-1680		
Carboxylic acid:	1120-1200, 1665-1760, 2500-3300		
Lactones:	1160-1170, 1675-1750		
Carboxylic anhydride:	980-1300, 1740-1830		
C-H (stretching)	2800-3000		

**Table 2.6 Assignment of bands in IR to surface functional groups [7].**

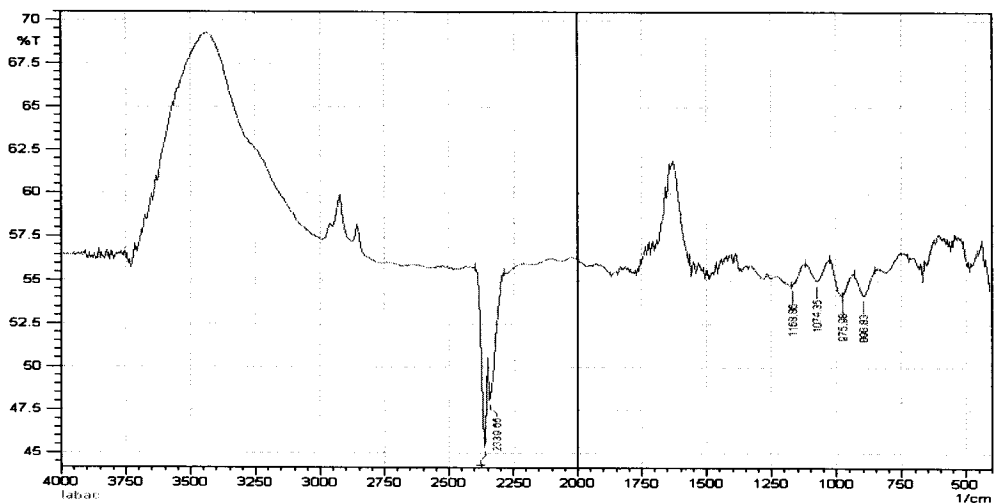
IR data showed the presence of carboxyl groups, lactones and nitrogen containing groups [7]. CMC- N showed surface functional groups in the region 2500-3500 cm<sup>-1</sup>, 1150 -1750 cm<sup>-1</sup>, 1000-1350 cm<sup>-1</sup> which are attributed to COOH and phenolic OH groups while the peak at approximately 3700 cm<sup>-1</sup> is due to possible presence of some neutral OH groups. In addition C- N groups could be present with absorption bands overlapping with carboxylates. The acidic and basic functional groups indicate that the carbon is amphoteric in nature.

C1 and C2 carbons showed functional groups in the range of 750 -1750 cm<sup>-1</sup> which are attributed to carboxylic acid and lactones.



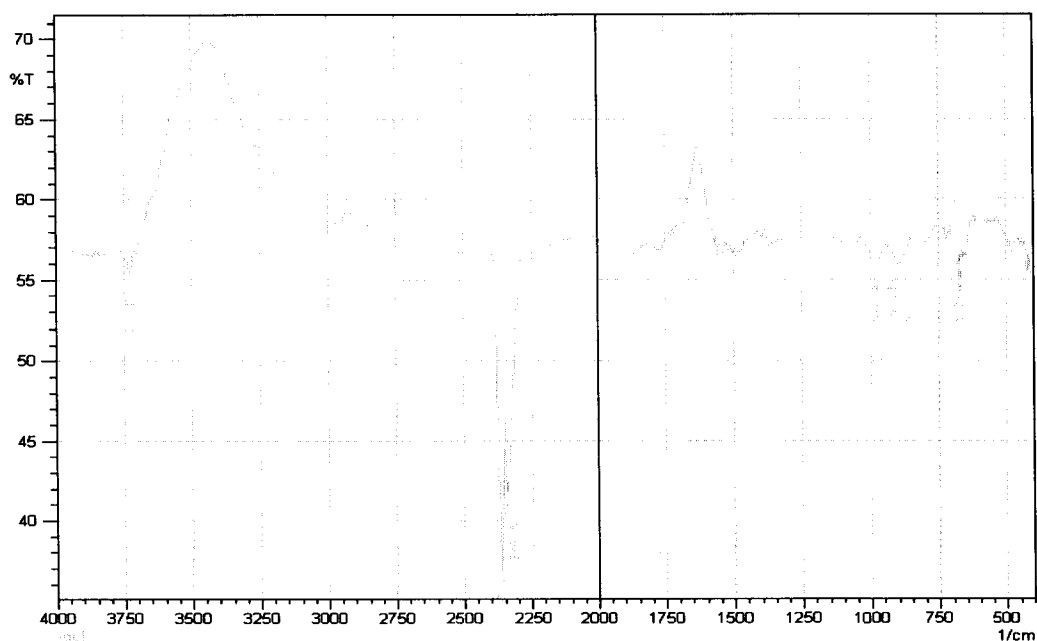
CMC N

Fig 2.30 IR of activated carbon CMC-N



C1

Fig 2.31 IR of activated carbon C1



C2

**Fig 2.32 IR of activated carbon C2**

Zawadzki[8] who carried out IR studies of basic carbons observed bands at  $1590\text{ cm}^{-1}$  with overlapping band in the range  $1500\text{-}1100\text{ cm}^{-1}$  which he attributed to carboxylic carbonate structures. The adsorption of oxygen at room temperature intensified the  $1590\text{ cm}^{-1}$  through the formation of complexes of condensed aromatic ring systems.

The absorption bands at low wave numbers  $1500\text{-}1100\text{ cm}^{-1}$  were attributed to chromene structures as suggested by Garten Weiss [9].

CMC-N showed absorption bands in this region indicating basic groups.

Monterra [10] prepared basic cellulose chars by degassing C at high temperature followed by room temperature exposure to oxygen. Examination of the IR of basic C revealed no evidence of the formation of any oxide species on any of the basic cellulose chars. These workers however did not rule out the possibility of

chemisorption of oxygen, but suggested that whatever oxygen that was chemisorbed did not produce structures that could be detected in the spectra under experimental conditions. Such spectra may be either IR inactive due to structure symmetry conditions or IR active but present in relatively small amounts so that the discrete weak bands could not be detected in the presence of strong background or they strongly coupled to the surface and made IR modes extremely broad.

These workers are of the view that the basic properties of carbon cannot be assigned to well defined oxygen structures. Thus suggesting that the adsorption of acids on carbon was due to the physical forces or due to Lewis co-ordination of proton on electron donor centres.

#### *2.4.7 Energy Diffraction Spectra.*

An elemental analysis was done by EDS to ascertain the elements present in the sample. The high percentage of carbon and presence of oxygen was confirmed.

EDS analysis showed that there was no nitrogen. During IR analysis the presence of nitrogen was speculated as there could be an overlapping of carboxylate and C- N bands.

The elemental analysis showed the presence of inorganic elements.

- CMC N carbon showed the presence of Na, K, Ca, Mg, Al and Si with the percentage of sodium being more.
- C 1 showed the presence of K, Ca, and Si.
- C2 showed the presence of K only which was significant.

Na was absent in the commercial carbons while a significant amount was present in CMC-N carbon. Since the precursor was sodium salt of CMC, the presence of Na is imminent.

K salts like carbonates are known to catalyse gasification of carbons. Hence their presence can result in catalytic reactions.

In all the carbons, chlorine was detected.

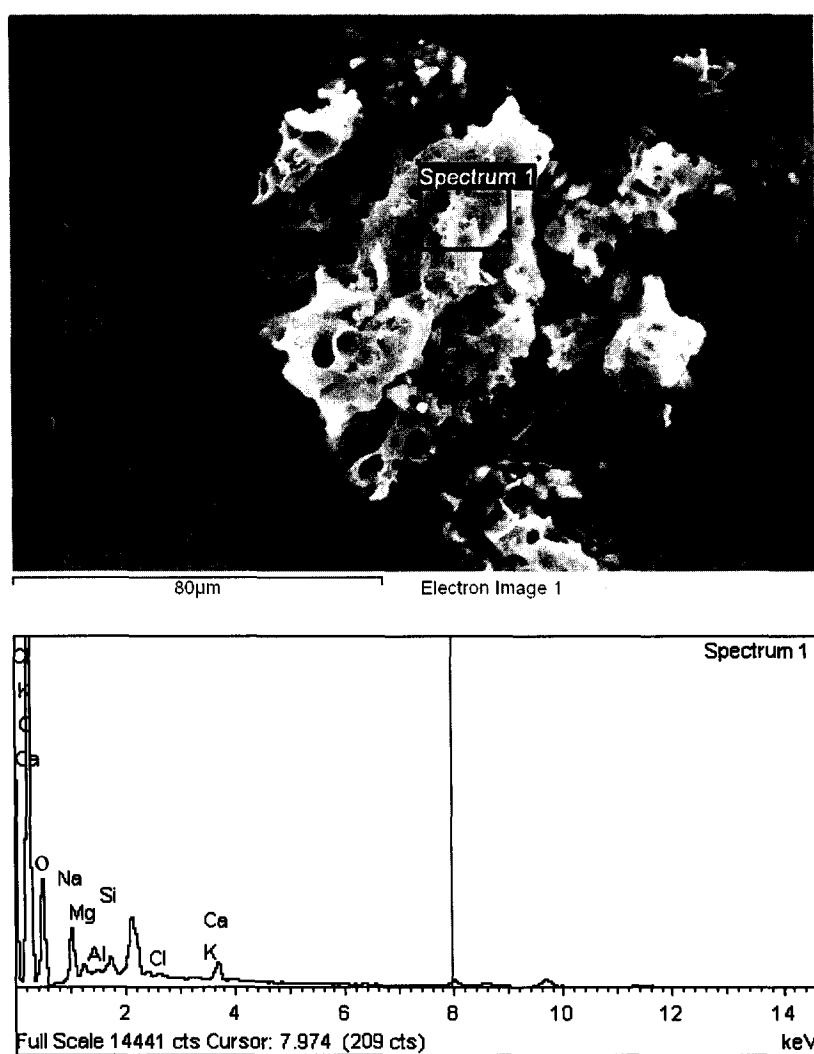


**Fig 2.33 Energy diffraction spectra of activated carbon from CMC**

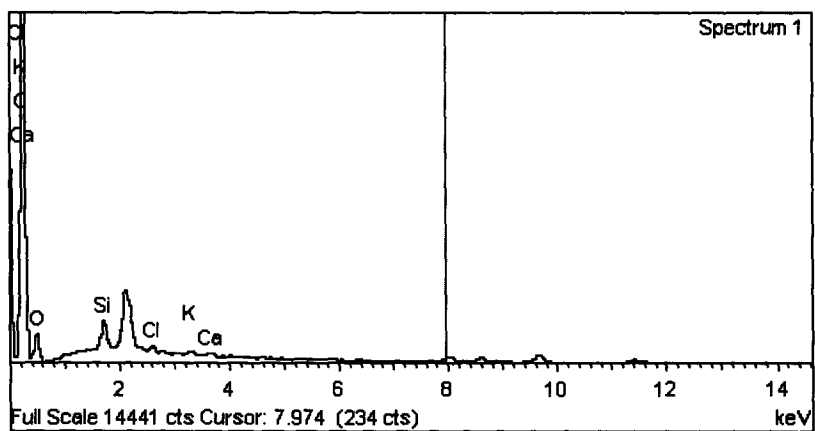
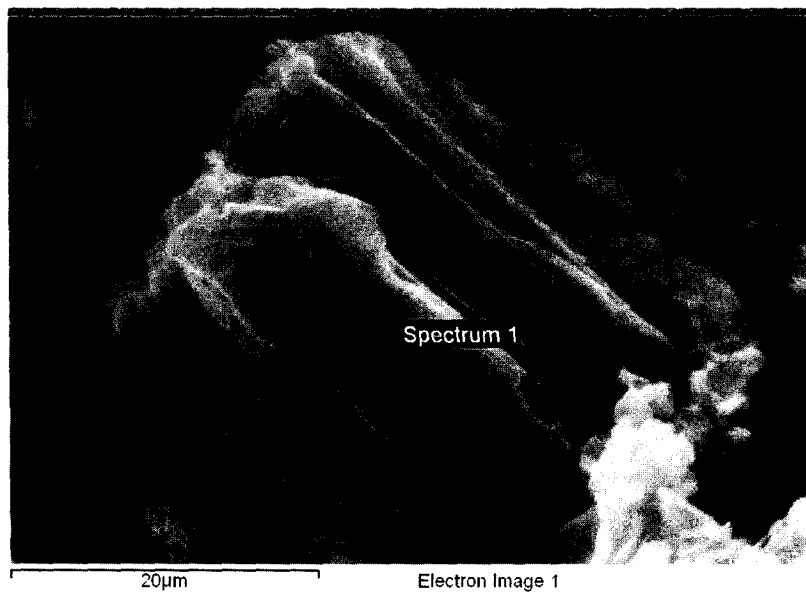


*Fig 2.34 Energy diffraction spectra of commercial activated carbon C1*

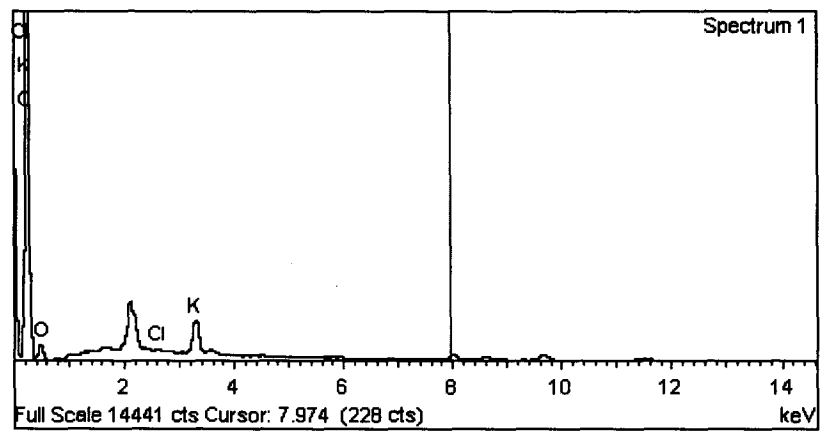
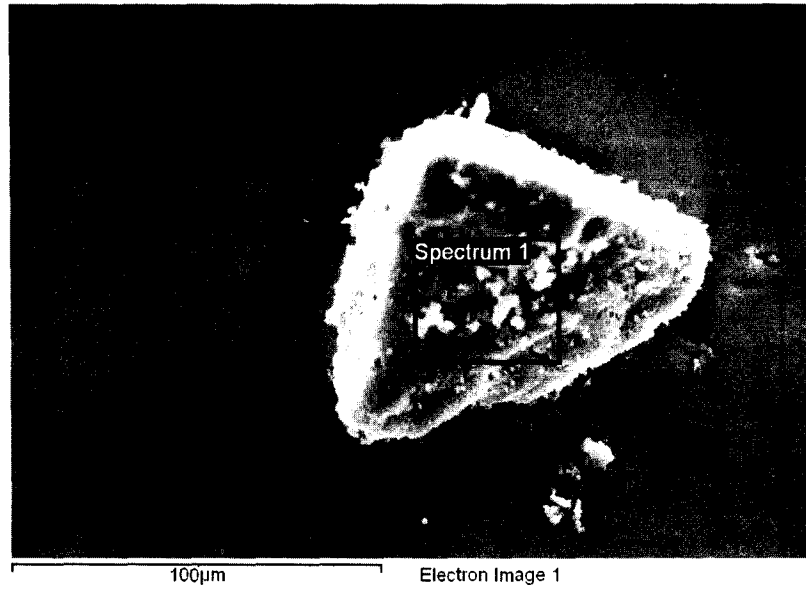


*Fig 2.35 Energy diffraction spectra of commercial activated carbon from C2*

#### 2.4.8 Acidity and Basicity titrations

CMC-N showed the most basicity and least acidity as compared to the other carbons.

Studebaker[11] suggested that the carbons prepared by various pyrolytic processes were like poly condensed aromatic hydrocarbons, which are known to be Lewis bases and can release OH<sup>-</sup> ions from water or aqueous solutions giving rise to basic character.

Carbon	ACIDITY millimoles g <sup>-1</sup>	BASICITY millimoles g <sup>-1</sup>
C1	9.24 x 10 <sup>-4</sup>	4.32 x 10 <sup>-4</sup>
C2	8.58x10 <sup>-4</sup>	1.056 x 10 <sup>-3</sup>
CMC-N	3.3 x 10 <sup>-4</sup>	3.264 x 10 <sup>-3</sup>

*Table 2.7 Acidity and Basicity of carbons in millimoles g<sup>-1</sup>*

#### 2.4.9 pH

The acidic and basic character of the carbons was studied by pH measurements. CMC-N carbon was most basic. Air oxidized carbons are reported to have basic properties

Carbons	C1	C2	CMC N
pH	7.44	8.49	8.71

*Table 2.8 pH of carbons in solution*

2.4. 10 TPD of ammonia

CARBON	Acid sites
C1	Weak and moderate
C2	moderate ,strong
CMC-N	Weak, large moderate, strong

**Table 2.9 Temperature programmed Desorption profiles of C1, C2, CMC-N using ammonia as probe molecule**

CMC-N carbon showed the least acidity values with C1 showing the highest

Though the amounts of acidic sites were less in case of CMC-N carbon, they were very strong and it also had a large amount of moderate acidic sites. C1 and C2 showed high acidic sites which were weak to moderate

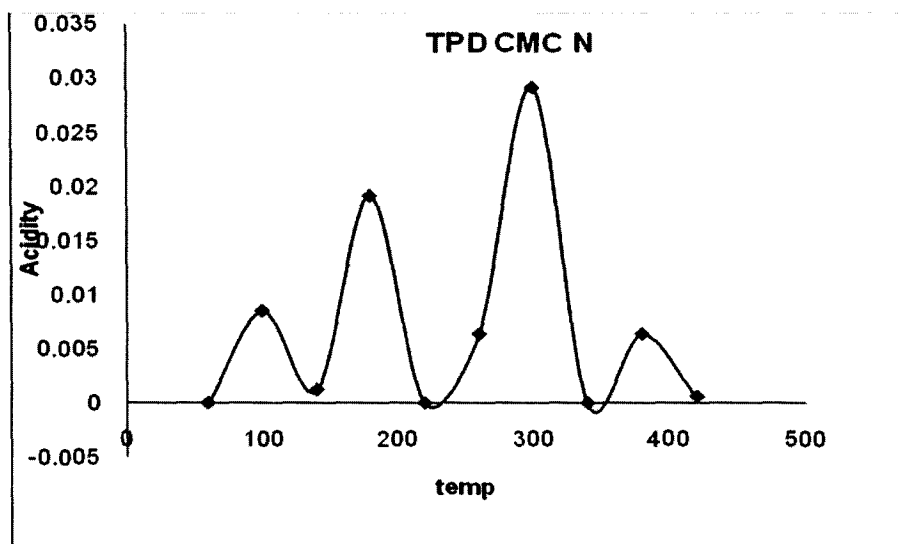


**Fig 2.36 Temperature Programmed Desorption of activated carbon CMC- N using ammonia as probe molecule**

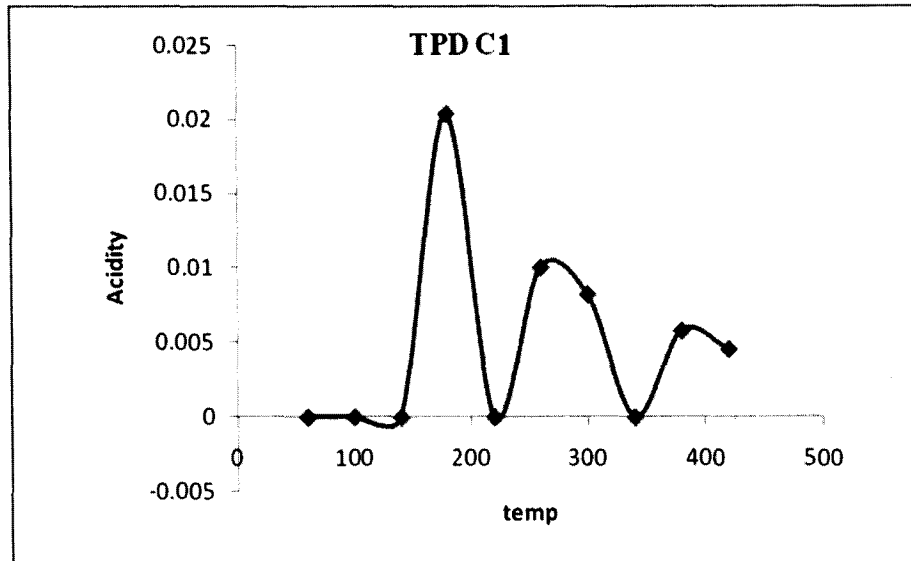


**Fig 2.37** *Temperature Programmed Desorption of activated carbon C1 using ammonia as probe molecule*

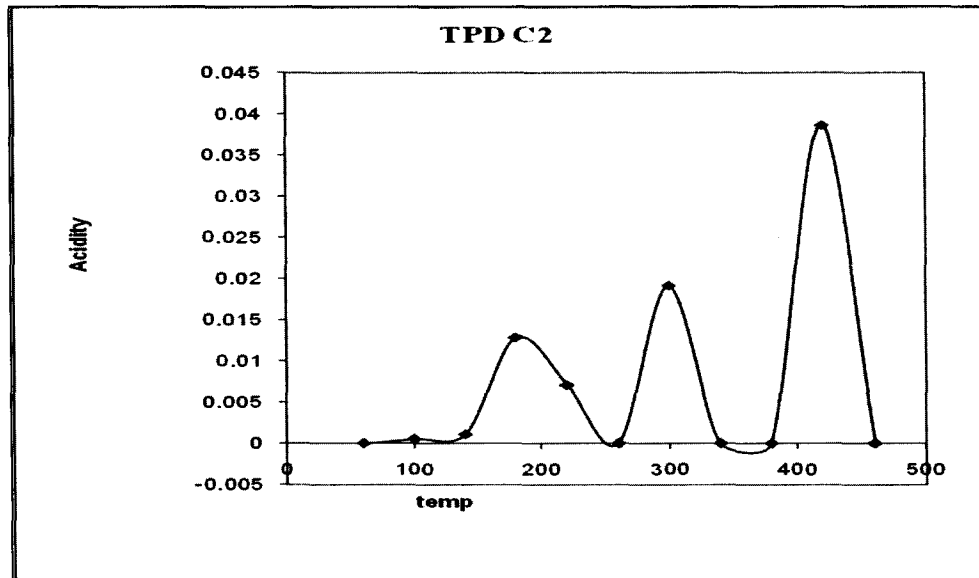


**Fig2.38** *Temperature Programmed Desorption of carbon C2 using ammonia as probe molecule*

#### 2.4.11 Decomposition of hydrogen peroxide.

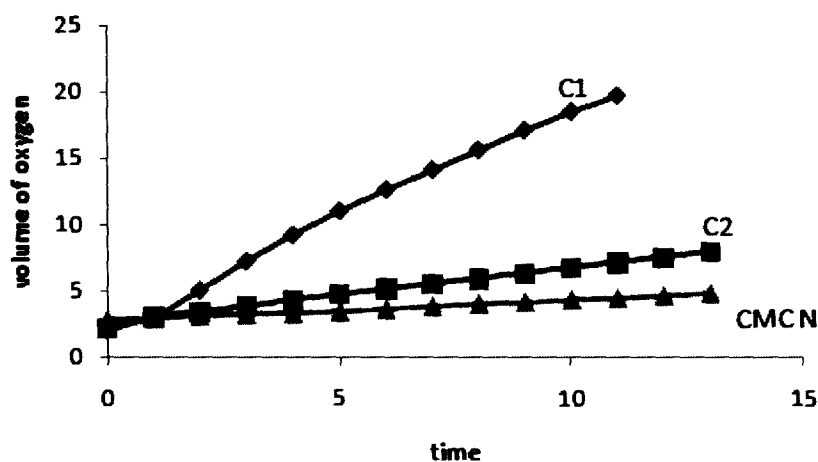


**Fig 2.39** Volume of oxygen evolved on decomposition of hydrogen peroxide using CMC-N, C1 and C2

Decomposition of hydrogen peroxide depended on the strength of acidic sites of carbon [12]. More the strength of the acidic sites, slower is the rate of hydrogen peroxide decomposition. It was found that the CMC-N carbon showed lesser degree of decomposition of hydrogen peroxide indicating that the strength of the acidic sites overrode the effect of basic sites in hydrogen peroxide decomposition. CMC-N had lesser amount of weak acid sites and large amounts of moderate sites. It also possessed some strong acidic sites. Since C1 had more of weak acidic sites, the volume of oxygen evolved on decomposition was most in case of C1, followed by C2 and least by CMC-N. C2 had a fair amount of moderate acidic sites lesser than CMC-N and also strong acidic sites.

#### 2.4.12 Conclusions

- Activated carbon has been synthesized from sodium salt of carboxyl methyl cellulose by low temperature physical activation.
- The activated carbon from CMC-N has high surface area comparable to commercial carbons.
- It has both acidic and basic sites; hence it is amphoteric in nature.
- It has less, but strong acidic sites.
- The solution of CMC-N carbon is basic.
- High porosity and surface functional groups makes it an ideal adsorbent.
- The paramagnetic nature of the carbon makes it a potential material for electrochemical applications.
- Its surface chemistry can be utilized to catalyse reactions.
- Its porosity provides large surface area to support catalyst.

## REFERENCES

1. [aic.stanford.edu/sg/bpg/annual/v01/bp01-04.html](http://aic.stanford.edu/sg/bpg/annual/v01/bp01-04.html)
2. <http://www.freepatentsonline.com/6472343.html>
3. Smisek M and Cerny S, Active Carbons, Elsevier, Amsterdam, 1970
4. Mackay D. M and Roberts P.V, Carbons, 20 (1982) 95
5. Rand B, Marsh H, Carbon, 9 (1971) 79
6. Tourkow K, Siemienieswka T et al, Fuel, 56 (1977) 121
7. Figueiredo J. L, Pereira M.F.R, Freitas M. M. A, Orfao J. J. M, Carbon, 37 (1999) 1379-1389
8. Zawadzki J, Carbon, 16 (1978) 491
9. Garten V.A and Weiss D. E, Rev.Pure and Applied Chemistry, 7 (1957) 69
10. Morterra C, Low M. J. D and Servedia A. G, Carbon, 22 (1984) 5
11. Studebacker M L, Huffmann E W D et al, Ind Eng Chem, 48 (1956) 156
12. Puri B. R and Kalra K. C, Indian Journal of Chemistry, (1969) 149-152.

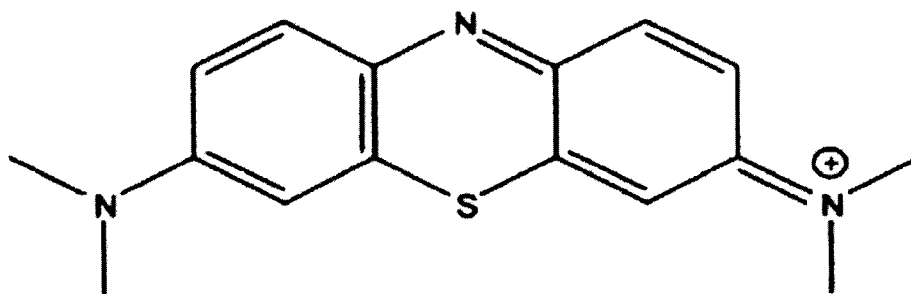
*CHAPTER III*

**ADSORPTION STUDIES**

### 3.1 ADSORPTION OF METHYLENE BLUE

#### 3.1.1 Introduction

Dye pollutants in water have been a major concern. Organic and inorganic dyes are major pollutants since colouring matter is used in wide range of industries like textiles, leather, toys, plastics etc [1]. These dyes are harmful to water systems as they do not allow sunlight to pass through, are toxic to organisms, cause hazards and environmental pollution [2, 3]. The dyes are made up of complex molecular structures which are not biodegradable [4]. The molecular structure of methylene blue is



While several techniques like chemical oxidation, coagulation, flocculation [5], ozonisation [6] and membrane separation [7] etc. have been used, adsorption technique, being the most often used, owing to its simplicity of operations. Various adsorbents such as alumina [8], silica, metal hydroxides have been used. However, activated carbons are widely used for commercial applications such as methylene blue adsorption [9, 12].

Biomass, which is a renewable source for cellulose has been historically used to prepare activated carbons for adsorption of various organic and inorganic substances. Activated carbon has been prepared from palm-tree cobs [13], plum kernels [14], assava peel [15], bagasse [16], jute fiber [17], rice husks [18], olive stones [19], date

pits [20], coir pith carbon [21], fruit stones and nutshells [22]. The surface chemistry and porosity of carbons determines its adsorption properties [23].

Langmuir and Freundlich isotherms are most often used for quantitative studies of adsorption. A simple experiment illustrating both the adsorption isotherms was carried out by J .H Poteiger [24].

Methylene blue adsorption experiments were carried out using different activated carbons using the method reported in [24]

### *3.1.2 Experimental*

#### *Materials*

The following carbons were obtained

1. C1: activated carbon was obtained from SD Fine Chemicals Ltd.
2. C2: activated carbon from coconut shell from IGCL, Kerala
3. CMC-N: activated carbon from CMC

Methylene Blue from Loba Chemie

#### *Method*

In the first run, 20mg of carbon sample was put in 100ml of 25mg/l methylene blue in 7 separate flasks at room temperature. Optical density of the blank solution was first found. The solution was stirred on a mechanical stirrer. At regular intervals, the supernatant solution was centrifuged and the optical density was found out of the clear solution using the colorimeter. The equilibration time was found out for each carbon.

Different weights of the carbon were taken in 100ml of 25mg/l methylene blue, separate flasks at room temperature and kept on the mechanical stirrer for 24 hours. The solution was then centrifuged and the optical density of the clear solution was found. The experiment was repeated for each of the 3 samples with the same weight and period of contact.

Langmuir and Freundlich adsorption isotherms were plotted for adsorption of methylene blue by the above procedure by keeping the equilibration time as period of contact of the carbon with methylene blue.

### 3.1.3 RESULTS AND DISCUSSIONS

#### 3.1.3.1 Equilibration time for methylene blue

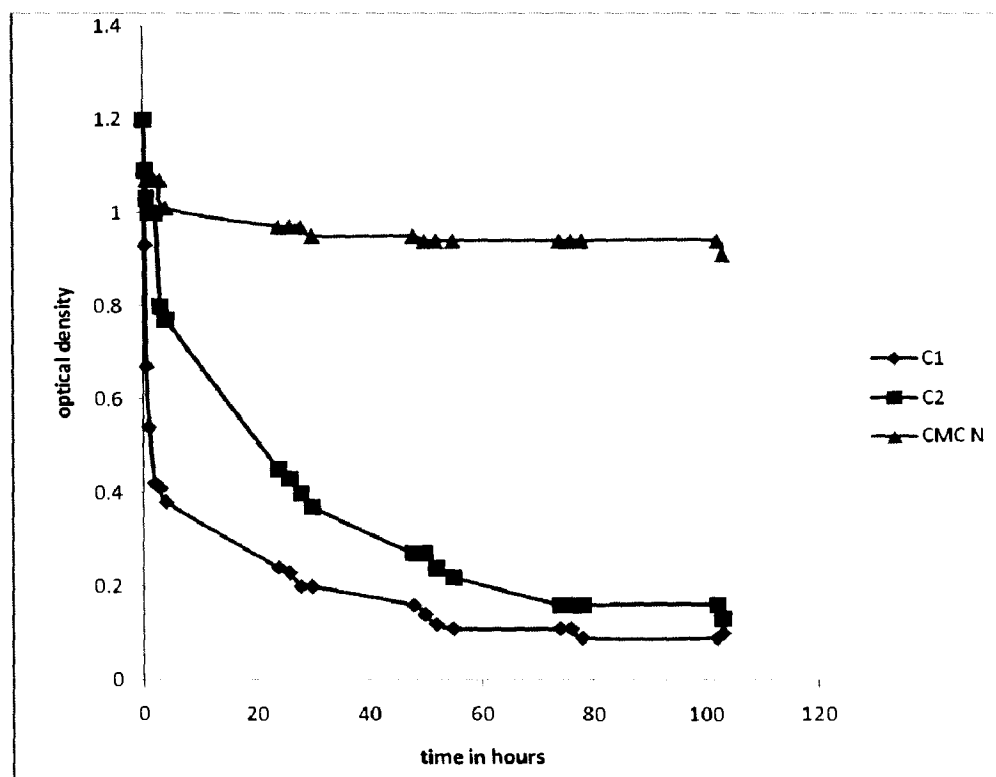


**Fig 3.1 Equilibration time for methylene blue adsorption by activated carbons C1, C2 and CMC N**

The equilibration time for C1 was 48 hrs whereas for C2 was 72 hours. CMC-N showed the least equilibration time as 24 hrs. C1 had more macropores and hence the dye molecule could diffuse faster into the pores and attain equilibrium. Since C2 had more of mesopores as well as acidic sites, the dye molecule took time to reach the pores. Since the acidic sites were less in CMC N, the equilibrium was probably reached faster than the other two carbons.

*3.1.3.2 Comparative study of methylene blue adsorption by different carbons for a fixed weight of sample and a fixed time period*

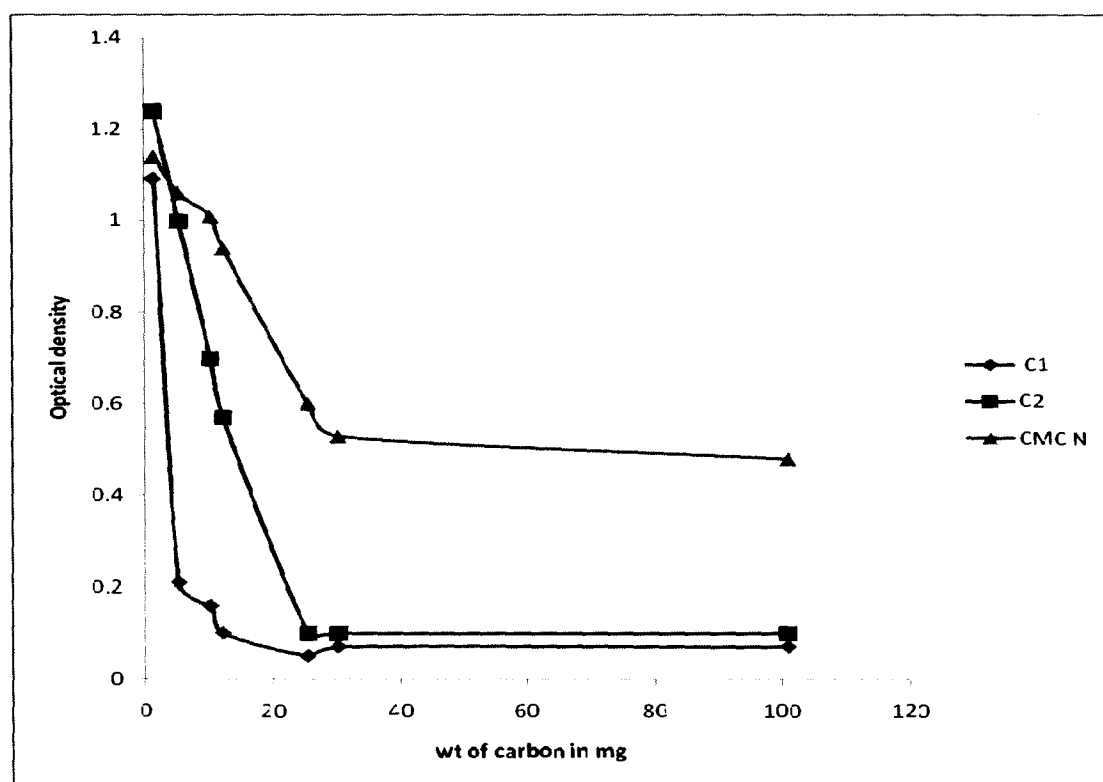


**Fig 3.2** *Comparative study of methylene blue adsorption by different carbons for a fixed weight of sample and a fixed time period*

It was observed that the amount of methylene blue adsorbed varied when the amount was less than 30 mg. However, the adsorption pattern remained steady for weights more than 30 mg. C1 and C2 carbons showed better adsorption of methylene blue as compared to CMC-N.

### 3.1.3.3 Langmuir adsorption isotherms

The adsorption isotherms were plotted based on the adsorption experiments [24].

The Langmuir adsorption isotherm is written as  $1/x = 1/x_m k \cdot 1/c + 1/x_m$  where  $x$  is the amount of solute (Methylene Blue) adsorbed per unit mass of adsorbent (activated carbon),  $x_m$  = the limiting amount of adsorbate that can be taken by per unit mass of the adsorbent and  $c$  is the concentration of the solute in the solution that is in equilibrium with the adsorbent. Thus the plot of  $1/x$  against  $1/c$  should be linear with a gradient of  $1/x_m k$  and intercept of  $1/x_m$  on the  $1/x$  axis.

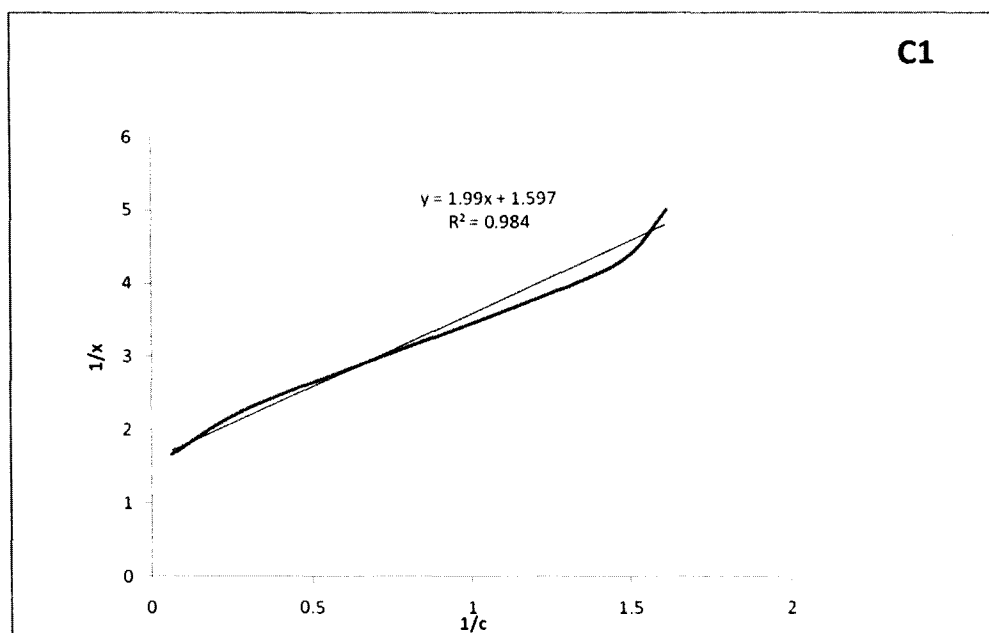
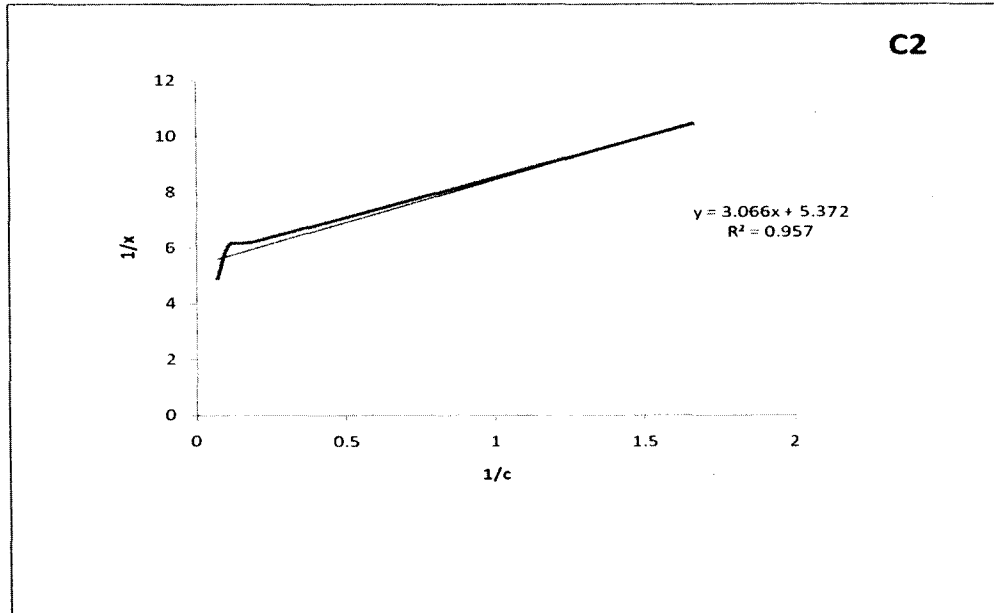
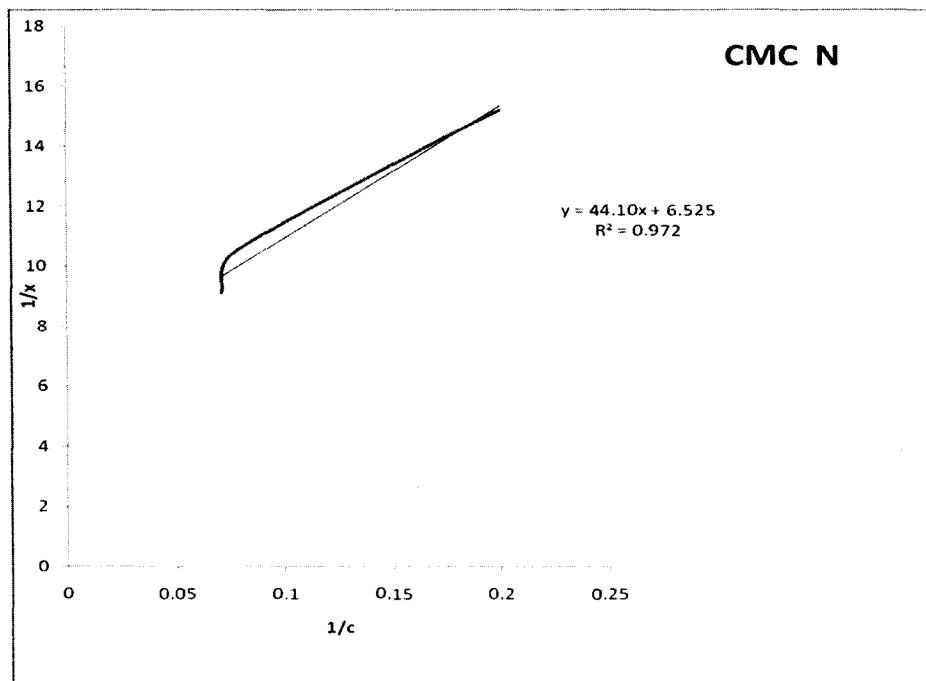


**Fig 3.3 Langmuir's adsorption isotherms for Methylene Blue adsorption by commercial carbon C1**



**3.4 Langmuir's adsorption isotherms for Methylene Blue adsorption by commercial activated carbon from IGCL, Kerala (C2).**



**3.5 Langmuir's adsorption isotherms for Methylene Blue adsorption by carbon synthesized from carboxyl methyl cellulose (CMC-N).**

Carbon	Linear Regression R <sup>2</sup>	Maximum amount adsorbed x <sub>m</sub>	Langmuir's constant K
C1	0.984	0.1626	3.178
C2	0.957	0.1861	16.48
CMC-N	0.972	0.1532	287.8

*Table 3. 1 Linear Regression and maximum amount adsorbed for Langmuir adsorption isotherms for Methylene Blue adsorption by the activated carbons C1 C2 and CMC-N*

#### *3.1.3.4 Freundlich Adsorption Isotherm*

The equation describing the Freundlich isotherm can be defined as

$$\log x = \log K + 1/n \log c$$

where K and n are constants and x and c have the same meaning as in Langmuir isotherm. A plot of log x against log c should be a straight line with a slope of 1/n and an intercept of log K.

Where x is the amount of solute (Methylene Blue) adsorbed per unit mass of adsorbent (activated carbon), x<sub>m</sub>= the limiting amount of adsorbate that can be taken by per unit mass of the adsorbent and c is the concentration of the solute in the solution that is in equilibrium with the adsorbent.

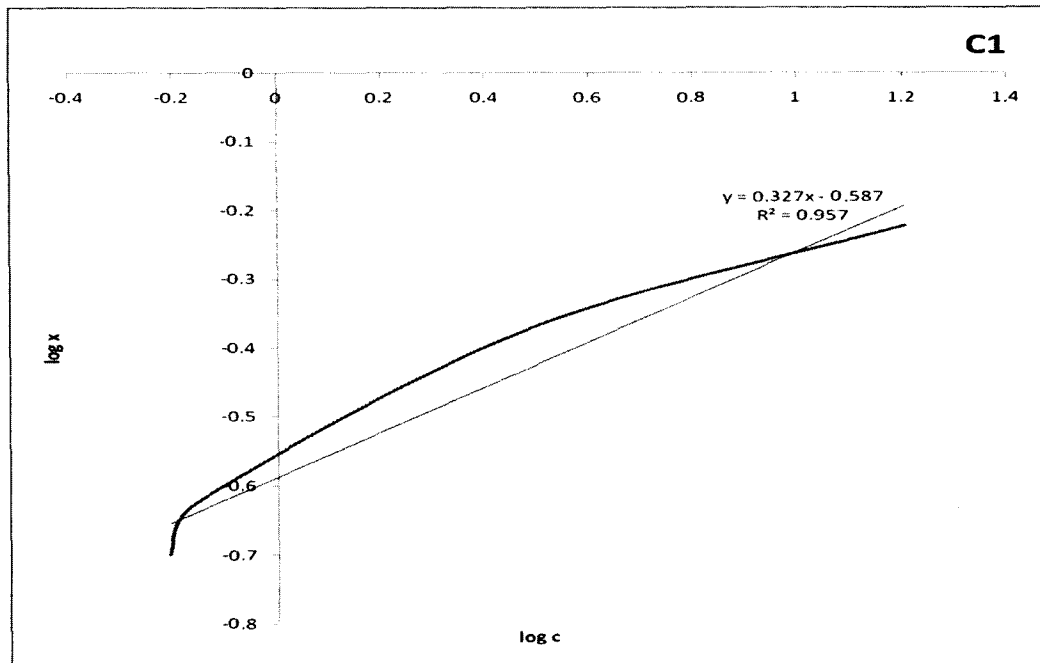


**Fig 3.6** Freundlich adsorption isotherms for Methylene Blue adsorption by commercial activated carbon (C1).

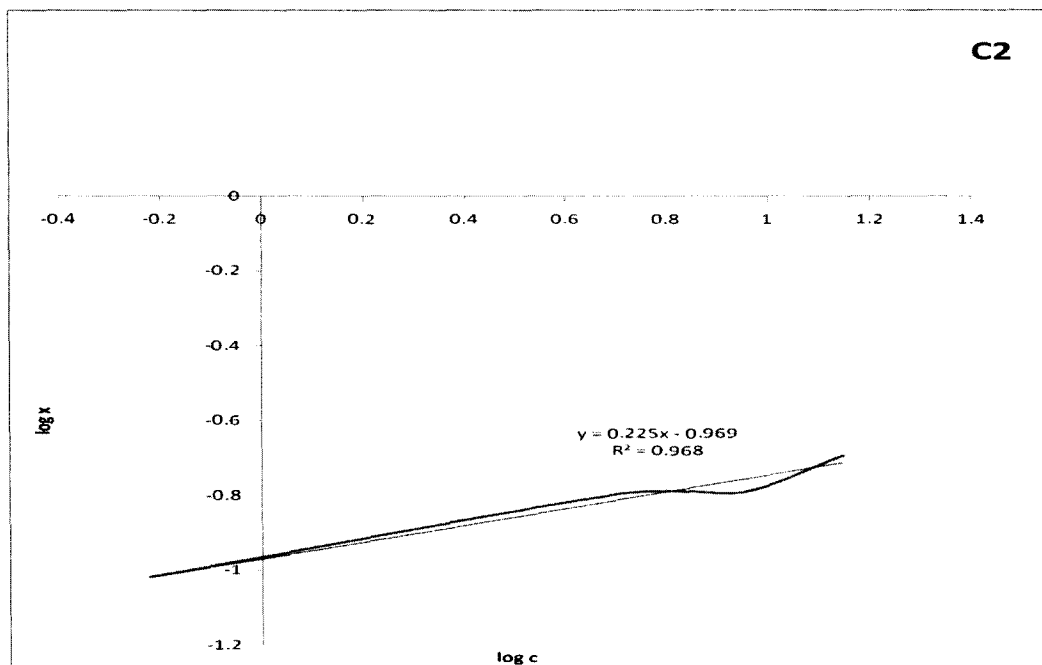


**Fig 3.7** Freundlich adsorption isotherms for Methylene Blue adsorption by commercial activated carbon from IGCL, Kerala (C2).

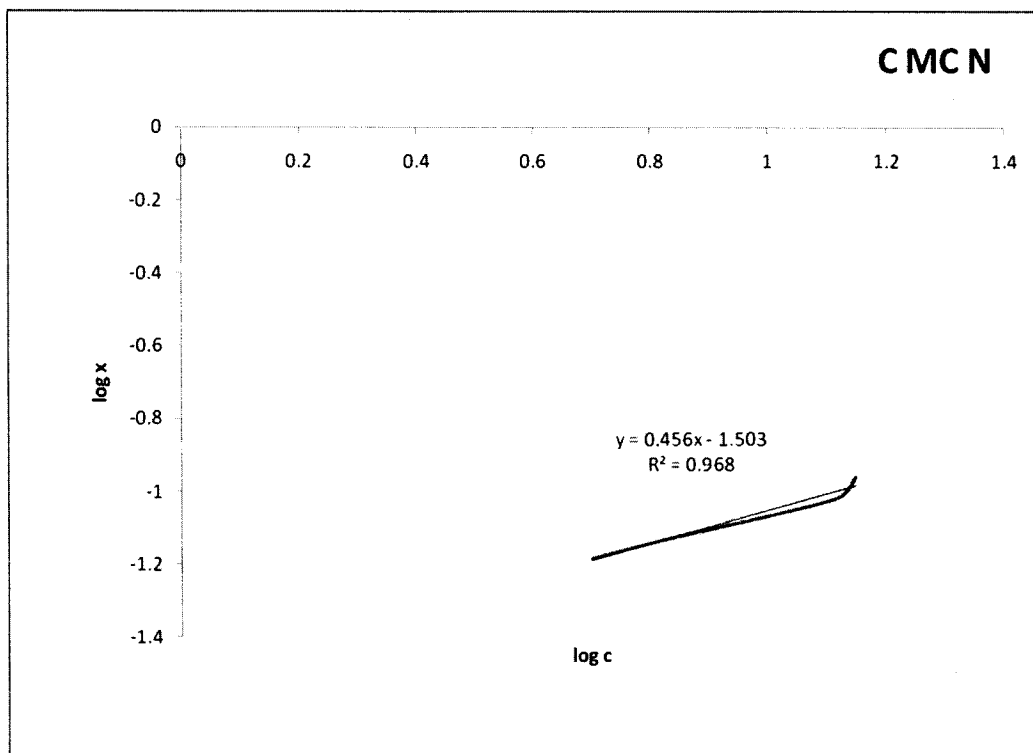


**Fig 3.8 Freundlich adsorption isotherms for Methylene Blue adsorption by activated carbon synthesized from CMC-N**

<b>Carbon</b>	<b>Linear Regression R<sup>2</sup></b>	<b>Constant n</b>
C1	0.957	3.058
C2	0.968	4.444
CMC-N	0.968	2.192

**Table 3.2 Linear Regression and Freundlich adsorption constant for Methylene Blue adsorption by activated carbons C1, C2 and CMC-N**

From the Regression data it follows that all the three carbons obey the adsorption isotherms of Langmuir and Freundlich. The maximum amount of adsorbate adsorbed is by C2 followed by C1 and least by CMC N.

Methylene blue dye is a cationic dye. Its adsorption is facilitated on acidic sites. C1 and C2 have more acidic sites hence the adsorption of methylene blue is more. CMC N shows less adsorption of methylene blue because it has less acidic sites.

The pore size also determines the adsorption capacity of the carbon. Methylene blue being a large molecule the pore diameter should be large enough for the molecule. C1 and C2 shows fairly good adsorption of methylene blue but CMC-N does not. This could be attributed to the surface chemical structure of CMC-N which has less acidic sites. A cationic dye will therefore show adsorption correlating to the acidic sites. This explains why though C2 and CMC-N have mesopores of the same diameter CMC-N shows less adsorption.

## **3.2 ADSORPTION OF METAL IONS: Mn<sup>2+</sup> and Cu<sup>2+</sup>**

### *3.2.1 Introduction*

Industrialisation has brought along with itself a lot of environmental concerns due to the pollution of ground water, soil and air. This may be caused due to the leaching of metal ions, chemicals in water, or release of polluting gases into the atmosphere.

The high risk areas of pollution by metal ions include the vicinity of industrial estates where plants dealing with heavy metals are located. The mining areas are other potential hazardous area where the possibility of mining rejects entering the water bodies is high, thus exceeding the permissible level of contaminants in the water [25].

It has been the constant endeavour of environmentalist to see that the gains of development are not frittered away on huge environmental costs. Hence the need for cost effective development of technology to deal with the negative fallouts has been a prime area of concern.

Adsorption by activated carbon has been widely studied as an effective technique for removing heavy metals from wastewater [26-28]. The removal efficiency is influenced by various factors, such as solution concentration, solution pH and ionic strength, and adsorbent modification procedure. Numerous attempts have been made to correlate the adsorption capacity of activated carbons with their surface areas and pore structures, but such a relationship seems to be limited to pure physical adsorption. In many applications, the adsorption properties of activated carbons may be correlated with the chemical nature of the carbon surface rather than with the surface area and the porosity of the carbon.

Activated carbons being cheap, readily available, easily modified for various applications are most preferred. Silver, gold, lead, cadmium, iron, manganese, copper, nickel, cobalt and chromium are some metal ions where activated carbons have been used for their removal. The most established procedure for removal of the methylene blue dye has been the adsorption by activated carbon [29].

Mostafa (1997) studied adsorption of mercury, lead and cadmium on activated carbon modified with sulphuric acid and observed a significant increase in metal ion adsorption. He proposed that sulphuric acid might introduce acidic surface oxides on the carbon surface [30].

#### **Adsorption of $Mn^{2+}$**

The adsorption of manganese ions from aqueous solution on activated carbons, obtained from olive waste (extracted olive pulp) was studied. These carbons were prepared by water vapour activation and oxidation with  $HNO_3$ . The results show that carbons, produced by chemical and physical activation of solvent extracted olive pulp, are efficient adsorbents in regard to manganese ions. It is established that the adsorbent, obtained from extracted olive pulp by chemical activation with  $HNO_3$ , shows a higher adsorption activity than the carbon, obtained by water vapour activation [31].

The removal of  $Fe^{2+}$  and  $Mn^{2+}$  from ground water has been studied wherein it has been observed that the adsorption of iron and manganese by granular activated carbon varies. It has been attributed to the ionic radius and the electronegativity [32].

### **Adsorption of Cu<sup>2+</sup> ions**

Activated carbon has been found successful to remove Cu. Several attempts have been made to modify the surface chemistry of carbons for metal ion adsorption. Toles et al. (1999) reported that air oxidation of phosphoric acid activated carbons yielded carbons with greater copper uptake capacity. Copper adsorption showed good correlation with surface functional groups [33].

Activated carbon with high capacity for Cu adsorption was prepared from pecan shell by air and phosphoric acid oxidation for development of oxygen or oxygen phosphorous containing groups on the carbon [34]. Similarly activated carbons were also prepared from casurina barks for Cu adsorption [35].

Activated carbon prepared from *Ceiba pentandra* hulls, an agricultural solid waste by-product, for the removal of copper and cadmium from aqueous solutions has been studied. C=O and S=O functional groups present on the carbon surface were the adsorption sites to remove metal ions from solution [36].

We report here the removal of Mn and Cu ions by activated carbon prepared from carboxyl methyl cellulose and commercial activated carbons C1 and C2.

#### *3.2.2 Experimental*

##### **Material**

MnSO<sub>4</sub>, CuCl<sub>2</sub>, EDTA, Eriochrome Black, Sulphon black

All the chemicals used were A R Grade from Loba Chemicals

### *Adsorption of Mn<sup>2+</sup>*

Different weights of carbons in the range of 2 to 50 milligrams was put in 10 ml of 0.005 M MnSO<sub>4</sub> solution and equilibrated for 2 hours with constant stirring at room temperature. The solution was centrifuged and the supernatant titrated against 0.005 M EDTA using Eriochrome Black T as the indicator after adjusting the pH of the solutions. Colour change was from pink to blue.

### *Adsorption of Cu<sup>2+</sup>*

Different weights of carbon (5- 50 mg) was put in 10 ml of 0.005 M of Copper chloride solution and equilibrated for 2 hours with constant stirring at room temperature. The solution was centrifuged and the supernatant titrated against 0.005 M EDTA using Fast Sulphon Black as the indicator. The colour change was from purple to dark green.

Langmuir Adsorption isotherms were plotted.

### 3.2.3 Results and Discussions

The commercial carbons C1 and C2 did not show any significant adsorption of the metal ions. However, CMC-N carbon adsorbed both Mn and Cu ions.

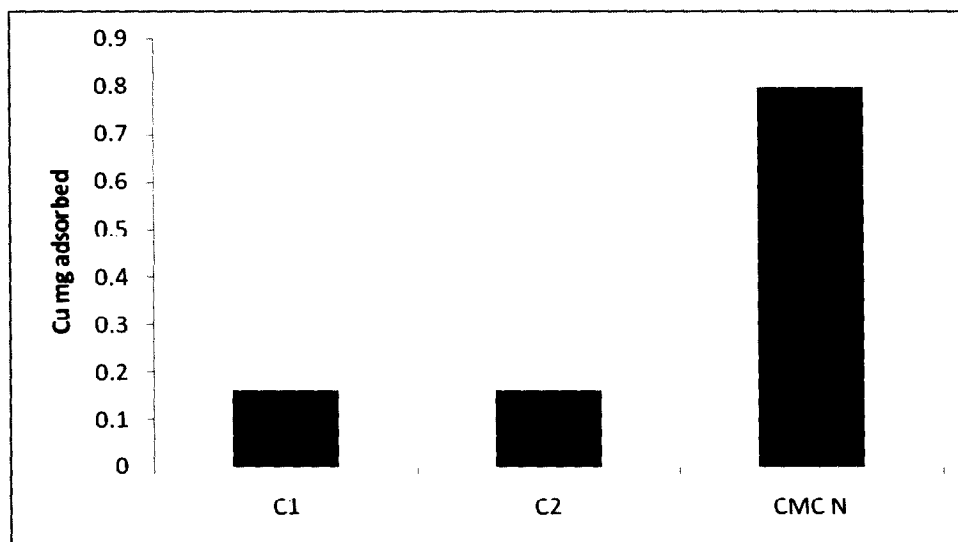


**Fig 3.9 Comparative study of  $\text{Cu}^{2+}$  adsorption by activated carbons C1, C2 and CMC-N when 10 ml of 0.005 M of  $\text{CuCl}_2$  solution was equilibrated for 2 hours**

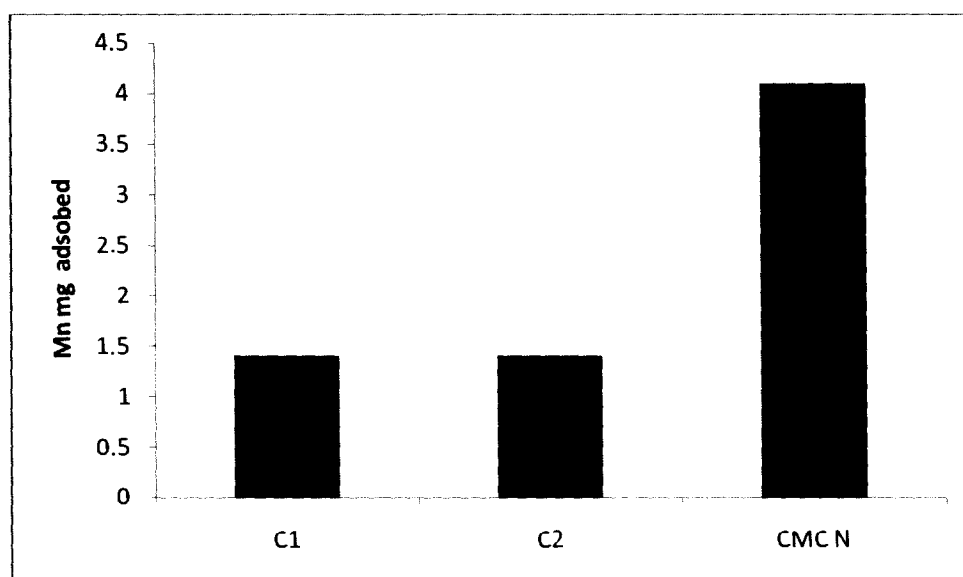


**Fig 3.10 Comparative study of  $\text{Mn}^{2+}$  adsorption by activated carbons C1, C2 and CMC-N when 10 ml of 0.005 M of  $\text{MnSO}_4$  solution was equilibrated for 2 hours**

Langmuir adsorption isotherms were plotted for Mn and Cu ion adsorption by CMC-N.

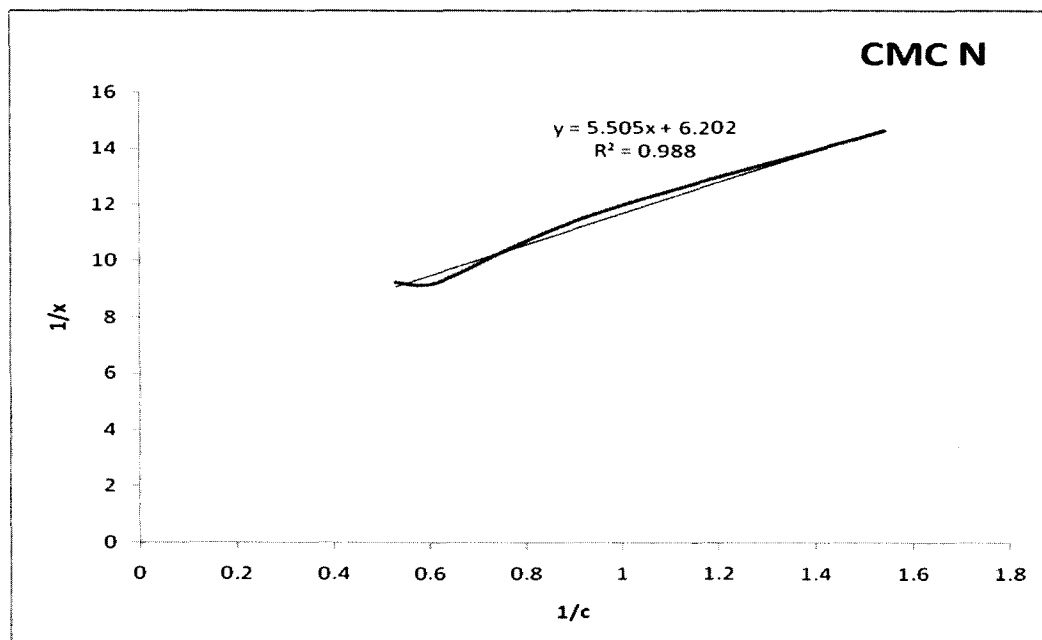


*Fig 3.11 Langmuir's adsorption isotherms for Mn<sup>2+</sup> ion adsorption by CMC N carbon*

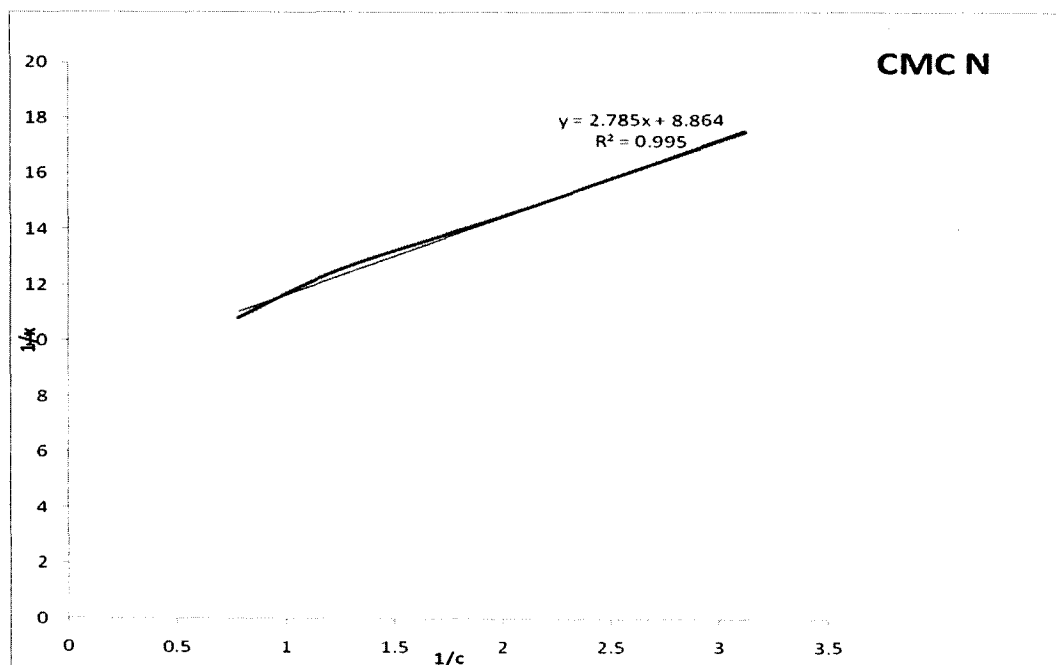


*Fig 3.12 Langmuir's adsorption isotherms for Cu<sup>2+</sup> ion adsorption by activated carbon CMC N*

	Linear Regression R <sup>2</sup>	Maximum amount adsorbed x <sub>m</sub>
Cu <sup>2+</sup>	0.995	0.1128
Mn <sup>2+</sup>	0.988	0.1612

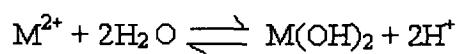
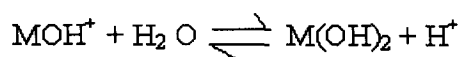
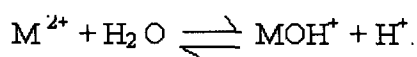
**Table 3.3 Linear Regression constant and the maximum amount of Cu<sup>2+</sup> and Mn<sup>2+</sup> ions adsorbed X<sub>m</sub> calculated from Langmuir adsorption isotherm for adsorption by CMC N carbon**

Amongst the three carbons, it is CMC N which showed adsorption of Cu<sup>2+</sup> and Mn<sup>2+</sup> ions. It obeyed the Langmuir adsorption isotherm. C1 and C2 did not show significant adsorption for Cu<sup>2+</sup> and Mn<sup>2+</sup> ions

CMC-N carbon obtained by physical activation, showed the highest amount of removal of Mn<sup>2+</sup> ions. It has been reported that lactone groups on carbon assist in copper and nickel adsorption.

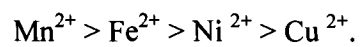
This result most probably arises from the differences between the hydrolysis constants and the ionic diameters of heavy metal ions. The hydrolysis constant for Mn<sup>2+</sup>, Fe<sup>2+</sup>, Ni<sup>2+</sup>, Cu<sup>2+</sup> is 10.7, 10.1, 9.40, 7.53 respectively. The ionic diameters are 80, 76, 72, 70 pm respectively. Since the CMC-N carbon has larger pore size it allowed better diffusion of the metal ions during adsorption.

The hydrolysis reaction equilibrium is mentioned below



According to the magnitude of the hydrolysis constants of heavy metal ions, namely  $\text{MOH}^+$  in the first step is formed and the adsorption event is completed through prompt interaction of the heavy metal ions with negative groups on activated carbon.

According to Pearson's hard acid-hard base theory, hard acid reacts to hard base. The hardness order of acidities of the heavy metal ions used is



$\text{OH}^-$  is also a hard base. CMC- N carbons have strong acid sites as indicated by temperature programmed desorption data using ammonia as a probe [37-38].

### **3.3 COMPARATIVE STUDY OF ADSORPTION ON FUNCTIONALISED AND NON FUNCTIONALISED CARBONS**

#### *3.3.1 Introduction*

Activated carbons have been chemically treated with nitric acid to modify the surface properties for specific applications as has been cited earlier.

To study the effect of nitric acid treatment on the adsorption properties of carbon, the following carbons were functionalized by treating it with 5 M nitric acid for 3 hours using the soxhlet apparatus.

- a) C1: activated carbon obtained from SD -Fine Chemicals Ltd
- b) C2: activated carbon from coconut shell IGCL
- c) CP: meso porous carbon from polymer
- d) CMC-N: activated carbon from CMC

They were labelled FC1, FC2, FCP, FCMC-N respectively.

A comparative study of functionalised and non functionalised carbons was done to study the influence of nitric acid treatment on adsorption properties.

#### *3.3.2 IR of functionalised and non functionalised carbons*

To study whether there was any change in surface functional groups, IR measurements were carried out and a comparative study of functionalised and non functionalised carbons was done.

From the IR, it was evident that there was a modification in the surface functional groups. The intensity of the peak in the 2750 to 3000  $\text{cm}^{-1}$  range increased for all the

carbons. This is attributed to carboxylic acid groups. This region is also indicative of C-H stretching. One can infer that the acidity of the carbons increased with nitric acid functionalisation.

Figures give a comparative view of the change in the surface functional groups.

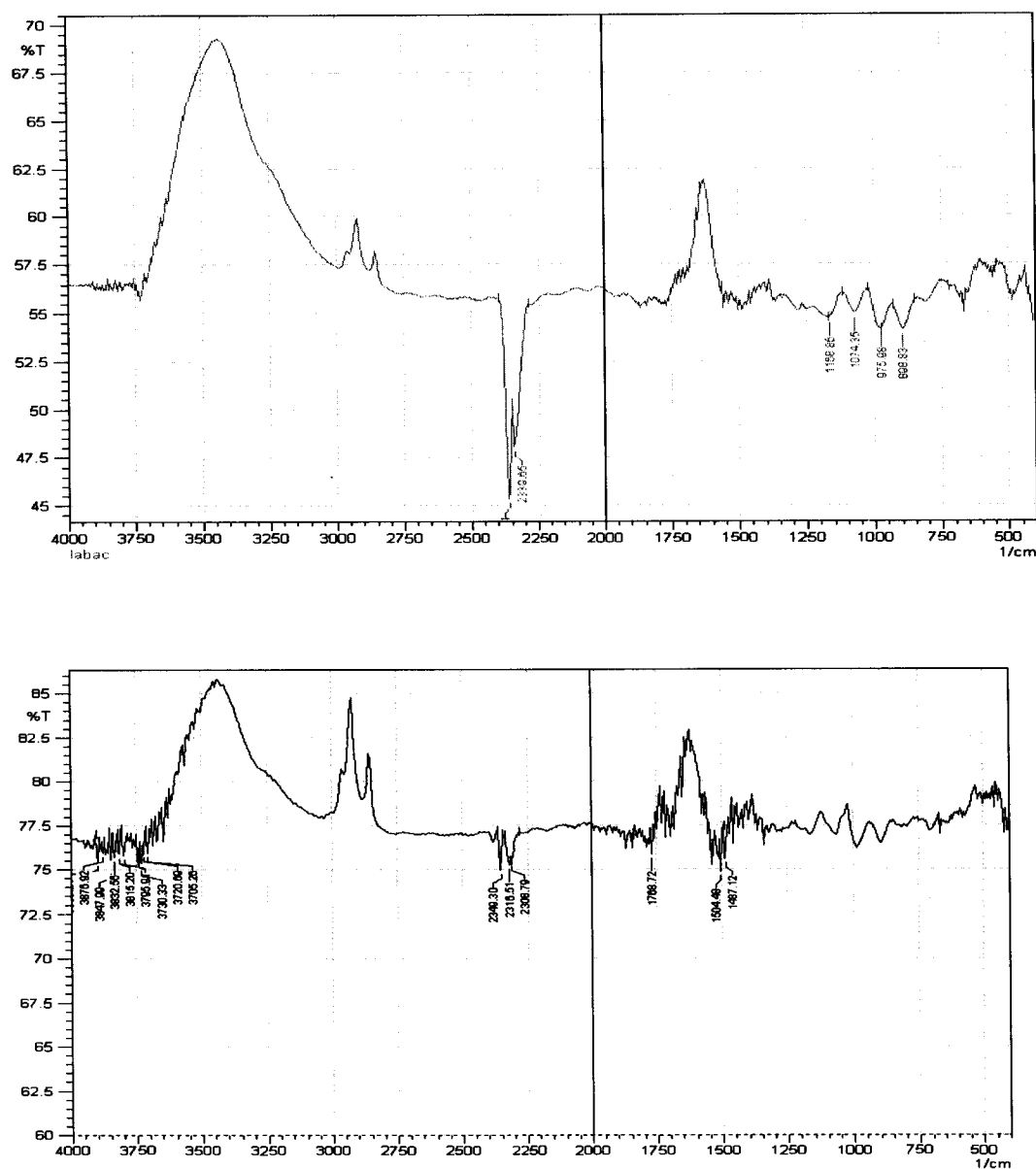


**Fig 3.13 IR of activated carbon C1 and nitric acid functionalized C1**



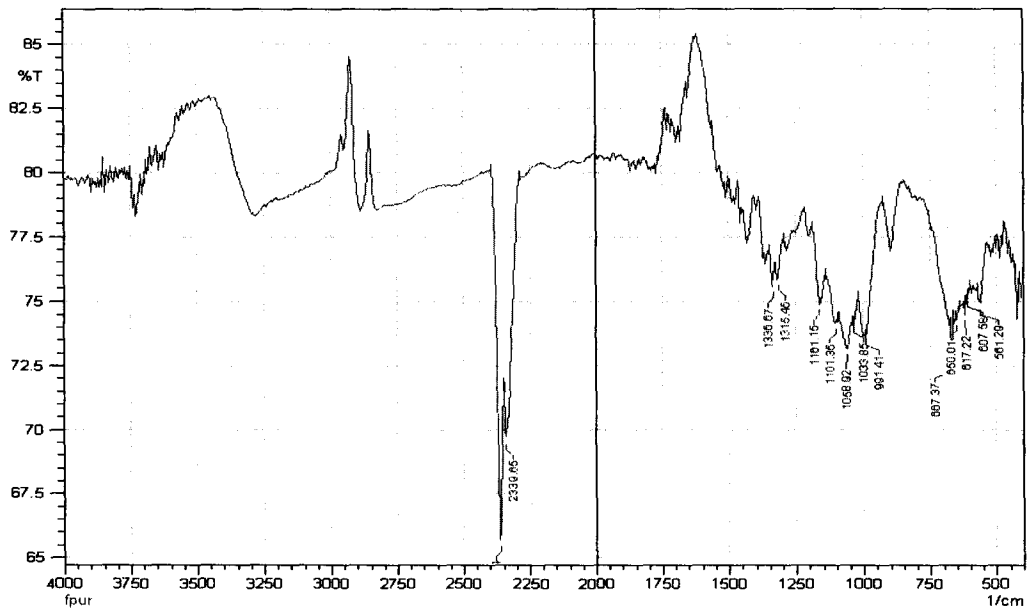
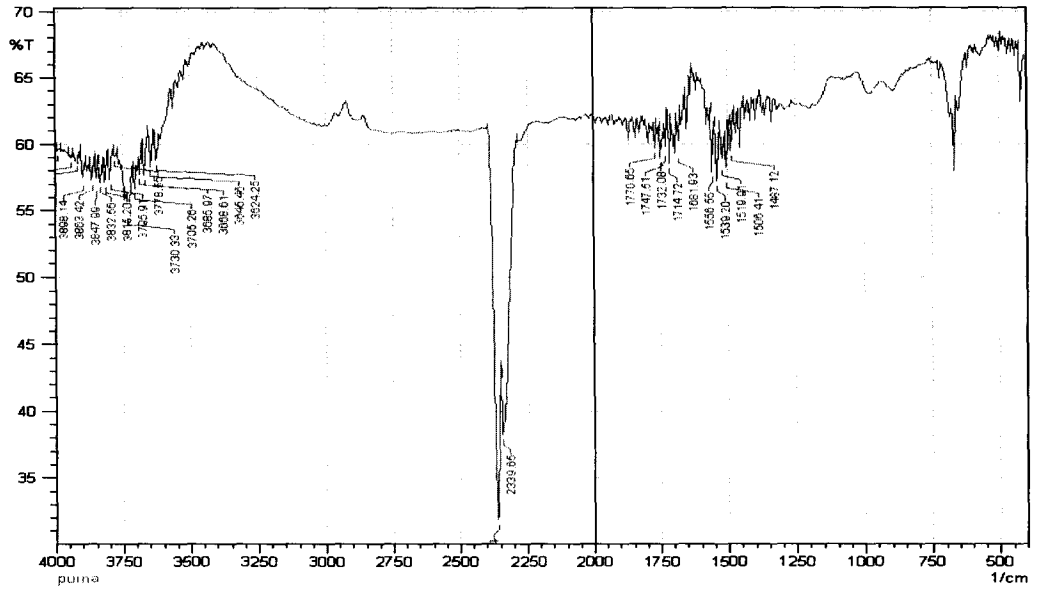


**Fig3.15 IR of activated carbon CP and nitric acid functionalized CP**

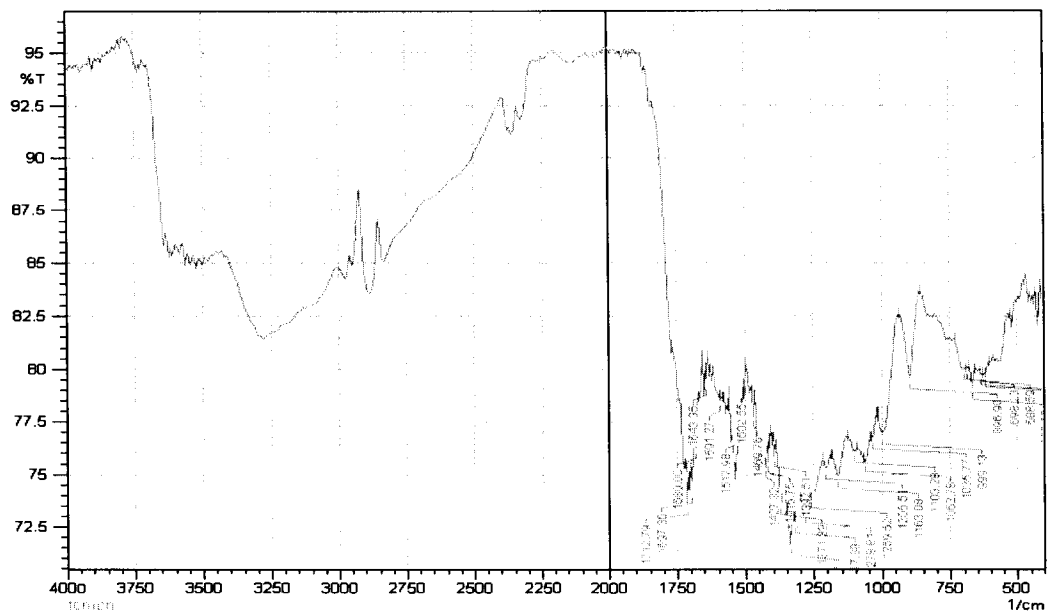
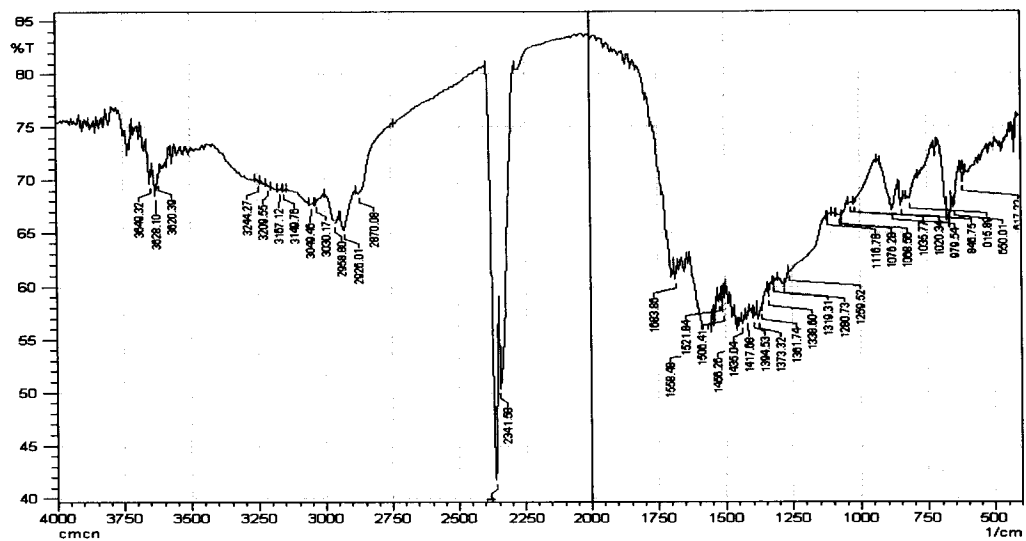


Fig 3.16 IR of activated carbon CMC-N and nitric acid functionalized CMC-N

### 3.3.3 Hydrogen peroxide decomposition

It is a known fact that an increase in acidic groups on carbon catalysts inhibits the decomposition of hydrogen peroxide [39]. To evaluate whether the same was true for the nitric acid functionalized carbons, hydrogen peroxide decomposition was carried out to do a comparative study of functionalized and non functionalized carbons.

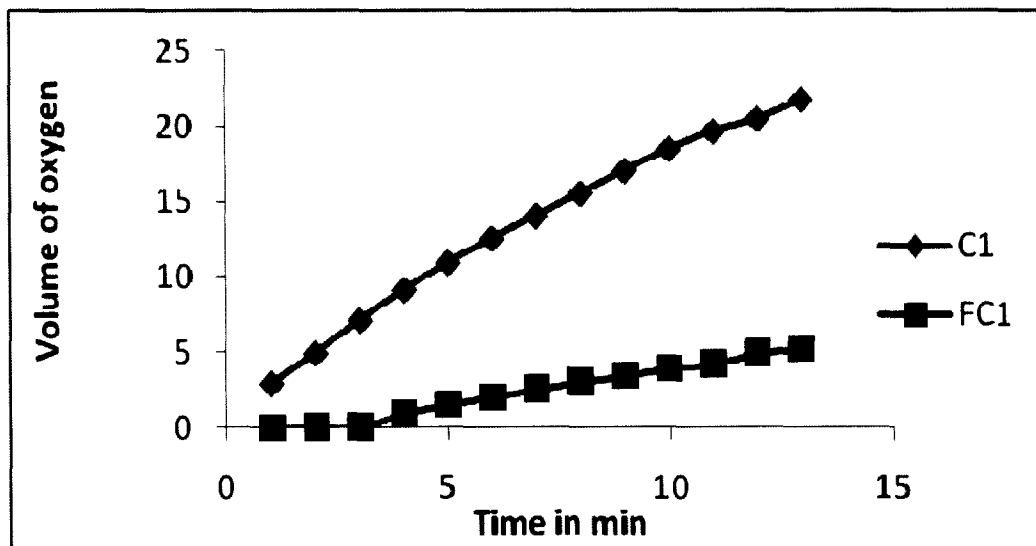


Fig 3.17 Volume of oxygen evolved on  $H_2O_2$  decomposition by activated carbon C1 and nitric acid functionalized C1

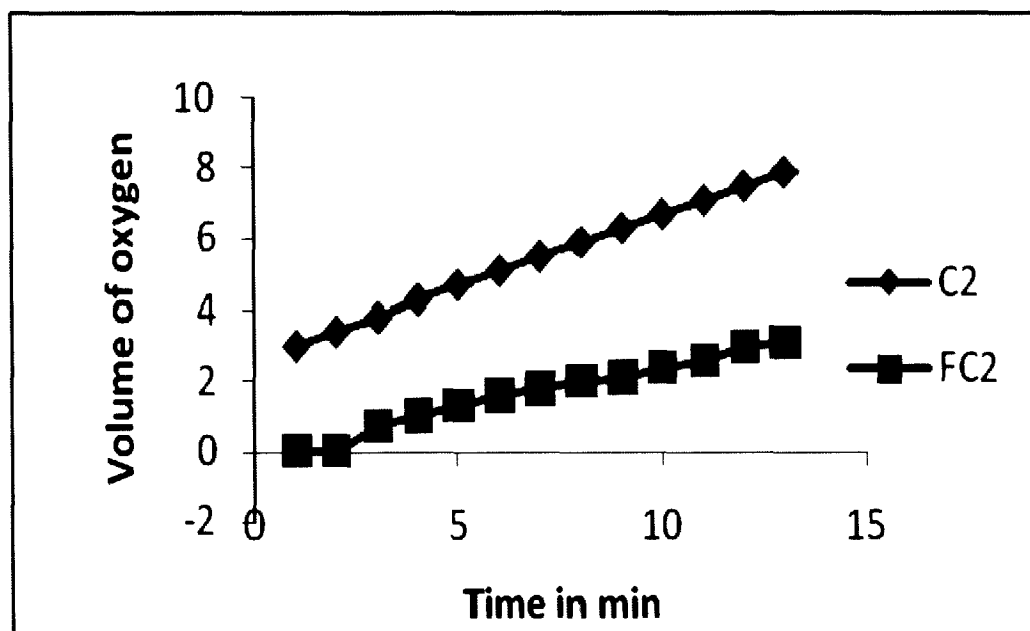
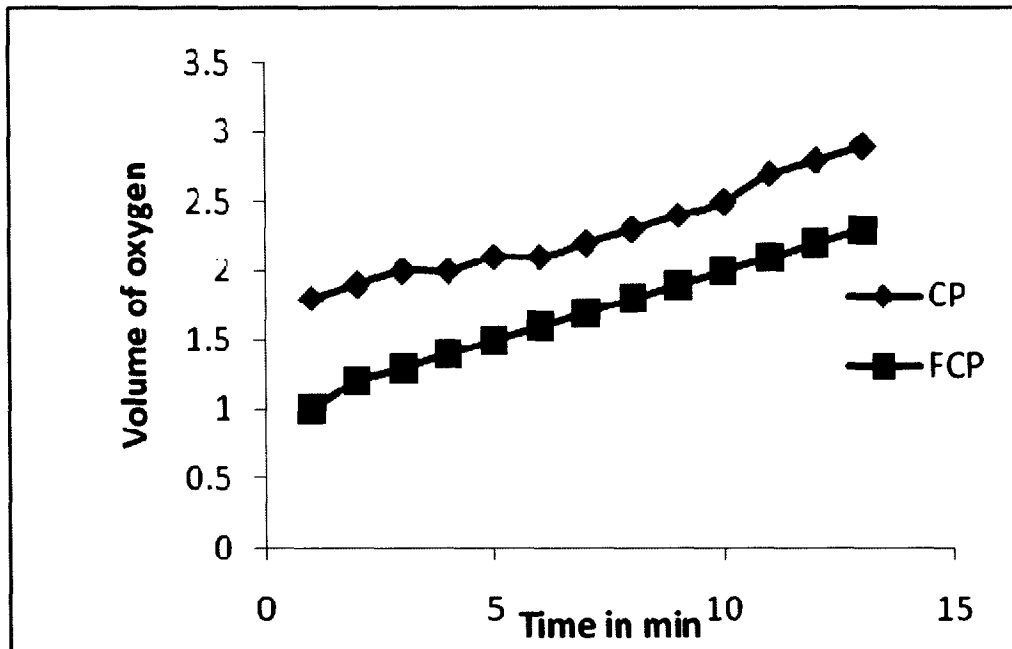
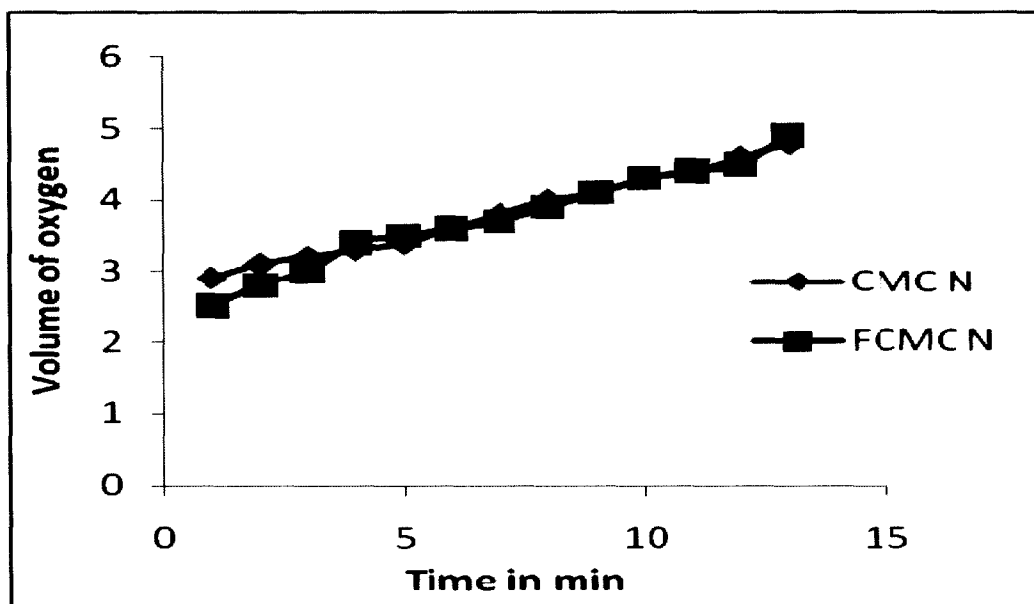


Fig 3.18 Volume of oxygen evolved on  $H_2O_2$  decomposition by activated carbon 2 and nitric acid functionalized C2



*Fig 3.19 Volume of oxygen evolved on H<sub>2</sub>O<sub>2</sub> decomposition by activated carbon CP1 and nitric acid functionalized CP*



*Fig 3.20 Volume of oxygen evolved on H<sub>2</sub>O<sub>2</sub> decomposition by activated carbon CMC N and nitric acid functionalized CMC N*

It is evident from the figures that decomposition of hydrogen peroxide decreased when nitric acid functionalized carbons FC1, FC2 and FCP carbons were used. However for CMC-N carbon there was no much change. The reason could be that CMC-N already had carboxylic groups and nitric acid oxidation did not affect the strength of these to produce any significant results.

### 3.3.4 Methylene Blue adsorption

The functionalized and non functionalized catalyst were methylene blue adsorption and the equilibration time for each catalyst was determined.

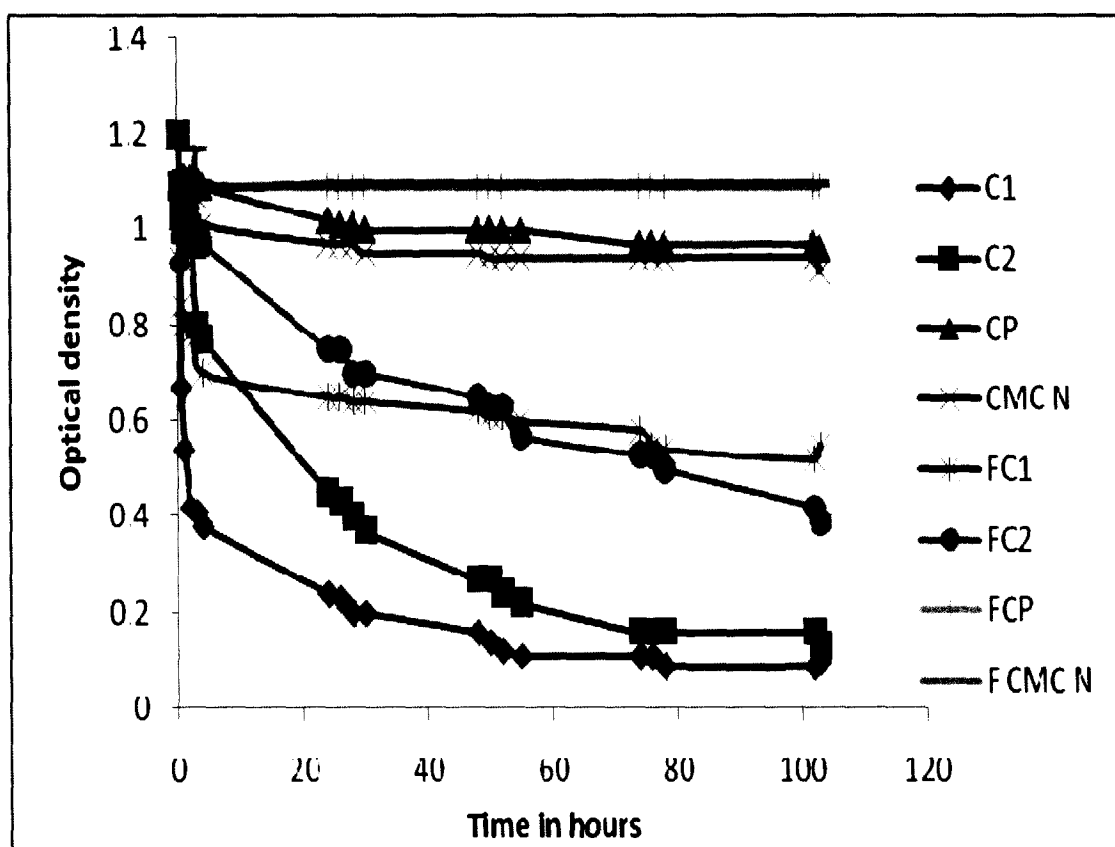


*Fig 3.21 gives the equilibration time for methylene blue adsorption by activated carbons and nitric acid treated carbons*

<b>CARBON</b>	<b>HOURS</b>
C1	50
C2	74
CP	24
CMC-N	24
FC1	76
FC2	100
FCP	1
FCMC-N	1

***Table 3.4 Equilibration time for activated carbon and nitric acid treated carbons for methylene blue adsorption***

It was observed that the equilibration time increased for functionalized C1 and C2 but decreased for functionalized CP and CMC-N carbons.

### 3.3.5. Adsorption of metal ions: $Mn^{2+}$ and $Cu^{2+}$ ions

A comparison was done of metal ion adsorption by activated carbons and their nitric acid treated counterparts.

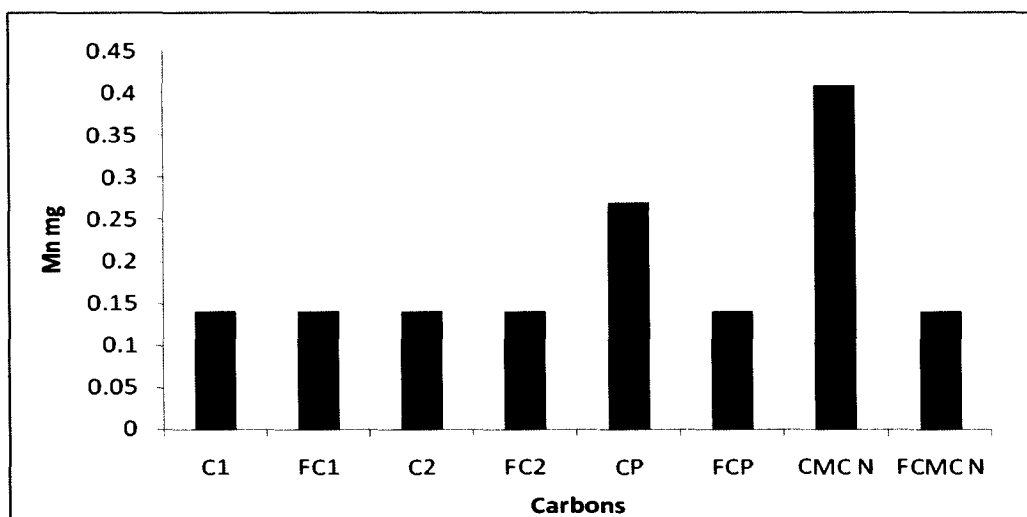


**Fig 3.22 Comparative study of adsorption of Mn ions by nitric acid functionalized and non functionalized activated carbons**

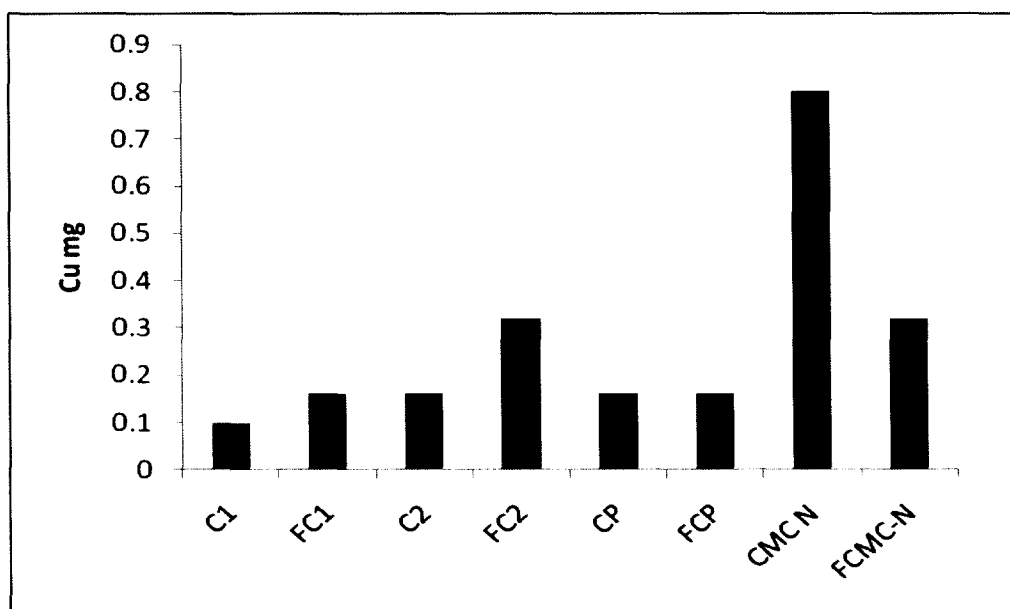


**Fig 3.23 Comparative study of adsorption of Cu ions by nitric acid functionalized and non functionalized activated carbons**

### **3.4 Conclusions**

- Surface functional groups were altered on treatment with nitric acid.
- Due to the increased acidity on carbons decomposition of hydrogen peroxide decreased. CMC-N showed no significant change.
- It was observed that the equilibration time increased for functionalized C1 and C2 but decreased for functionalized CP and CMC N carbons.
- It was observed that there was no adsorption of Mn ions by the treated and untreated carbons except for CMC-N carbon.
- In case of Cu ions adsorption it was observed that there was a marginal increase in case of C1 and slightly more in case of C2.

## **REFERENCES**

1. O. Gulnaz, A. Kaya, F. Matyar, B. Arikan, *Journal of Hazardous Materials*, 108 (2004) 183-188.
2. W. T. Tsai, C. Y. Chang, M. C. Lin, S. F. Chien, H. F. Sun, M. F. Hsieh, *Chemosphere*, 45 (2001) 51-58.
3. K. Santhy, P. Selvapathy, *Bioresource Technology*, 97 (2006) 1329-1336.
4. B. E. Barragán, C. Costa, M. C. Márquez, *Dyes and Pigments*, 75 (2007) 73-81
5. J. J. M. Órfão, A. I. M. Silva, J. C. V. Pereira, S. A. Barata, I. M. Fonseca, P.C.C. Faria, M.F.R. Pereira, *Science*, 296 (2006) 480-489.
6. P. K. Malik, S. K. Saha, *Separation and Purification Technology*, 31 (2003) 241-250.
7. G. Ciardelli, L. Corsi, M. Marussi, *Resource Conservation and Recycling*, 31 (2001) 109-113.
8. S. Y. M. Josefa, E. De Oliveira, *Advance Environmental Research*, 7 (2003) 263-272.
9. F. Wu , R. Tseng, *Journal of Colloid and Interface Science*, 294 (2006) 21-30
10. D. J. Malik, V. Strelko Jr, M. Streat, A. M. Puziy, *Water Research*, 36 (2002) 1527-1538.
11. F. N. Arslanoglu, F. Kar, N, *Arslan Journal of Food Engineering*, 71 (2005) 156-163.
12. S. Senthilkumaar, P. R. Varadarajan, K. Porkodi, C. V. Subbhuraam, *Journal of Colloid Interface Science*, 284: (2005) 78-82.

13. J. Avom, J. K. Mbadcam, C. Noubactep, P. Germain, *Carbon*, 35 (1997) 365-369.
14. F. C. Wu, R. L. Tseng, R. S. Juang, *J. Hazard. Mater*, 69 (1999) 287-302.
15. Rajeshwarisivaraj, S. Sivakumar, P. Senthilkumar, V. Subburam, *Bioresour. Techno*, 80 (2001) 233-235.
16. W. T. Tsai, C. Y. Chang, M. C. Lin, S. F. Chien, H. F. Sun, M. F. Hsieh, *Chemosphere* 45 (2001) 51-58.
17. N. H. Puan, S. Rio, C. Faur, L. L. Coq, P. L. Clorrec, T. H. Nguyen, *Carbon for Energy storage and Env Protection*, 44 (2006) 2569-2577.
18. S. Senthilkumaar, P. R. Varadarajan, K. Porkodi, C. V. Subbhuraam, *Sci.* 284 (2005) 78-82.
19. N. Yalcin, V. Sevin, *Carbon* 38 (2000) 1943-1945.
20. A. H. El-Sheikh, A. P. Newman, *J. Anal. Appl. Pyrol*, 71 (2004) 151-164.
21. B. S. Girgis, A. A. El-Hendawy, *Micropor. Mesopor. Mate*, 52 (2002) 105-117.
22. D. Kavita, C. Namasivayam, *Biores. Techno*, 98 (2007) 14-21.
23. M. Fernando, R. Pereira, S. F. Soares, J. J. M. Orfao, J. L. Figueiredo, *Carbon*, 41 (2003) 811-821.
24. J. H. Potgieter, *Journal of Chemical Education*, 68 (1991) 4.
25. A. E. Q. M. Tata Energy Research Institute, Report No 93/EE/63, 1997.
26. M. O. Corapcioglu, C. P. Huang, *Water Res*, 21 (1987) 1031-1044.
27. M. R. Matsumoto, A. S. Weber, J. H. Kyles, *Chem. Engrg. Comm*, 86 (1989) 1-16.

28. B. E. Reed, M. R. Matsumoto, *J. Envir. Engrg, ASCE*, 119 (1993) 332-348.
29. I. Uzun, F.G. Uzel, *Turk J Chem*, 24 (2000) 291 - 297.
30. M. R. Mostafa, *Adsorption Sci. Technol*, 15 (1997) 551-557.
31. D. Savova, T. budinova, N. Petrov, *Belgium Chem Com*, 38 (2006) 283-288.
32. B. J. Ahmad, W. H.Cheng, W. M. Low, N. Ali, M. I. M. M. Noor, *Desalination*, 182 (2005) 347-353.
33. C. A. Toles, W. E. Marshall, M. M. Johns, *Carbon*, 37 (1999) 1207-1214.
34. S.A Dastgheib, D. A Rockstraw, *Carbon*, 39 (2001) 1849-1855.
35. S. Mohan, K. Sumitha, *Environmental Engineering Science*, 25 (2008) 497-506.
36. M. Rao, A. Ramesh, P. Chandra Rao, K. Seshiah, *Journal of Hazardous Materials*, 124 (2006) 123-129.
37. J. E. Huheey, "Inorganic Chemistry", Harper International Edition, New York, (1978) 20.
38. N. Tunal, S. Ozkar, "Inorganic Chemistry", Gazi Univ. Press No: 185 (1993).
39. B. R. Puri, K. C. Kalra, *Indian Journal of Chemistry*, 7 (1969) 149-152.

***CHAPTER IV***

**ADSORPTION ON C-TiO<sub>2</sub>**

**AND PHOTOCATALYSIS**

#### 4.1 Introduction

Photocatalysts are being increasingly used for environmental applications. The ability to photodecompose the contaminants in ordinary sunlight without any sophisticated machinery makes it commercially viable in day to day applications.

TiO<sub>2</sub> is one such photocatalyst which has been extensively used for degradation of pollutants [1]. Titanium dioxide is a semiconductor whose photocatalytic activity arises due to the favourable band gap [2] of the semiconductor.

It is amphoteric in nature and has high room temperature resistivity. It is insoluble in water and acids and becomes basic on heating. TiO<sub>2</sub> has a melting point of 1610° C and boiling point below 3000° C [ 3].

The treatment of dilute water borne pollutants by semiconductor photocatalysis is one of the fast growing areas in terms of academic research and commercial activity. The potential benefits of semiconductor photocatalysis can be reflected by the large number of literature generated in the past decade. Among many chalcogenides and metal oxide semiconductors, colloidal TiO<sub>2</sub> particles are frequently used as the photocatalyst. This is because TiO<sub>2</sub> is non-toxic, chemically stable, and possesses relatively high photocatalytic activity. Laboratory studies have demonstrated that organic compounds such as alcohols, carboxylic acids, phenolic derivatives, and chlorinated aromatics can be readily mineralized by TiO<sub>2</sub> into harmless carbon dioxide, water, and simple mineral acids, using molecular oxygen as the primary oxidant.

## 4.2 Phases of TiO<sub>2</sub>

TiO<sub>2</sub> exists in three polymorphic forms –Rutile, Anatase and Brookite – built from (TiO<sub>6</sub>) octahedra whose chains are differently assembled [4-5].

Rhombohedral Brookite is rather unstable and is rarely encountered in chemical applications [6]. It has a rather complex structure with both edge and corner sharing. Anatase on the other hand is most widely investigated due to its high surface area and other favourable properties. Here the cation, Ti<sup>4+</sup> is surrounded by an octahedron of oxygen anions. There is an edge – shared bonding amongst the [TiO<sub>6</sub>] octahedra and 4 edges are shared by the octahedron. In rutile, likewise, the cation is surrounded by the octahedron of anions. The octahedron in rutile is not regular and shows slight orthorhombic distortion; while the octahedron in anatase is significantly distorted [7]. In rutile there is edge sharing along the C – axis to form chains which link to each other by corner O atoms to form three dimensional frameworks.

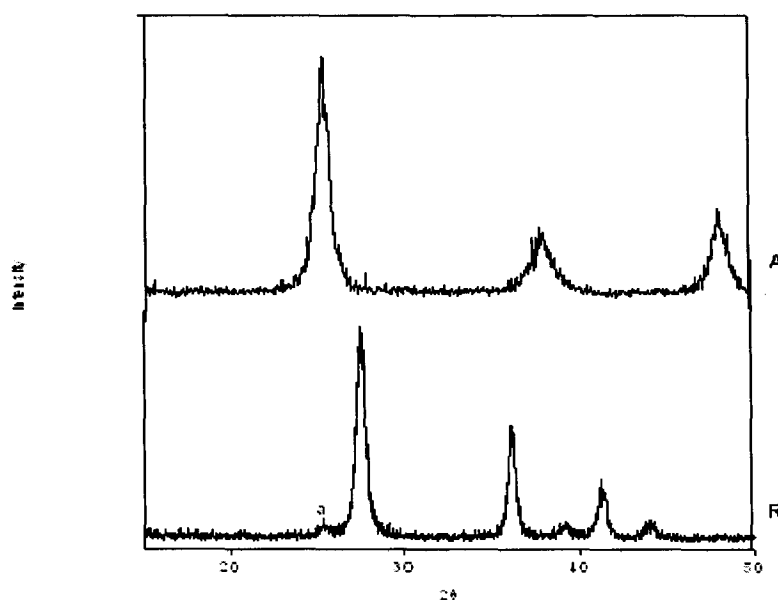


*Fig 4.1 XRD profiles of Anatase (A) and rutile (R) phase of TiO<sub>2</sub>*

Thus the number of edges shared by an octahedron increase from 2 (out of 12) for brookite, 3 for rutile and 4 for anatase [8]. Fig 4.1 gives XRD profiles of Anatase (A1) and rutile (R1) phase of  $\text{TiO}_2$ .

The characteristic peaks for the rutile and anatase forms of  $\text{TiO}_2$  and the corresponding (hkl) values are as reported in Table 4.1 [9].

Rutile			Anatase		
d	I/I <sub>0</sub>	hkl	d	I/I <sub>0</sub>	Hkl
3.2483	100	110	3.5169	100	101
3.1871	20	111	2.3785	21	004
1.6874	69	211	1.8925	33	200

**Table 4.1 Characteristic peaks of rutile and anatase  $\text{TiO}_2$**

### 4.3 Mechanism of photodegradation

When photocatalyst titanium dioxide ( $\text{TiO}_2$ ) absorbs Ultraviolet (UV) radiation from sunlight or illuminated light source (fluorescent lamps), it will produce pairs of electrons and holes. The electron of the valence band of titanium dioxide becomes excited when illuminated by light. The excess energy of this excited electron promoted the electron to the conduction band of titanium dioxide therefore creating the negative-electron ( $e^-$ ) and positive-hole ( $h^+$ ) pair. This stage is referred as the semiconductor's 'photo-excitation' state. The energy difference between the valence band and the conduction band is known as the 'Band Gap'. Wavelength of the light necessary for photo-excitation is 388 nm [10].

$$1240 \times (\text{Planck constant, } h) / (\text{band gap energy, } 3.2 \text{ eV}) = 388 \text{ nm [10]}$$

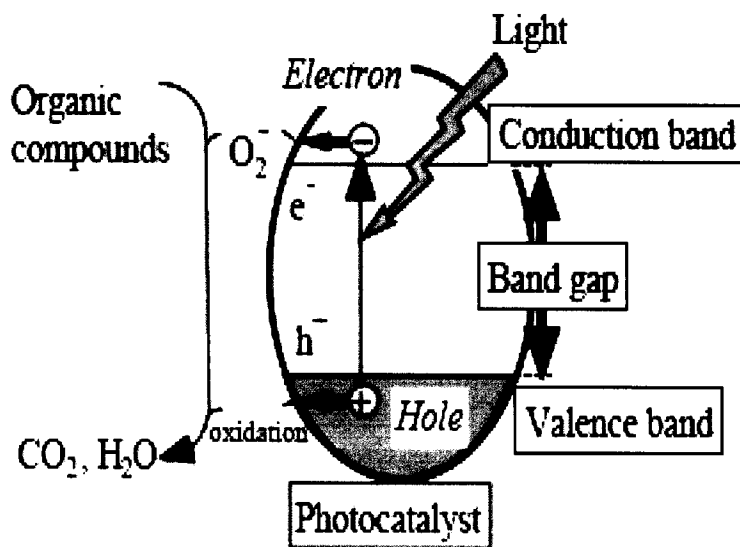


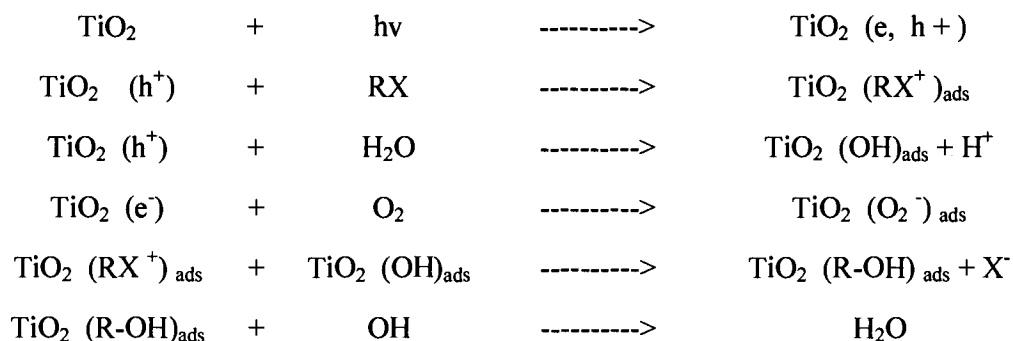
*Fig 4.2 Mechanism of photocatalytic degradation of a dye molecule*

Under illumination, the TiO<sub>2</sub> photocatalyst absorbs photons with energy equal or higher than its band gap energy (385 nm). This will delocalize a valence electron and excite it to the conduction band of the semiconductor. These photoexcited charge carriers can initiate the degradation of the adsorbed chemical species by one or more forms of electron transfer reactions. Alternatively, they can recombine radiatively or non-radiatively and dissipating the input energy as heat.

As in classical heterogeneous catalysis, the size of TiO<sub>2</sub> particles usually defines the surface area in a system available for adsorption and decomposition of the organic pollutants. In many occasion, nanosized TiO<sub>2</sub> particles are considered desirable.

The TiO<sub>2</sub> mediated oxidation of coloured pollutants such as dyes may occur by the process known as photosensitization. In this process a coloured compound adsorbed on to the TiO<sub>2</sub>, absorbs radiation in the visible range, becomes photochemically excited, and transfers an electron to the semiconductor particle which, in turn, reduces molecular O<sub>2</sub> to form a superoxide anion radical. The radical generated from the dye may then undergo degradation reactions possibly with other dye molecules, with super oxide anion, or other active oxygen species that might be generated.

The usual mechanistic steps of TiO<sub>2</sub>/UV process are as in Scheme 4.1 below.



*Scheme 4.1 Mechanism for the TiO<sub>2</sub>/UV process*

#### 4.4 Synthesis of pure and suggested TiO<sub>2</sub>

Anatase is known to be metastable with respect to rutile under all conditions of temperature and ambient pressure [11-13]. Factors like temperature, pH, type of solvent, route of synthesis, presence of certain ions in solution are known to influence the phase composition [14].

In most synthesis routes, employment of lower synthesis temperatures (< 500°C) generally yields anatase phase whereas higher temperatures yield predominantly rutile phase [15-21]. However the synthesis of rutile phase around room temperature has also been reported [23].

TiO<sub>2</sub> nano particles have been synthesized by several methods. Some of them being thermal oxidation of Ti, plasma spraying,, anodization and chemical vapour deposition [7]. But all these techniques require special apparatus, which is a major disadvantage. Highly active nanosize TiO<sub>2</sub> is also prepared by sol-gel route, either using Ti alkoxide or chlorides as the source of Ti [8]. It can also be obtained by the hydrothermal treatment of the alkoxide gel [11]. Moreover high cost of alkoxide limit commercialization of this process

S. Yang et al. extended the growth unit model of anion co-ordination polyhedron to phase formation in liquid reaction systems. As per that, there exists a competition among the rutile and anatase growth units in a liquid reaction system. Owing to the low formation energy, intense structure and short bond length of Ti-O in rutile, its growth unit is more stable and appears more at lower temperature. So rutile TiO<sub>2</sub> could also be obtained at lower temperatures. Phase formation is also influenced by the presence of certain anions. It has been reported that presence of sulphate anions

gives anatase phase while the presence of perchlorate anions in the thermolysis of a very acidic solution of  $\text{TiCl}_4$  leads to only rutile phase [23-24].

It is well known that there are two routes in sol - gel synthesis depending on the chemical nature of the precursors [25].

- i. Aqueous route: It is based on inorganic salts dissolved in water.
- ii. Metal – organic route : Alkoxides dissolved in organic solvents.

#### 4.5 TiO<sub>2</sub> on Supports

To enhance the photocatalytic activity of TiO<sub>2</sub>, various materials have been used as supports such as Al<sub>2</sub>O<sub>3</sub> and SiO<sub>2</sub> [27], cellulose and activated carbons [28]. The purpose is to concentrate the organic compounds around the loaded TiO<sub>2</sub> catalyst.

It has been observed that carbon supports for TiO<sub>2</sub> gave better photocatalytic activity [29]. There is a synergy created between the acid and basic sites of TiO<sub>2</sub> and the surface area and porosity provided by the carbon [30]. The sol – gel synthesis of inorganic and carbonaceous supports or catalysts, is a frequently used method to enhance pore volumes where many reactions in the gas phase is carried out [31-38].

In the case of inorganic solids, the method involves the hydrolysis and condensation of inorganic alkoxides. One of the most commonly used techniques to prepare carbonaceous materials is the aqueous poly condensation of resorcinol with formaldehyde, producing organic polymers. When they are pyrolysed in an inert atmosphere, carbon aerogels or xerogels are obtained [35-37].

TiO<sub>2</sub>/C composite xerogels and aerogels were obtained by polymerization of mixture of resorcinol, formaldehyde and tetrabutyl orthotitanate. Samples so obtained were dried with supercritical CO<sub>2</sub> to obtain aerogels or at 110<sup>0</sup>C in an oven to obtain xerogel. The aerogel was prepared with two different percentages of TiO<sub>2</sub> contents of 30 and 49%. The aerogel as well as the xerogel were subsequently carbonized in an inert atmosphere of 500 to 900 <sup>0</sup>C [39].

Composites of Carbon/TiO<sub>2</sub> microspheres have been prepared by carbonization of cellulose/TiO<sub>2</sub>. Cellulose/TiO<sub>2</sub> microspheres were in turn made by one step phase

separation method using cellulose xanthate aqueous solution and polyacrylate aqueous solution. The distribution of  $\text{TiO}_2$  was adjusted by addition of polyethylene glycol as diluents [40]

C/ $\text{TiO}_2$  microsphere composites have been used for removal of acetaldehyde the efficiency of which was much higher than that of cellulose/ $\text{TiO}_2$  composites [41]. C/ $\text{TiO}_2$  have also been used as catalyst in the decomposition reaction of isopropanol. [39].

The present investigation describes a simple method to prepare carbon supported  $\text{TiO}_2$  for photocatalytic degradation of dyes.

## 4.6 EXPERIMENTAL

### 4.6.1 Synthesis of $TiO_2/C$

$TiO_2$  was supported on carbon. Two methods were employed, namely, mechanical mixing and insitu preparation.

#### *General Procedure*

##### 1. Activated carbon C 2

Activated carbon prepared from coconut shell was obtained from Indo German Company Limited (IGCL), Alwaye , Kerala

Chemicals:  $TiCl_3$ ,  $HNO_3$ , Urea, Oxalic acid, of AR grade chemicals of Loba Chemie (India) make, were used for synthesis purpose.

##### 2. Synthesis of rutile $TiO_2$

The rutile  $TiO_2$  was synthesized by a method reported in [26].

Calculated quantity of  $TiCl_3$  was taken in an evaporating dish, followed by dropwise addition of 0.5 M  $HNO_3$ , till the colour changed from violet to colourless. This was followed by addition of urea, such that the  $TiCl_3$ : Urea molar ratio was 1:2. It was stirred on a magnetic stirrer for 15 minutes. The resultant mixture was then evaporated to dryness on a steam bath. The dry residue was transferred to a glass column and heated in a horizontal muffle furnace at  $400^{\circ}C$ , with continuous flow of nitrogen for 3 hours. The product was then cooled to ambient temperature and then homogenized to obtain the final samples.

### *3. Carbon + TiO<sub>2</sub>*

Mechanical mixing: C2 and TiO<sub>2</sub> as mentioned above were mixed together mechanically

### *4. In-situ preparation of 10% TiO<sub>2</sub> R2/C2*

Calculated quantity of TiCl<sub>3</sub> was taken in an evaporating dish, followed by the drop – wise addition of 0.5 M HNO<sub>3</sub>, till the colour changed from violet to colourless. This was followed by the addition of urea, such that the TiCl<sub>3</sub>: Urea molar ratio was 1:2 and stirred for 15 minutes.

In a separate container, calculated amount of C2 was taken and 2 propanol was added along with water for wetting. The contents from the evaporating dish were added to the beaker and stirred with a magnetic stirrer for 15 minutes.

The resultant mixture was then evaporated to dryness on a steam bath. The dry residue was transferred to a glass column and heated in a horizontal muffle furnace at 400<sup>0</sup>C, with continuous flow of nitrogen for 3hrs. The product was cooled to ambient temperature and then homogenized to obtain the final samples.

### *5. In-situ preparation of 30% TiO<sub>2</sub> R2/C2*

Sample was prepared by the above insitu method, by taking calculated amount of chemicals to get 30% TiO<sub>2</sub> R2/C2 .

### *6. In-situ preparation of 10% TiO<sub>2</sub>*

TiCl<sub>3</sub>, oxalic acid, urea were taken in the ratio 1:2:2 and prepared by the same insitu method, using calculated amounts to get 10% anatase TiO<sub>2</sub>

7. Methylene blue solution of various concentrations were prepared. 0.200 g/L, 0.025 g/L, and 0.012 g/L.

#### *4.6.2 Photocatalytic Degradation of Methylene Blue*

##### *Comparative study of adsorption of dyes on the activated carbon*

Optical density was found out of blank solutions of 200 mg/L solutions of congo red, methylene blue and methyl orange. 0.100g of activated carbon was placed in the solution of the three dyes and allowed to equilibrate for an hour at room temperature. The solution was stirred at regular intervals. After an hour, it was centrifuged and the clear aliquot was used to determine the optical density.

##### *Comparative study of adsorption of methylene blue by C2 , TiO<sub>2</sub>, TiO<sub>2</sub>+C2 and TiO<sub>2</sub>/C2.*

10 mg each of the above catalysts were put in separate 250 ml conical flasks containing 100ml of 0.025mg/L methylene blue solution. The solution was kept in sunlight and stirred at regular intervals.

At definite time intervals 10ml of the solution was centrifuged and the clear supernatant liquid was used to find the optical density. A graph of optical density v/s time in minutes was plotted.

##### *Comparative study of adsorption of methylene blue by the other TiO<sub>2</sub>/C catalysts*

A similar procedure for analysis was adopted to make a comparative study of the effect of percentage loading as well as in the case of a comparative study of anatase and rutile forms of TiO<sub>2</sub> supported on carbons by taking 0.12g/L methylene blue.

## 4.7 Results and Discussion

### 4.7.1 Comparative study of adsorption of dyes by C2

Activated carbon has the ability to adsorb dyes and thus used extensively in the dye industry to treat dye effluents in the water. Fig 4.3 gives a comparative optical density of congo red, methylene blue and methyl orange by activated carbon. It was observed that the optical density decreased when carbon was added. This could be attributed to the adsorption of the dye on the carbon, resulting in a lesser concentration in the solution.

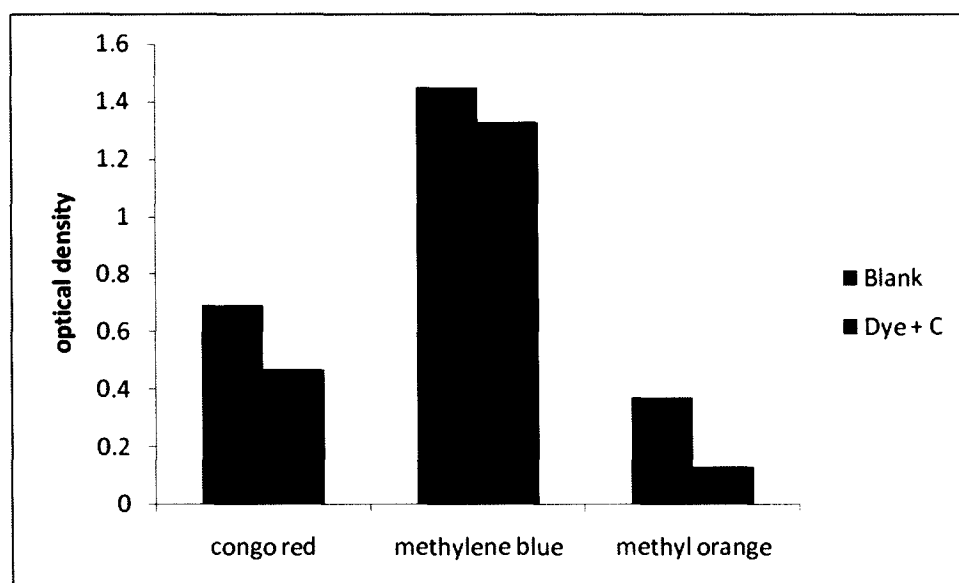


*Fig 4.3 gives a comparative optical density of congo red, methylene blue and methyl orange with and without activated carbons. Decrease in optical density gives a measure of extent of adsorption.*

The adsorption of dyes on to the carbon depends upon several factors such as porosity, pH of solution, surface functional groups, nature of the dye, contact time between the adsorbate and adsorbent and temperature.

C2 has a high surface area and pore volume as indicated in chapter 2. The porosity is visible in the SEM images.

It is seen that the carbon used here showed significant adsorption of all the three dyes tested.

#### 4.7.2 Comparative study of adsorption of methylene blue by C2, Methylene blue+C, methylene blue +TiO<sub>2</sub>.

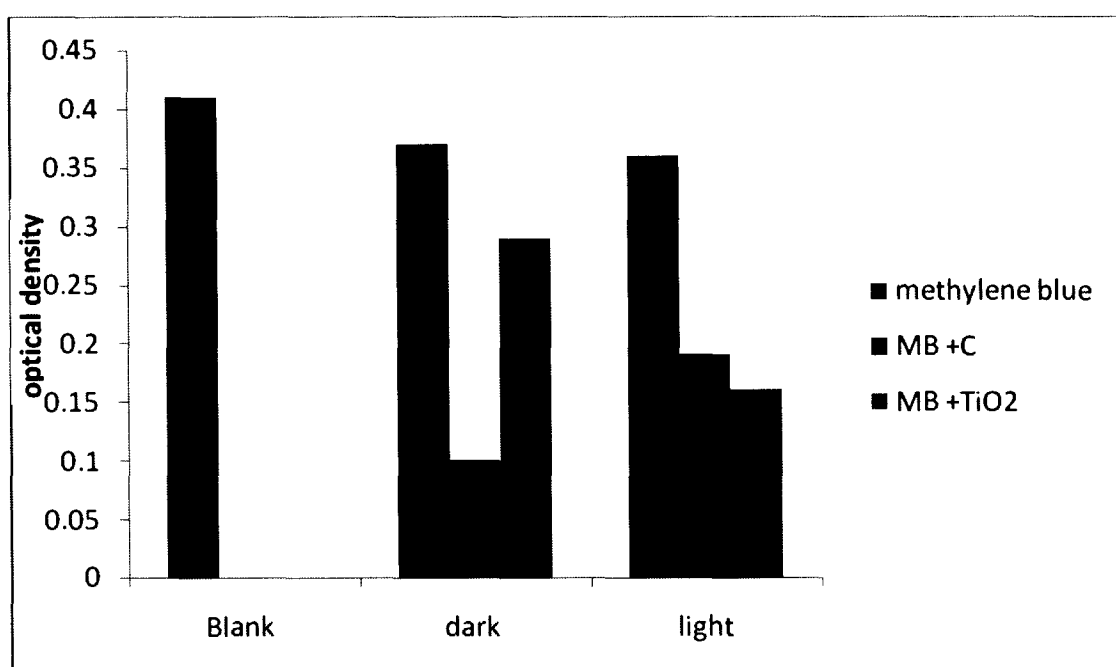


**Fig 4.4 gives a comparative optical density of methylene blue, MB and TiO<sub>2</sub>, MB and C2 when in dark and in light**

With reference to Fig 4.4 it is evident that methylene blue degrades slightly when kept for some time even when no catalyst is added.

On the other hand it is clear that carbon removes the dye by adsorption. When kept in the dark the adsorption is more. However, in the light the adsorption of the dye is less due to the increase in temperature. Rise in temperature slows down the adsorption

process. Though C2 showed better adsorption in the dark, its efficiency decreases when exposed to sunlight.

TiO<sub>2</sub> removes the dye by photodegradation. The amount of dye that remains in the solution is much less as can be seen by the optical density measurements as compared to the measurements of the solution with carbon. Though, overall, the removal of methylene blue due to adsorption by carbon in the dark, is much better than photo degradation by TiO<sub>2</sub>.

#### 4.7.3 Photocatalytic degradation of methylene blue.

The efficiency of removal of dye can be improved by combining the adsorption properties of carbon and photodegradation property of TiO<sub>2</sub>. TiO<sub>2</sub> is a well known photocatalyst. When supported on activated carbons, it has been observed that the property is enhanced. There is a synergy created between the acid and basic sites of TiO<sub>2</sub> and the surface area and porosity provided by the carbon [12]. This can be achieved by loading TiO<sub>2</sub> on carbon support either by directly mixing the two or by insitu loading.

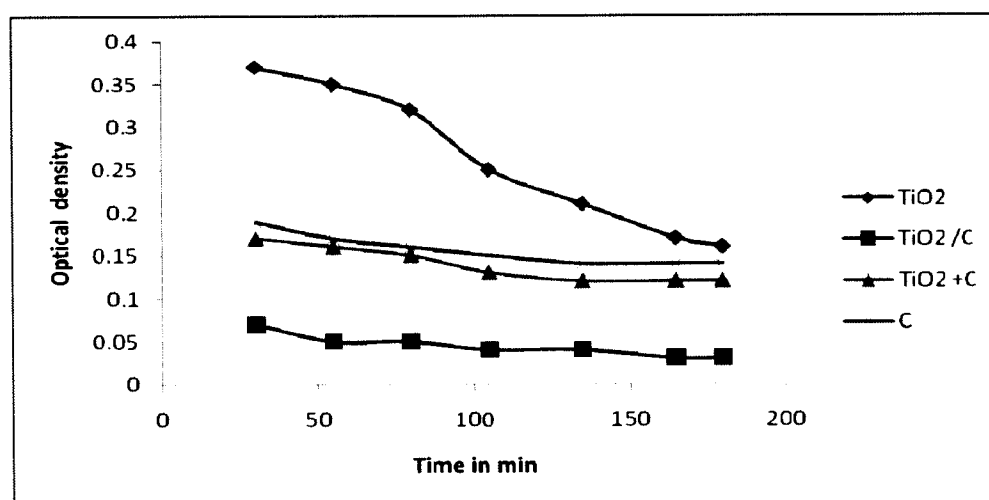


**Fig 4.5 Graph of optical density v/s time indicating photocatalytic degradation of 0.012 g/L methylene blue by the various catalysts**

As indicated by Fig 5.3 It was found that the insitu preparation of C2/TiO<sub>2</sub> showed significantly better photocatalytic activity, followed by TiO<sub>2</sub> + C2.

This could be the result of more dispersive loading of TiO<sub>2</sub> in the pores of carbon during insitu preparation as compared to mechanical mixing. The large surface area provides for more interaction of the dye with the catalyst.

#### 4.7.4 Comparative study of anatase and rutile phase on the degradation of methylene blue

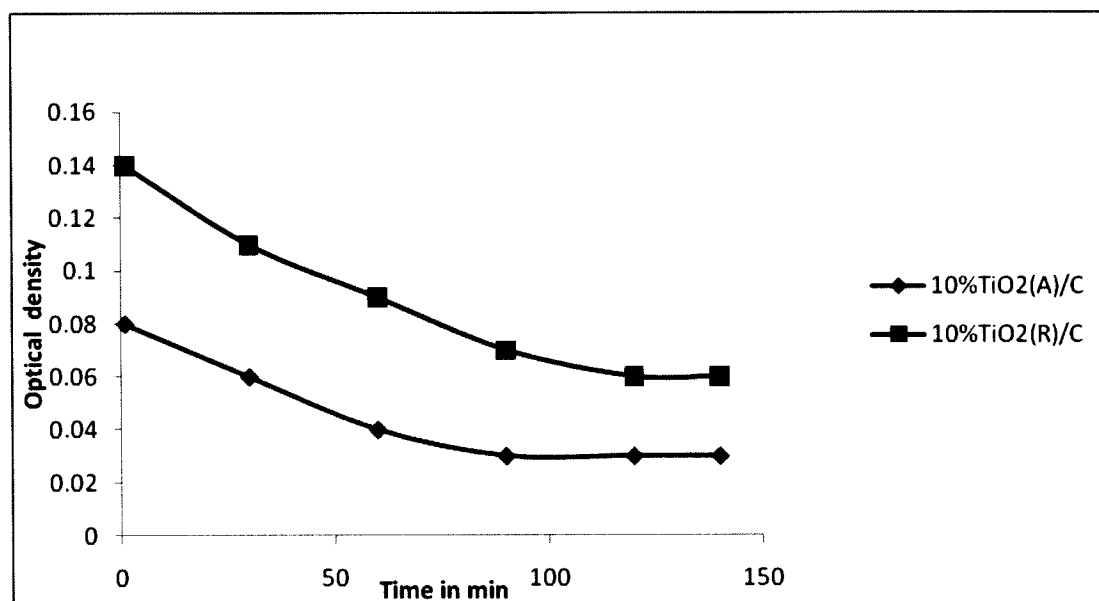


**Fig 4.6 Graph of optical density v/s time indicating photocatalytic degradation of 0.012g/L methylene blue by 10% TiO<sub>2</sub>A2/C2, 10% TiO<sub>2</sub>R2/C2.**

The X-ray powder diffraction patterns (XRD) have been recorded on a Shimadzu LabX -700 diffractometer, using Ni filtered CuK $\alpha$  radiation ( $\lambda=1.5406 \text{ \AA}$ ) by step scanning with a scan rate of  $2^\circ 2\theta/\text{min}$ . The crystallite size was determined by

Scherrer formula. The weight percent for anatase in the rutile phase was obtained from the equation

$$XA=(1+1.26(IR/IA) [42]$$

Where XA is the weight fraction of anatase and rutile diffractions respectively.

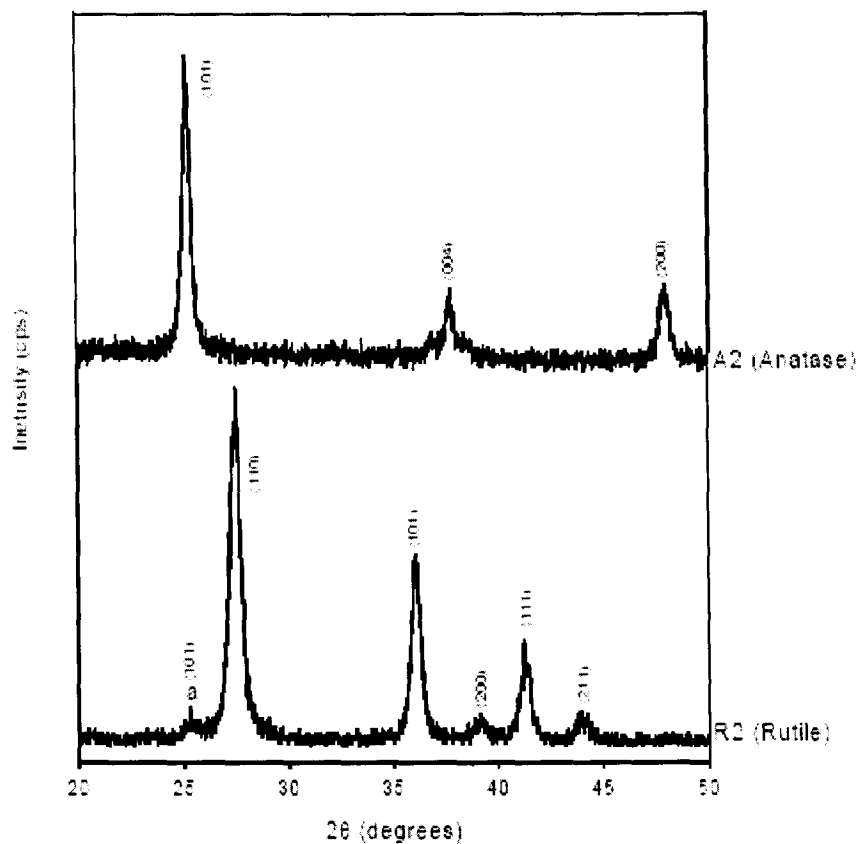


*Fig 4.7 XRD images of A2 (anatase ) and R2 (rutile ) phases*

**10%TiO<sub>2</sub> (A2)/C2**

2 theta	d	I	phase
25.2	3.52	100	(A)
37.8	2.37	20	(a)
48.2	1.89	40	(a)

**10%TiO<sub>2</sub> (R2)/C2**

2theta	d	I	phase
25.2	3.52	20	(a)
27.5	3.25	100	(R)
36.2	2.49	50	(R)
37.6	2.39	20	(a)
42.2	2.1	30	(r)
44.5	1.89	20	®

**Table 4.2 Characteristic peaks of A2 (anatase) and R2 (rutile) TiO<sub>2</sub>**

It was observed that the anatase phase was more photocatalytically active as compared to the rutile phase in agreement with literature reports.

#### 4.7.5 Comparative study of percentage loading of $\text{TiO}_2$ on Carbon

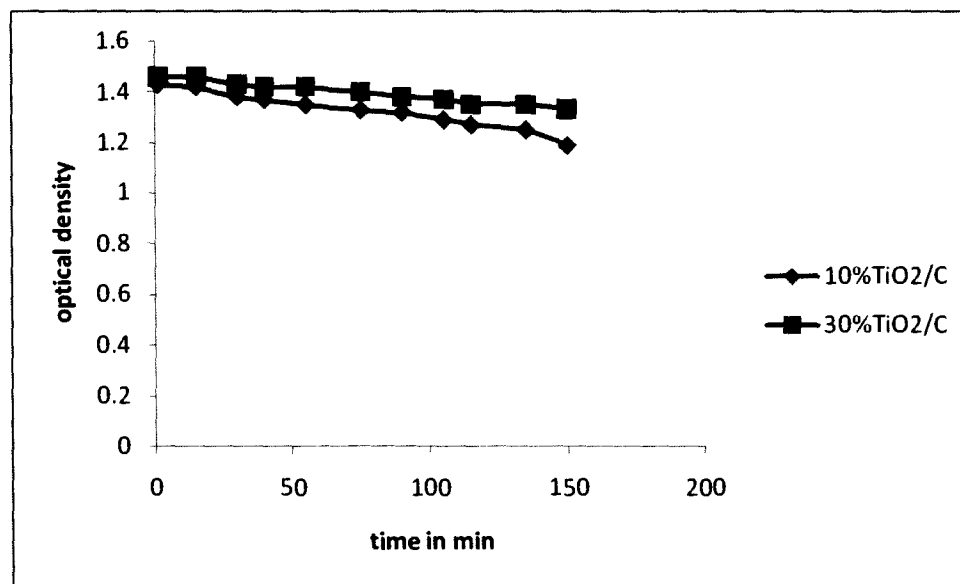


**Fig 4.8 Graph of optical density v/s time indicating photocatalytic degradation of methylene blue by , 10%  $\text{TiO}_2$  R2/C2 and 30%  $\text{TiO}_2$  R2/C2.**

It was observed that 10% loading of  $\text{TiO}_2$  showed better results as compared to 30%. This could be as a result of the blockage of pores in carbon by excess % of  $\text{TiO}_2$ . The pores are normally the conduits for passage of dye inside the carbon. Hence the internal surface where  $\text{TiO}_2$  is present may not be available.

#### 4.7.6 Comparative study of Carbon and Silicon dioxide as supports for $\text{TiO}_2$

$\text{SiO}_2$  is itself a catalyst and is also known to be a good support.  $\text{TiO}_2/\text{SiO}_2$  catalyst have been studied reactions for various heterogeneous catalytic reactions such as decomposition of  $\text{NO}_2$ , Friedel Crafts alkylation etc.

A comparative study of  $\text{TiO}_2/\text{SiO}_2$  and  $\text{TiO}_2/\text{C}$  was done to study the photodegradation of methylene blue.

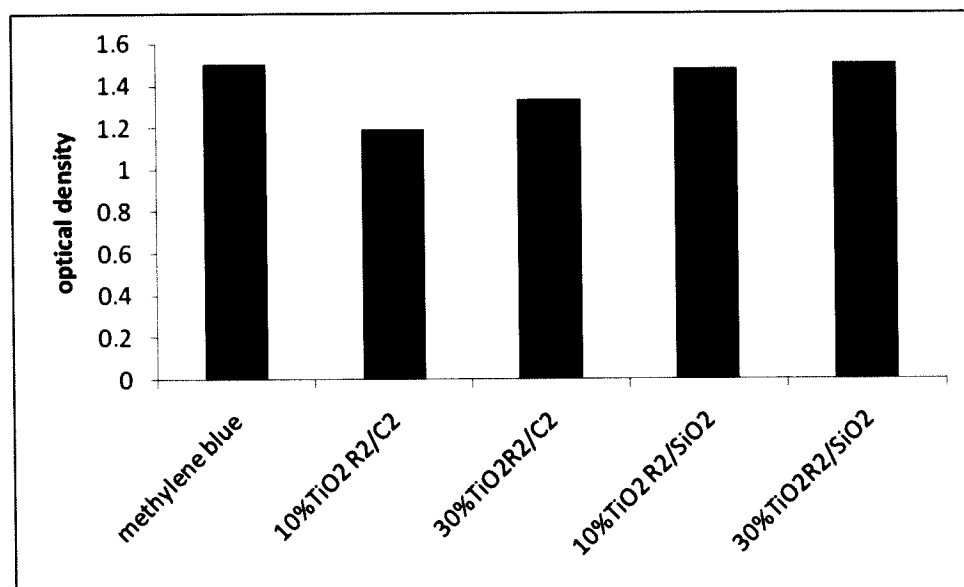


***Fig 4.9 Comparative study of TiO<sub>2</sub>/SiO<sub>2</sub> and TiO<sub>2</sub>/C on the photodegradation of methylene blue.***

It was observed that TiO<sub>2</sub>/SiO<sub>2</sub> did not show any significant decomposition of methylene blue for the time tested. Therefore, carbon supported TiO<sub>2</sub> is a better catalyst as use of carbon enhances adsorption cum photocatalysis.

#### 4.8 CONCLUSIONS

- $\text{TiO}_2/\text{C}$  was used to test photocatalytic degradation of methylene blue dye. It was found that the insitu preparation of  $\text{TiO}_2/\text{C}$  showed better photocatalytic activity as compared to mechanically mixed sample  $\text{TiO}_2+\text{C}$ .
- C2 showed better adsorption of methylene blue in the dark but decreased in the light.  $\text{TiO}_2/\text{C}$  showed better photodegradation of the dye in the light as compared to carbon.
- Photocatalytic activity was also tested for the anatase and rutile phase of  $\text{TiO}_2$ . It was observed that the carbon supported anatase phase gave better photodegradation.
- C2 was a better support for  $\text{TiO}_2$  as compared to  $\text{SiO}_2$ .  $\text{TiO}_2/\text{SiO}_2$  did not show any significant decomposition of methylene blue.
- Effect of percentage loading of  $\text{TiO}_2$  on carbon was studied. It was observed that 10% loading showed better photocatalytic activity as compared to 30% loading.

## REFERENCES

1. C. H. Ao, S. C. Lee, C. L. Mak, L.Y. Chan , Appl. Catal, B 42 (2003) 119.
2. K.T. Ranjit, B. Viswanathan, J. Photochem. Photobiol, A 180 (1997) 79.
3. [www.ktf-split.hr/periodni/en/ti.htmlbk](http://www.ktf-split.hr/periodni/en/ti.htmlbk).
4. V.E. Henrich, P. A. Cox, 'The Surface Science of Metal Oxides'. Cambridge Univ. Press, Cambridge. U.K, 1994.
5. A. L. Linsebigler, G. Lu, J T. Yates, Chem. Rev, 95 (1995) 735.
6. G. A. Tompsett, G.A. Bowmaker, R.P. Cooney, J. B. Metson, K.A. Rodgers, M. A. Seakins, J. Raman, Spectosc., 26 (1995) 57.
7. A. Fahmi, C. Minot, Surf. Sci , 304 (1994) 343.
8. K. Shaw, P. Christenson and A. Hamnet, Electrochemica. Acta, 41 (1996) 719.
9. [www.fis.unipr.it](http://www.fis.unipr.it)
10. <http://www.gensnano.com/photocatalysis-mechanism.php>
11. a) J. YU, X. Zhao, Q. Zhao, Thin Solid films, 379 (2000) 7.  
b) J. Yu, X. Zhao, Q. Zhao, Mat. Chem. Phys, 69 (2001) 25.
12. S. Sato, J. Phys. Chem, 87 (1983) 3531.
13. K. T. Ranjit, B. Viswanathan, J. Photochem. Photobiol, A, 180 (1997) 215.
14. C. Wang, J.Y. Ying Chem. Mater, 11 (1999) 3113.
15. B. L. Bischoff, M.A. Anderson, Chem. Mater, 7 (1995) 1772.
16. P. Amal, J. P. R. Corrie, D. Lecierque, P.H.Mutin, A. Vioux, J. Mater. Chem, 6 (1996) 1925.
17. P. Arnal, J. P. R. Corrie, D. Leclerque, P. H. Mutin, A. Vioux, Chem. Mater, 9 (1997) 694.

18. E. Santacesaria, M. Tonello, G. Storti, R. C. Pace, S. J.Caira, *J. Colloidal Interface Sci*, 111 (1986) 44.
19. G. Marci, V. Aug ugliaro, M. J. Lopez-Muoz, C. Martín, L. Palmisano, V. Rives, M. Schiavello, R.J.D. Tilley and A.,. Venezia, *J. Phys Chem*, 105 (2001) 1026.
20. S.D. Park, Y.H. Cho, L.W. Kim and S.Kim, *J. Solid State Chem*, 146 (1999) 230.
21. A. Kato, Y. Takeshita, .Y. Katatae, *Mater. Res. Soc. Symp. Proc*, 155 (1989).13
22. N. Negishi, K. Takeuchi, T. Ibusuki, *J. Mater. Sci*, 33 (1998) 5789.
23. Y. Tanaka, *Ceram Soc. Jpn*, 106 (1998) 344.
24. E. Stathatos and P. Lianos, *Langmuir*, 16 (2000) 2398.
25. J. Livage, M. Henry, C. Sanchez, *Progr. Solid State Chem*, 18 (1998) 259, J. Livage, *Catal. Today*, 41 (1998) 3.
26. A. R. Gandhe, J.B Fernandes, *Catalysis Communications*, 5 (2004) 89-94
27. C. Minero, F. Catozzo, E. Petizetti, *Langmuir*, 8 (1992) 481.
28. T. Ibusuki, K. Takeuichi, *J. Mol Caltal*, 88 (1994) 93.
29. T. Koretoh, *Kogyozairyou*, 45 (1997) 36.
30. M. Steigerwald, L. Bus, *Acc. Chem. Res*, 23 (1990) 183.
31. R. D. Gonzalez, T. Lopez, R. Gomez, *Catal. Today* 35 (1997) 293
32. G. M. Pajonk, *Catal Today*, 35 (1997) 319.
33. M. Schneider, A. Baiker, *Catal Today*, 35 (1997) 339.
34. R. W. Pekala, *J Mater.Sci*, 24 (1989) 3221.
35. C. Lin , J. A. Rittter, *Carbon*, 35 (1997) 1271.
36. F. J. Maldonado-Hodar, M. A. Ferro Garcia, J. Rivera-Utrilla, C. Moreno-Castilla, *Carbon* 37 (1999) 1199.

37. G. W. Scherer, *J. Am. Ceram. Soc.*, 73 (1990) 3.
38. M. J. Van Bammel, A. B. de Haan, *J. Mater. Sc.*, 29 (1994) 943.
39. F. J. Maldonado-Hodar, C. Moreno-Castilla, J. Rivera-Utrilla, *Applied Catalysis*, 203 (2000) 151-159
40. S. Nagaoka, Y. Harasaki, S. Ishara, M. Nagata, K. Lio, C. Nagaarva, H. Ihara  
*J Mol Catal A ; Chemical*, 177 (2002) 255-263.
41. H. Idriss, K. S. Kim, M. A. Barteau, *Surf. Sci.*, 262 (1992) 113.
42. R. A. Spurr, H. Myers, *Anal Chem*, 29 (1957) 760.

*CHAPTER V*

**ELECTROCHEMICAL AND  
CATALYTIC PROPERTIES OF  
CARBONS AND CARBON SUPPORTED  
Mn (IV) OXIDE**

## **5.1 ELECTROCHEMICAL PROPERTIES OF ACTIVATED CARBON, MnO<sub>2</sub>/C**

### *5.1.1 CAPACITORS*

There are three common forms of carbon – diamond, graphite, and amorphous carbon, but only the latter two are important for electrochemical applications. Between the extremes of graphite and amorphous carbon there is a wide range of carbons with properties that can be tailored, to some extent, for a specific application by controlling the manufacturing conditions and subsequent treatments (heat treatment, chemical oxidation, etc.). It is these latter treatments that are generally exploited by scientists and technologists who use carbon in electrochemical application [1].

The theoretical densities of these carbon structures are 3.51, 2.25, and 1.88 g/cm<sup>3</sup>, respectively. The ideal graphite structure consists of layers of carbon atoms arranged in hexagonal rings that are stacked in a sequence ABAB... This form of graphite is called hexagonal graphite. The graphite structure with the stacking sequence ABCABC... is called rhombohedra graphite. Amorphous carbon may be considered as sections of hexagonal carbon layers of varying size, with very little order parallel to the layers. The process of carbon graphitization consists essentially of ordering and stacking of these layers, generally achieved by high-temperature heat treatment.

The widespread use of carbon materials in electrochemical systems started in nineteenth century with the use of carbon electrodes in Volta batteries. The Leclanche cell also uses carbon in the cathode mix. The development of artificial graphite in 1896, led to the rapid growth of industrial electrochemical processes. The major

industrial applications for carbons are electrodes for steel arc furnaces and brushes for electric motors [2].

Manganese dioxide is also used for electrochemical super capacitors [3]. To optimize these properties, manganese dioxides are supported on carbon.

Super capacitors can be divided into two types on the basis of the charge-storage mechanism, principally, the capacitance of the electric double layer and the pseudo capacitance of redox reactions at/within the electroactive materials [3-5].

The double-layer capacitors are usually composed of very high surface area electrodes (e.g. carbon fibers) because the non-Faradaic capacitance of the electric double layer is directly proportional to the surface area accessible by electrolytes [5-9]. On the other hand, the electrodes of electrochemical pseudo capacitors mainly consist of electroactive materials with several oxidation states or structures [5, 10-12]. Recently, the electrochemical pseudo capacitors have been paid much attention because the capacitive characteristics (e.g. a higher energy density), estimated theoretically, of these devices are better than that of the double-layer capacitors [3-4]. Moreover, super capacitors with a high pulse-power and an acceptable energy capability are believed to be a potential device in several future applications, such as an energy manager or tuner in the electric power systems [13].

Carbon black, graphite, charcoals, glassy carbons and carbon fibres are commonly used electrochemical systems.

Numerous publications [14 -20] are available that present detailed reviews on the manufacture of carbon blacks. The formation of polyaromatic macromolecules in the vapor phase is followed by nucleation of these macromolecules into droplets, which are then converted into carbon-black particles [21-22].

Data on the chemical analysis, surface area, and thermal reactions of natural graphite are given by Mackles et al [23]. Natural graphite is not used much in electrochemical systems. Of greater importance for electrochemical applications is artificial graphite, which is produced from different precursors. Detailed description of the formation of pyrolytic graphite, its uses, and its properties are presented by Ishikawa and Nagaoki [24].

Rayon and polyacrylonitrile (PAN) are precursors for most of the carbon fibers that are produced, although other precursors such as pitch [25, 26], a by-product of the petroleum or coal-coking industry, phenolic resins [27, 28], and polyacetylenes [29] have also been used. In general, graphitized carbon fibers produced from pitch provide better electrical and mechanical properties than do those obtained from hard carbons, such as from a PAN precursor produced at the same temperature.

While carbon black and graphites are extensively used as electrode materials, porous activated carbon is also being investigated as their surface can be modified depending upon the applications.

### *5.1.2 Modification Porous Carbon for Electrode Materials*

Surface functional groups and porosity greatly influence the capacity of carbon electrodes.

Porous carbons have been used as electric double layer capacitance electrodes material. It was well known that the electric capacity of an electrode was affected by its physical and chemical properties [30-38].

The crystallographic structure has a considerable influence on the chemical reactivity of carbons. It is well known that the chemical reactivity at basal-plane sites is considerably lower than that at the edge or defect sites of carbon. Consequently, highly graphitized carbons with a homogeneous surface consisting of predominantly basal planes are less reactive than amorphous carbons. The edge carbon atoms have unpaired  $\alpha$  electrons that are available to form bonds with chemisorbed oxygen; in the basal-plane carbon atoms,  $\alpha$  electrons are tied up in chemical bonds with adjacent carbon atoms. The rate of carbon oxidation by  $O_2$  is about 17 to 20 times faster at edge sites than that at basal-plane sites [39-40].

Walker and co-workers [41-46] carried out investigations to understand the reactivity of carbon blacks especially in relation to their surface area. They reported decrease in reactivity on graphitization of the carbon black [47], confirming the hypothesis that oxygen attack on carbon blacks occurs preferentially at specific high-energy sites on the surface, such as the edge sites in the carbon lattice. This hypothesis is supported by electron and optical microscopy studies [41, 48],

The effects of oxygen-containing functional groups on electric characteristics had been investigated qualitatively in terms of temperature-programmed desorption [35, 36, 49]; and the result indicated that the presence of oxygenated groups on the surface of the activated carbon influence the wettability, surface reactivity, electrical properties such as increasing the capacitance and producing pseudo capacitance effects.

Oda *et al.* compared the effect of surface chemical property of commercial porous carbon on its application in electrolyte [50]. In the case of the aqueous electrolyte, the electric capacity depended more on oxygen functional groups than on BET surface area. It was considered that a larger number of functional group promoted not only the wettability of electrodes but also the negative charge of electrodes leading to an increase in capacity. In the case of the organic electrolyte, pore structure seemed to be a more dominant factor than functional group.

Fang *et al.* developed carbon electrode material through surface modification of Norit activated carbon [51,52], which improved the wettability of activated carbon in the electrolyte solution, resulting in not only a lower resistance to the transport of electrolyte ions within micropores of activated carbon, but also more usable surface area for the formation of electric double layer, and accordingly, higher specific capacitance, energy density, and power capability available from the capacitor based on modified carbon.

Variety in surface chemical character was achieved through modification of commercial activated carbons by heat treatment in vacuum, ammonia and ammonia-

oxygen atmospheres, as well as by oxidation in moist air and with concentrated nitric acid [53]. The importance of the surface chemistry of the carbon electrode materials was that the adsorbed lead species exhibited different electrochemical activities due to its different existing states on the carbon surface.

### *5.1.3 MnO<sub>2</sub> supported carbons*

Carbons have been used as electrode materials. MnO<sub>2</sub> is known for its electrochemical properties. MnO<sub>2</sub> supported on carbons has been studied for the use of electrochemical capacitors. Many researchers focused on developing the electrode materials such as transition metal oxides (e.g. oxides of Mn, Mo, V, Cr, W, Ru, Ir, Ni, Co, etc) and conducting polymers with several oxidation states/structures for applications in supercapacitors [54-68]. Although there are several oxidation states, including Mn(0), Mn(II), Mn(III), Mn(IV), Mn(V), Mn(VI) and Mn(VII), for manganese oxides [69], they were often employed as the cathode materials in rechargeable batteries [70-71]. Recently, manganese oxides have been considered as a potential candidate for the electrode material of super capacitors [63-65, 72, 73]. In addition, several methods have been developed for preparing manganese oxides, including chemical oxidation [74], sol gel-derived method [64], chemical co precipitation [63,65] and electrochemical deposition [71-73,75].

### *5.1.4 Cyclic voltammetry as an electro analytical technique*

Cyclic voltammetry [77] is a versatile technique used in electrochemical analysis. Its importance stems from the fact that it can observe redox reactions over a wide range of potentials.

CV consists of cycling the potential of an electrode, which is immersed in an unstirred solution, and the resulting current measured. The potential of this working electrode is controlled versus a reference electrode such as saturated calomel electrode or a silver /silver chloride electrode.

A cyclic voltammogram is obtained by measuring the current at the working electrode during the potential scan. The current can be considered as the response signal to the potential excitation signal. The voltammogram is a display of current (vertical axis) versus potential (horizontal axis). Because the potential varies linearly with time, the horizontal axis can also be thought of as a time axis. Fig 5.1 is an illustration of a cyclic voltammogram.

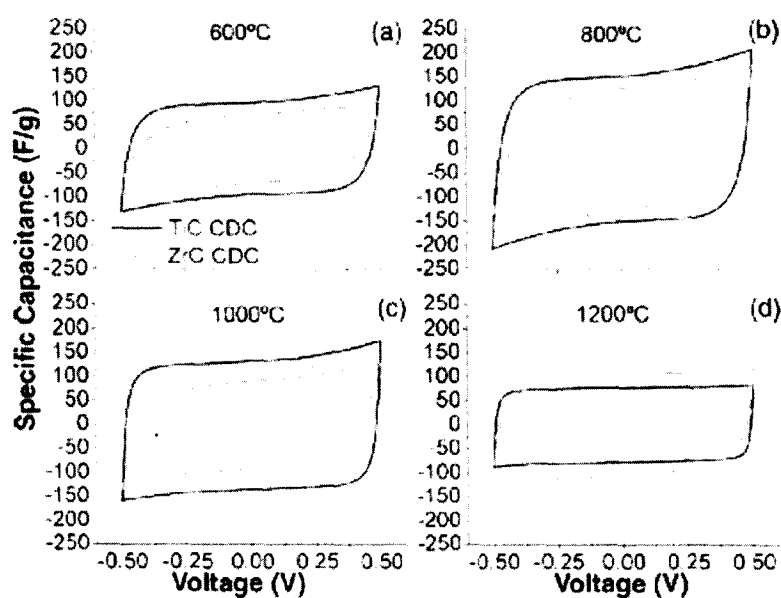


*Fig 5.1 Cyclic voltammogram of TiC and ZrC Carbide derived carbons [77].*

Though supercapacitors employing metal oxides or conducting polymers have been increasingly investigated, carbon based supercapacitors remain the most extensively studied and least expensive technology. Various carbonaceous materials such as activated carbons, aerogels, xerogels, templated carbons, nanotubes and more recently carbide derived carbons have been used extensively as super capacitors [77].

In the present investigation, CV profiles were carried out with working electrodes prepared from various carbons and compared with C-MnO<sub>2</sub>, OMS-2 and carbon nano tubes, to understand the relative capacitance of the electrodes. Capacitance studies were also done to observe the effect of OMS- 2 when mixed with carbon. The area enclosed by the CV profile was considered as a measure of capacitance.

#### *5.1.5 Experimental*

The electrodes were prepared from the following substances

1. C1: activated carbon was obtained from SD Fine Chemicals
2. C2: activated carbon from coconut shell from IGCL, Kerala
3. CP: mesoporous carbon from polymer [78]
4. CMC-N: activated carbon from CMC
5. MnO<sub>2</sub> /C1: MnO<sub>2</sub> was supported on carbon by calcining Manganese Nitrate and carbon C1 in the furnace at 400<sup>0</sup>C to obtain C-MnO<sub>2</sub> .
6. OMS-2 as synthesized in [79]
7. Carbon nanotubes

Samples 1-5 were mixed with OMS-2 in the ratio 1:1 and labeled

1. C1O,
2. C2O
3. CPO
4. CMC NO
5. MnO<sub>2</sub>/C O

The capacitance studies were done by cyclic voltammetry as mentioned in [80]. The working electrode was prepared by taking 50 mg of the sample along with 3 ml of isopropyl alcohol and mixed well in a mortar and pestle. Next three drops of 15% solution in isopropyl alcohol were added and mixed to make a homogeneous mixture for about 5 minutes till the solvent evaporated. The ink thus prepared was put on a 1 cm<sup>2</sup> active surface area on a 3 x 1cm platinised carbon paper which amounted to 10 mg of ink. The strip was dried in the oven at 120 °C for 1 hour.

CVs were done also for samples mixed with OMS-2 to make the working electrode. 25 mg of carbon and 25 mg of OMS were taken and the electrode was prepared as above. The same was done with MnO<sub>2</sub>/C sample.

### 5.1.6 Results and Discussion

The voltammograms for the samples with and without OMS is given in the Figures 5.2 -5.8.

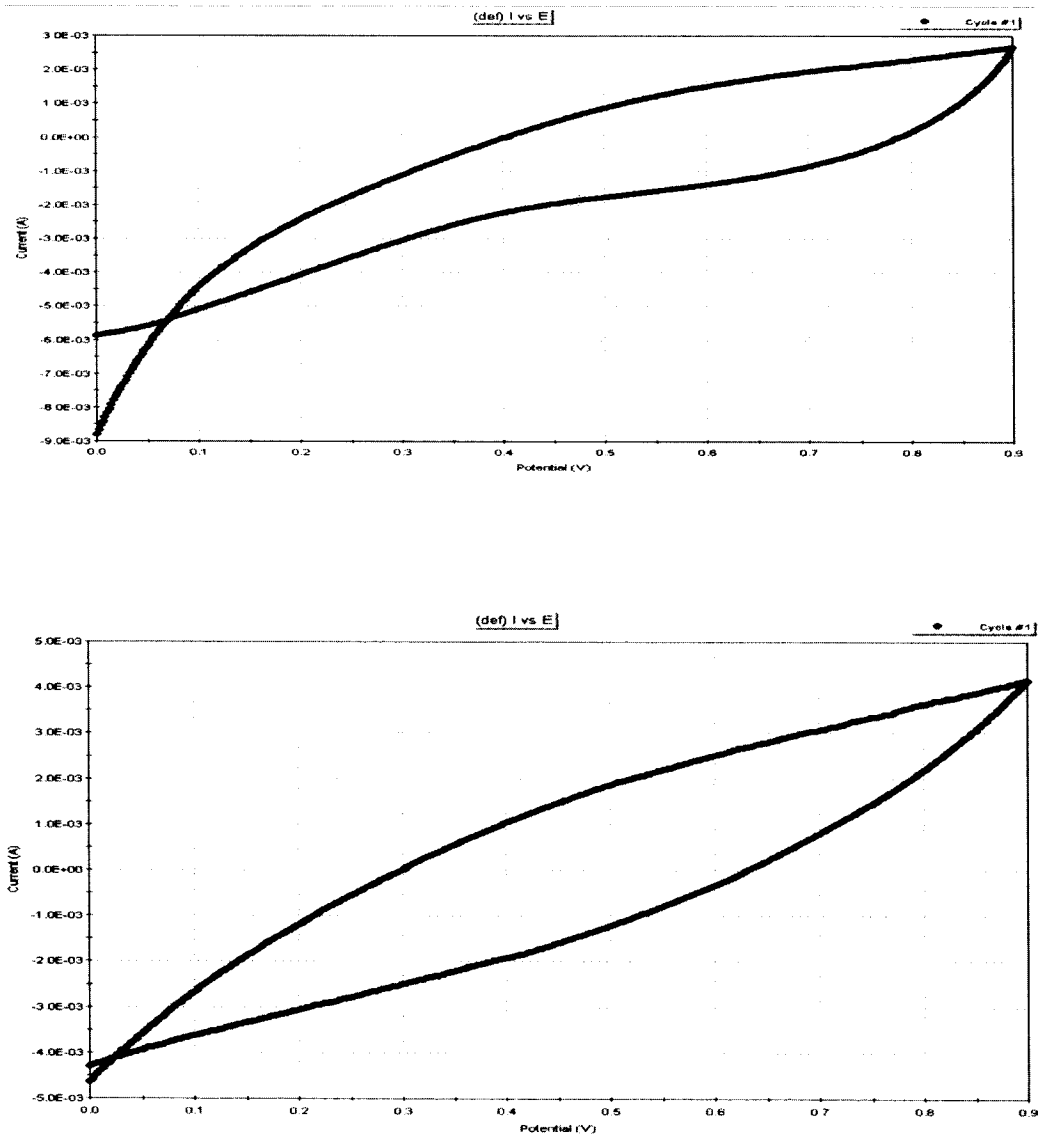


**Fig 5.2** Cyclic Voltammograms of activated carbons C1 and C1 with OMS-2

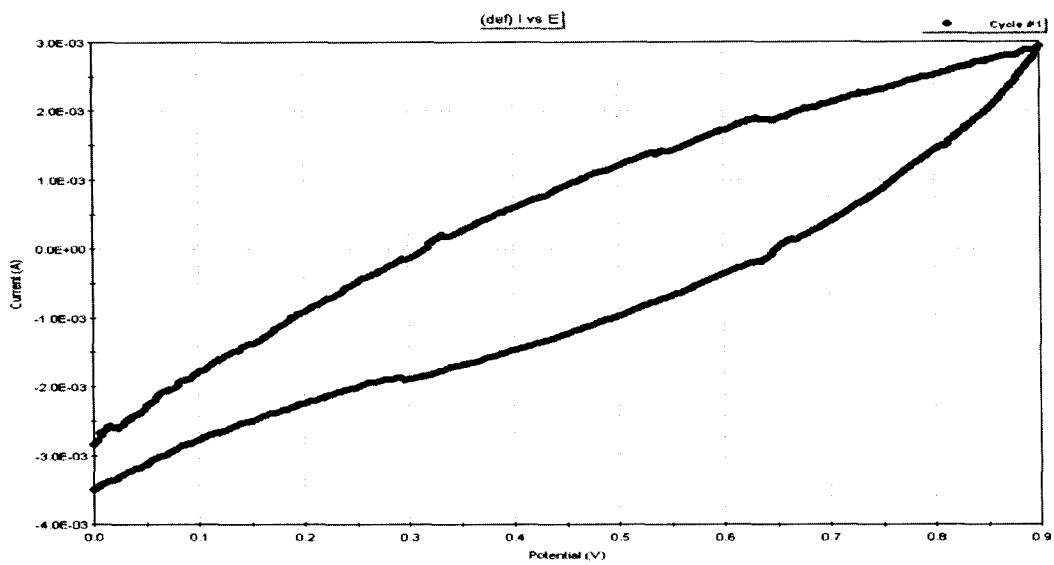
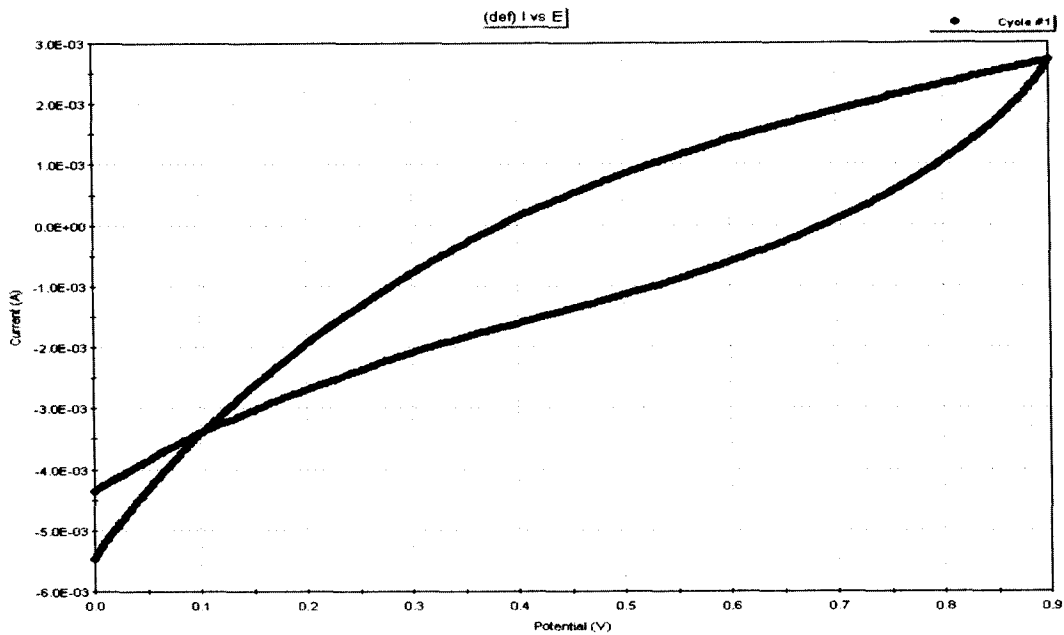


*Fig 5.3 Cyclic Voltammograms of activated carbon C2 and C2 with OMS-2*

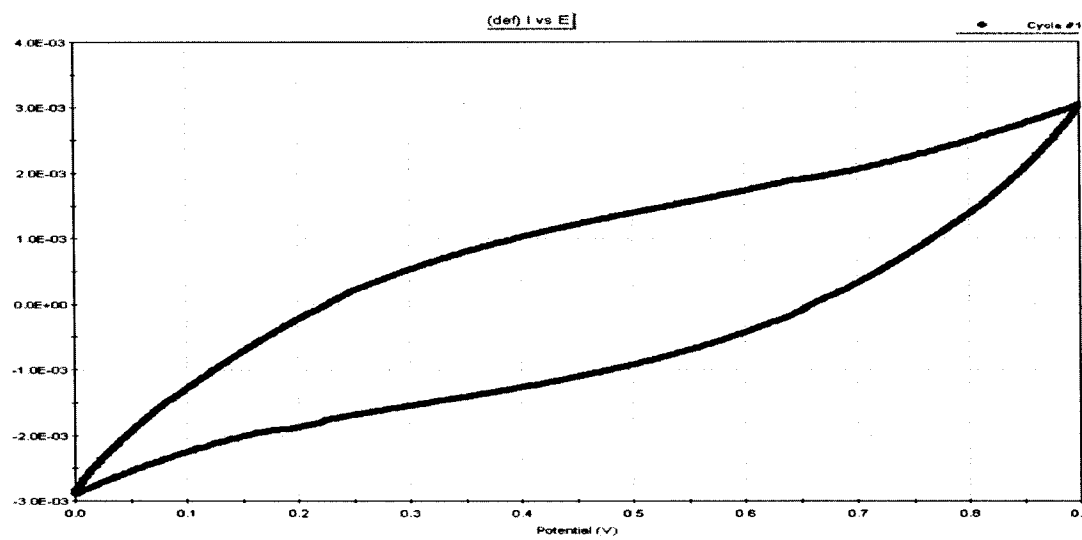
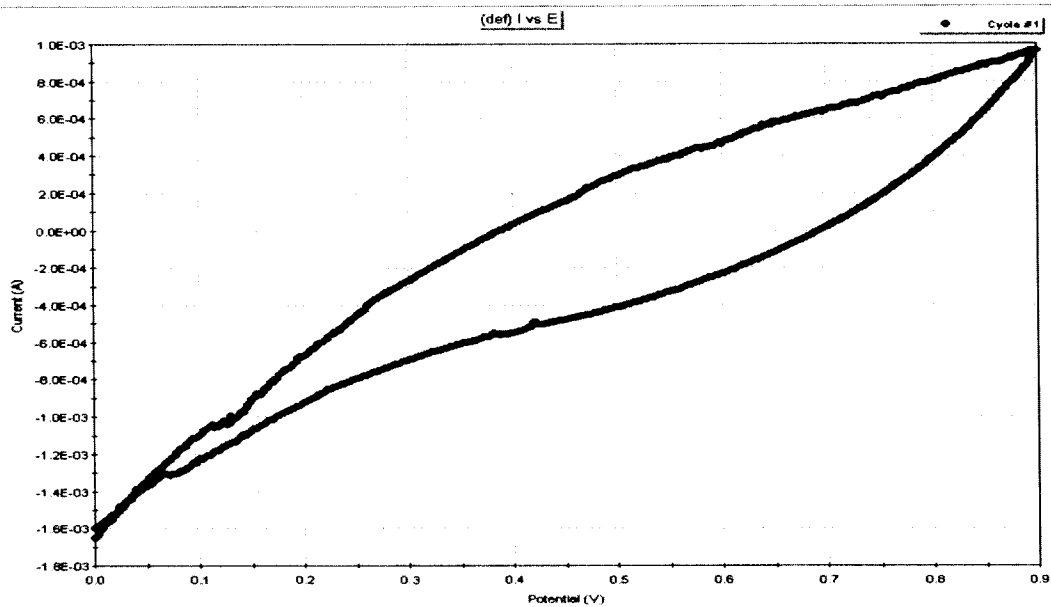


**Fig 5.4** Cyclic Voltammogram of CMC carbon (CMC N) and CMC N with OMS-2

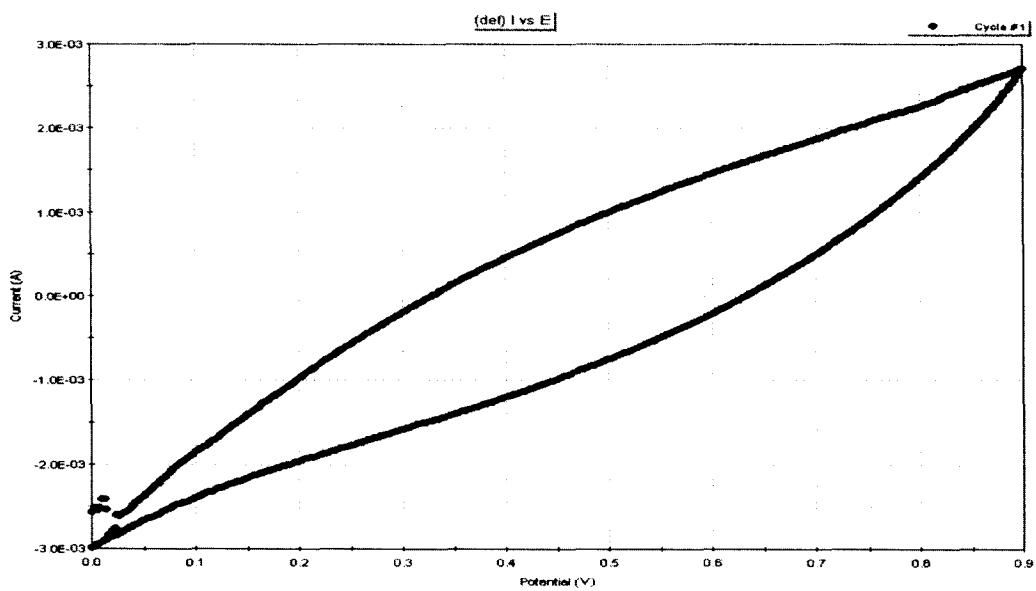
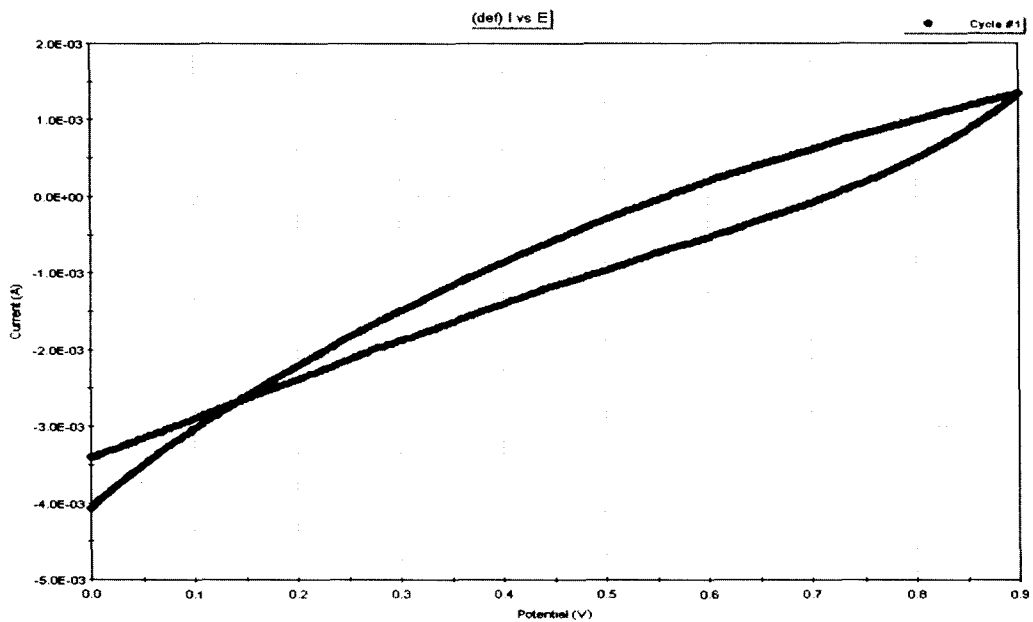


**Fig 5.5** Cyclic Voltammograms of polymer carbons (CP) and CP with OMS-2

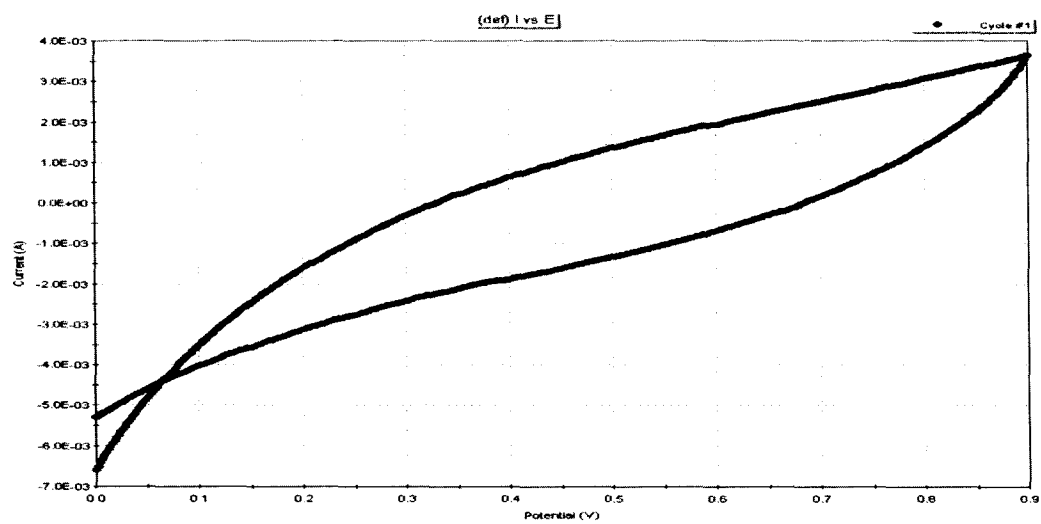
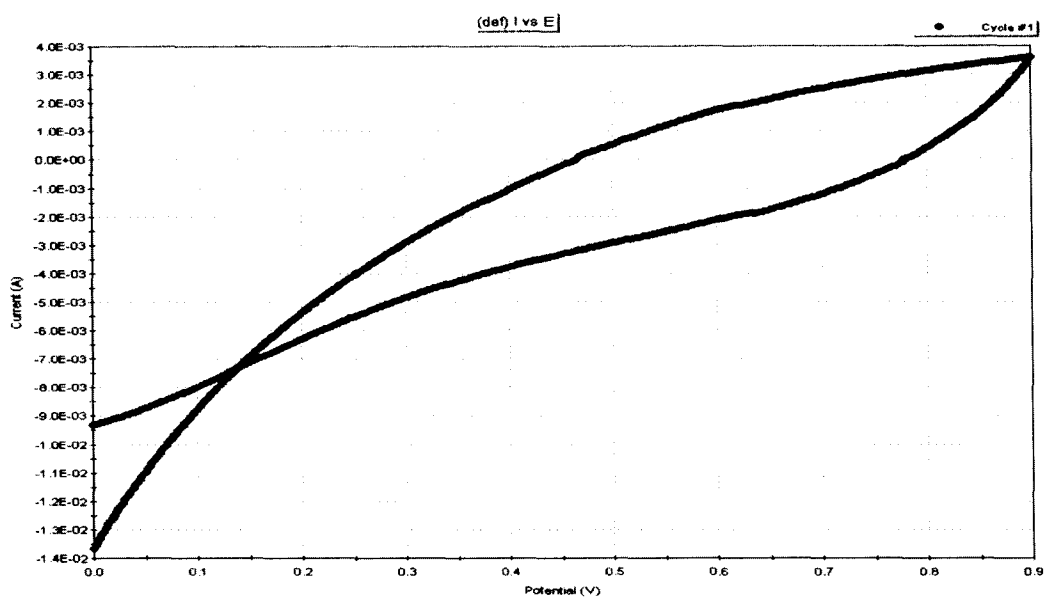


*Fig 5.6 Cyclic Voltammograms of manganese dioxide supported carbons*

*(MnO<sub>2</sub>/C 1) and MnO<sub>2</sub>/C 1 with OMS*

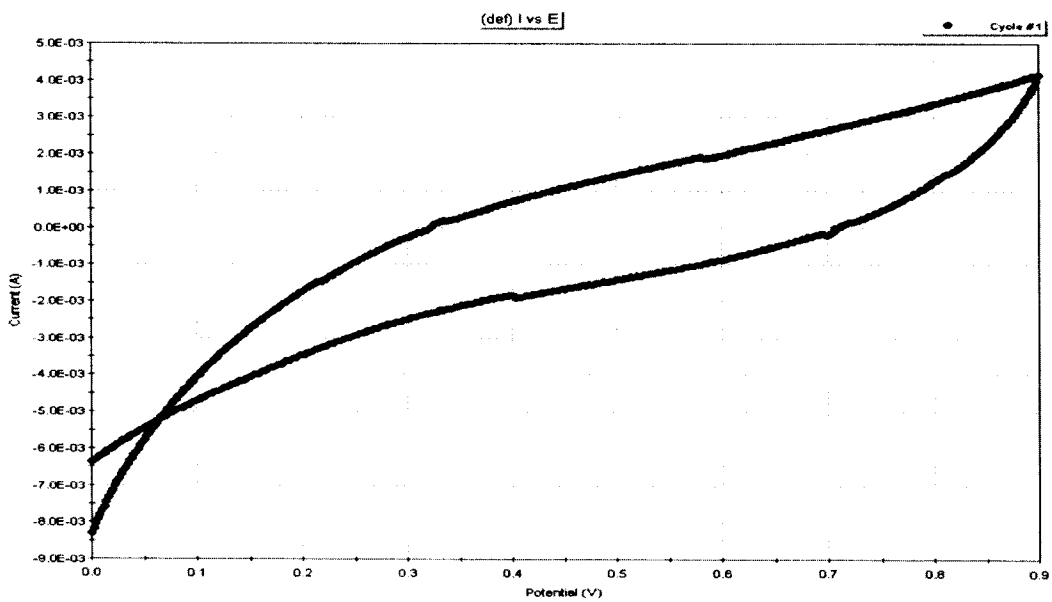


*Fig 5.7 Cyclic Voltammogram of OMS-2*

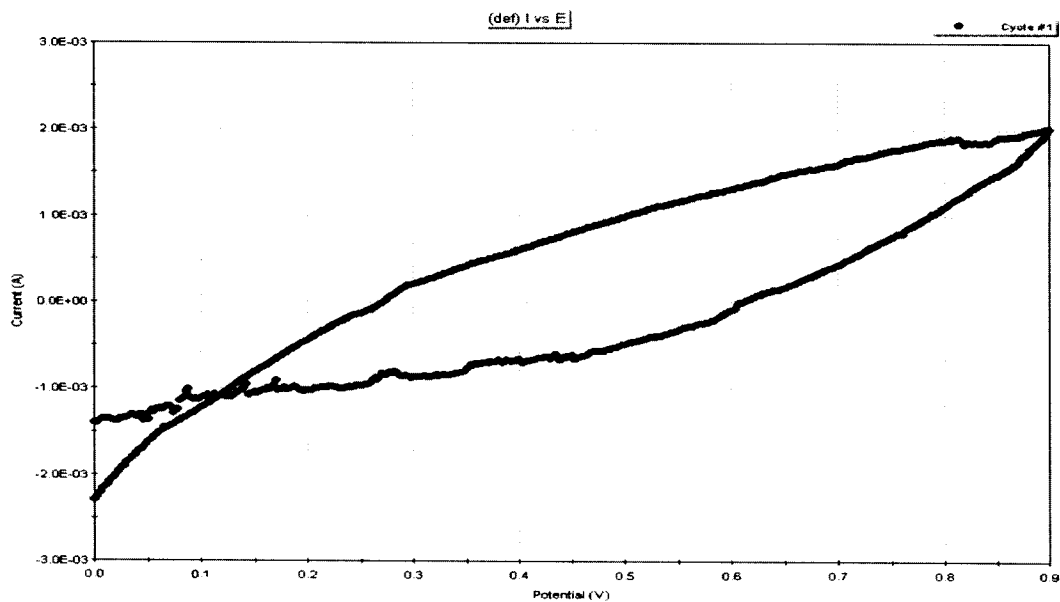


*Fig 5.8 Cyclic Voltammogram of Carbon nano tube*

The current that was produced at 0.5 V for the samples with and without OMS -2 is given in Table 5.1.

SAMPLE	Current I (A) at 0.5V	SAMPLE with OMS-2	Current I (A) at 0.5V
C1	$1 \times 10^{-3}$	C1 O	$2 \times 10^{-3}$
C2	$0.9 \times 10^{-3}$	C2 O	$1.2 \times 10^{-3}$
CP	$1.6 \times 10^{-3}$	CPO	$1 \times 10^{-3}$
CMC- N	$2.5 \times 10^{-3}$	CMC-N O	$1.4 \times 10^{-3}$
MnO <sub>2</sub> /C1	$0.5 \times 10^{-3}$	MnO <sub>2</sub> /C1 O	$1.4 \times 10^{-3}$
OMS	$1.4 \times 10^{-3}$	-	-
C nano tube	$1 \times 10^{-3}$	-	-

**Table 5.1** Current I (A) at 0.5V for carbons with and without OMS-2

It was observed that the maximum current of  $2.5 \times 10^{-3}$  A was produced for CMC-N carbon without OMS-2. CMC-N has large surface functional groups as well as porosity with surface area of 1025 m<sup>2</sup>/g. However with OMS-2, the current decreased to  $1.4 \times 10^{-3}$ . This could be attributed to the linking of OMS-2 to surface functional groups which affected the charge density. In all the other samples the current increased with the addition of OMS -2. The maximum increase being for C1 from  $1 \times 10^{-3}$  A to  $2 \times 10^{-3}$  A. C1 has a high surface area.

The current density was found out by calculating the surface area enclosed in the voltammogram.

Sample	Current density
C1O	$19.24 \times 10^{-2}$
C2O	$22.60 \times 10^{-2}$
CPO	$11.03 \times 10^{-2}$
CMC- NO	$14.93 \times 10^{-2}$
MnO <sub>2</sub> /C1 O	$17.29 \times 10^{-2}$
OMS-2	$21.68 \times 10^{-2}$
C nanotube	$8.61 \times 10^{-2}$

*Table 5.2 Current density of carbons C1, C2, CP, CMC N with OMS-2, MnO<sub>2</sub> supported carbons with OMS-2, OMS-2 and Carbon nanotube.*

The current density was maximum for C2O and was comparable to OMS. C1O also showed a considerable amount of charge density.

Fig 5.9 gives a comparative view of the charge densities of CMC NO, C2O and OMS.

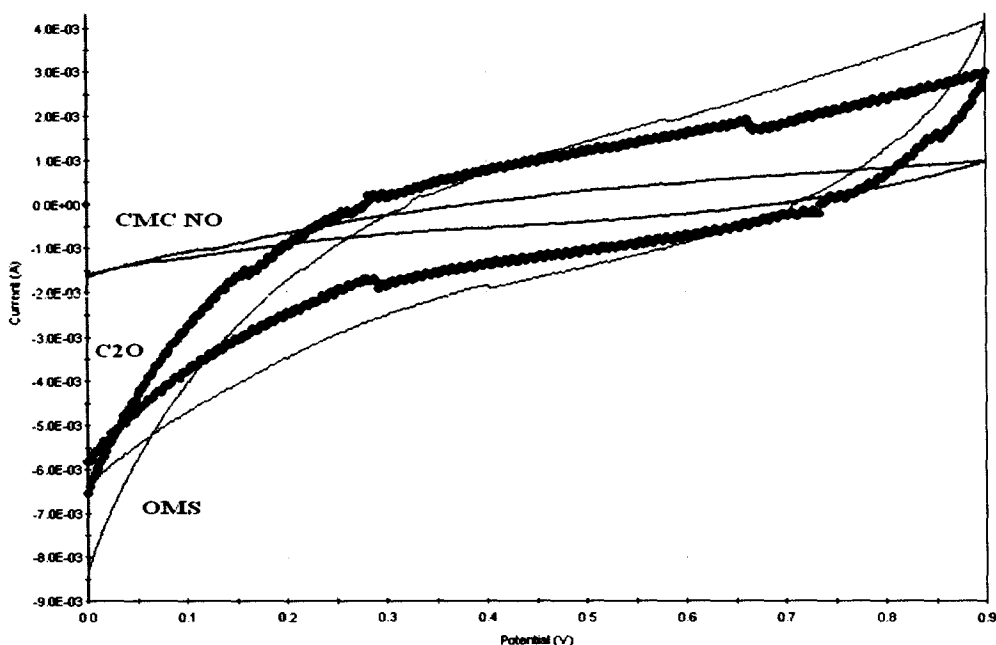


**Fig 5.9 Comparative cyclic voltammogram of activated carbon C1 with OMS-2, CMC -N with OMS -2 and OMS-2**

CMC NO which showed highest current at 0.5V without OMS shows a decrease in charge density on addition of OMS-2 as can be seen from the comparative CVs

High surface area carbons are desirable for enhancing electrochemical capacitance, when used as capacitors in combination with batteries and fuel cells and can also be good support materials for electrocatalysts such as Pt-C in fuel cells.

In the present investigation, it is observed that the capacitance of the carbon electrodes i) increase upon functionalisation ii) increase when mixed with OMS-2. OMS-2 which is an Mn (IV) oxide is believed to increase the capacitance of carbon supports by undergoing reversible charge-discharge cycles.

Thus the carbons investigated in the present work can be used as supports for catalytic and electrocatalytic materials for green processes.

## 2 ELECTROCATALYSIS

### 5.2.1 Introduction

Carbon is used in electrodes as an electro catalyst and or as a substrate for the catalyst. A wide spectrum of electrocatalytic properties is found in carbon electrodes because of their extensive variety and wide ranging physiochemical properties. Some of these include oxygen reduction/evolution, decomposition of hydrogen peroxide, hydrogen oxidation /evolution and other redox reactions.

*Electrocatalysis* is the enhancement of electrode kinetics by a material by minimizing the overpotential. *Overpotential* is the extra potential over the equilibrium value that must be applied to cause an electrodic reaction at a certain rate. An electrodic reaction may be anodic (oxidation) or cathodic (reduction) depending upon the direction of overpotential with respect to the equilibrium potential of the electrode.

### 5.2.2 Electrocatalysis using porous carbon supports.

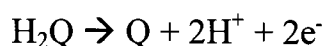
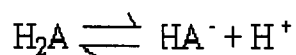
Traditionally fuel cell electrode catalysts are prepared using carbon black supports for Pt. It is recently shown that efficiency of methanol oxidation kinetics at an anode increases when Pt electrodes are prepared using carbon nanotubes or mesoporous carbons as supports. The efficiency further increases when the carbon supports are oxidized containing oxygenated surface groups [81].

Many carbon electrodes used in electroanalytical studies suffer from poor electro catalytic activity or exhibit poor selectivity in solutions containing several electro active species. Various procedures for improving the reproducibility of the

electrochemical measurements and enhancing the electrocatalytic activity and selectivity of the carbon surface have been evaluated. These procedures are often referred to as “electrode activation”. Many explanations have been advanced for the role of activation on carbon electrodes, such as to

- (a) remove contaminants from the electrode surface;
- (b) increase the concentration of surface functional groups that may act as electron-transfer mediators;
- (c) increase the surface area by increasing the surface roughness; and
- (d) expose fresh edge planes, micro particles, and defects that may be sites for electron transfer.

The surface oxygen groups produced by activation play a role in enhancing the electrocatalytic activity of carbon electrodes. The suggestion is made [82, 83, 84] that phenol-type groups may be important for enhancing the rates of reactions involving proton-coupled electron transfer (e.g., electrochemical reaction of H<sub>2</sub>A and DA). The pathway for proton-coupled electron transfer involving the oxidation of H<sub>2</sub>A, and the role of quinone (Q) and hydroquinone (HQ) groups on the carbon surface, is illustrated by the following reaction sequence:



### 5.2.3 Electrocatalysis by Manganese Oxides:

Manganese oxide-based solids having channels, layers, and pillars can be made to specification for applications ranging from detergents to sensors. They are generally prepared by permanganate or chlorate oxidation of Mn (II) salt. Recently manganese oxide of the type OMS-2 is synthesized using sulphate ion as a structure directing agent [85]. Fig.5.10 gives structure of OMS-2 and OMS-1.

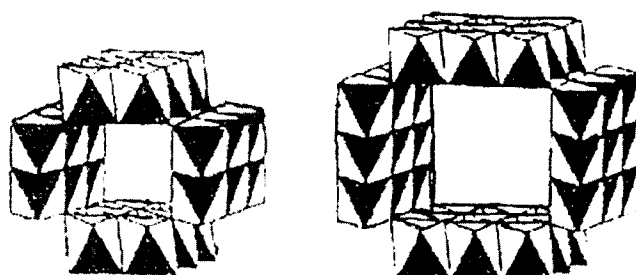


*Fig 5.10 (a) OMS-2*

*(b) OMS-1*

Manganese oxides are well known to be oxidation catalysts. Recently it is shown that they readily catalyse oxidation of benzyl alcohol initiated through its lattice oxygen.

OMS - 2 has shown high activity in anodic oxidation of methanol. The activity is enhanced by making appropriate electrode composites with carbon supported Ruthenium [79]

### 5.2.4 Hydrogen evolution reaction

Hydrogen is one of the most important chemical which is in high demand in industry as a general purpose fuel, in hydrogenation processes, in fuel cells for generation of electricity etc. On commercial scale it is produced by steam reforming of hydrocarbons. Hydrogen thus obtained is not very pure. Although there are several other non – conventional methods to produce H<sub>2</sub>, they are not yet economically viable for large scale production.

Hydrogen is often produced by electrolysis of water between steel cathodes and nickel anodes. Considering the over potentials and the IR drop, the operating cell voltage is about 2.0 V although the equilibrium cell voltage for decomposition of water is 1.23 V. A typical cell is known to generate current density of 10<sup>3</sup> A/m<sup>2</sup> and can deliver 500 m<sup>3</sup> H<sub>2</sub> per hour

Very pure hydrogen is produced by electrolysis of water Fig.5.11

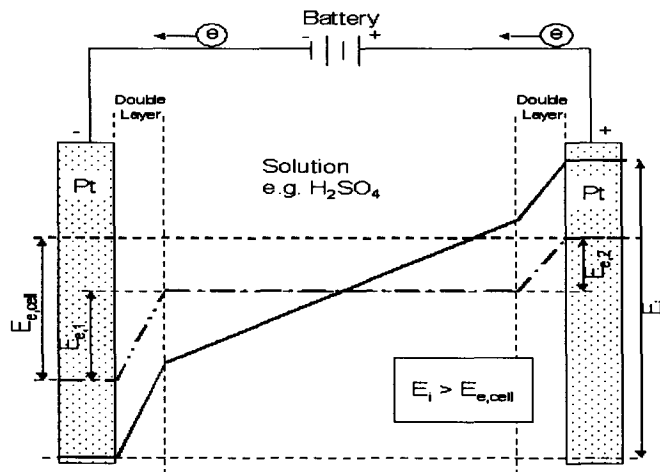


*Fig. 5.11 illustrates the excess potential  $E_i$  needed during electrolysis, over the equilibrium potential.*

$E_e$  [2].  $E_e, 1$  and  $E_e, 2$  represent the potential drops across the double layer at cathode and anode respectively. (the thick solid line is due to ohmic drop  $IR$  within the solution as well as due to cathodic and anodic overpotentials  $\eta_c$  and  $\eta_a$  [ 86]

### 5.2.5 Oxygen evolution

Despite all the attention devoted to electrocatalysis of oxygen reduction and evolution in aqueous solutions at low and moderate temperatures, the overpotential for these electrochemical reactions with practical electrocatalyst is high. Thus the challenge remains to reduce the overpotential of oxygen electrodes in such applications as fuel cells, metal/air batteries and industrial electrolytic processes.

The carbon electrode has an effect on the potential at which oxygen evolution is observed [88]. The Tafel slope for  $O_2$  evolution on graphite fibre in an epoxy – composite electrode ranges from 0.3 to 0.4V/decade in buffer solutions of 8.1 to 13.3 [89]. The Tafel slope (-0.3V) is independent of pH in acid and neutral solutions and tend to increase to higher values in alkaline solutions.

Owing to the high over potential oxygen evolution on carbon electrodes in alkaline solutions is generally accompanied by carbon erosion. This problem is exasperated with high surface area carbons which are susceptible to corrosion. The onset of corrosion of acetylene black in KOH occurs at about 0.0V versus Hg/HgO,  $OH^-$  [90].

At temperatures below 50 °C and potentials below 0.5 V, carbon corrosion forming carbonate is the primary anodic process in KOH solution but at 0.5 and 0.6 V evolution of oxygen and carbon corrosion occurs at the same rate [88].

### 5.2.6 Tafel relationship

The electrochemical cell set up to find the Tafel relationship is as shown in Fig 5.2.12

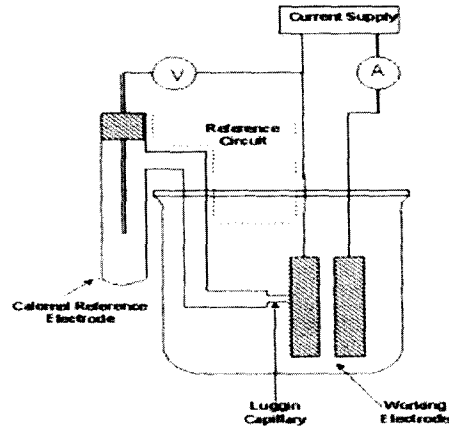


*Fig 5.12 Electrochemical cell set up for Tafel plot*

The salient features of the electrolytic cell are

- Counter electrode which is connected to the working electrode through a current source so that controlled current can be passed at the working electrode.
- A high impedance voltmeter measures the potential difference the potential difference between the reference and the working electrode.
- The use of luggin capillary between the two electrodes prevents minimizes the ohmic drop or IR drop.
- Currents to the working electrode can be measured as a function of various overpotentials.

Tafel relationship is given by the graph of  $\eta$  v/s  $\log i$ .

$$\text{where } \eta = 0.059/\alpha \log i_0 + 0.059/\alpha \log i$$

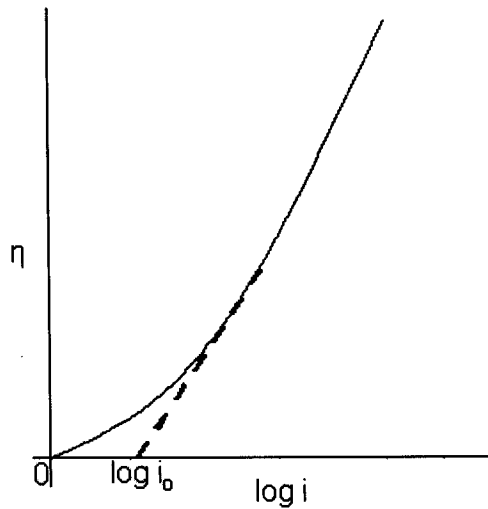


**Fig 5.13 Tafel graph of  $\eta$  v/s  $\log i$**

From the graph of  $\eta$  v/s  $\log i$ , it is possible to find out the exchange current density  $i_0$ . The linear portion of the Tafel plot intercepts the  $\log i$  axis at  $\eta = 0$ . From the intercept  $\log i_0$  the exchange current density  $i_0$  can be evaluated.

The slope of the linear portion also known as Tafel region is given by  $0.059/\alpha$  from which the value of transfer coefficient  $\alpha$  can be determined [91, 92].

### 5.2.7 Experimental

A comparative study was done with commercial Pt/ C electrode and Pt/CMCN electrodes during electrolysis of water acidified with sulphuric acid. The Pt/CMCN electrode was prepared by coating a thin film of CMC N carbon on the commercial Pt/C electrode.

An electrolytic cell was set up as in Fig 5.14 using the above electrodes as working electrode and current – overpotential data was recorded to obtain Tafel plots as given in Fig 5.1 was recorded.

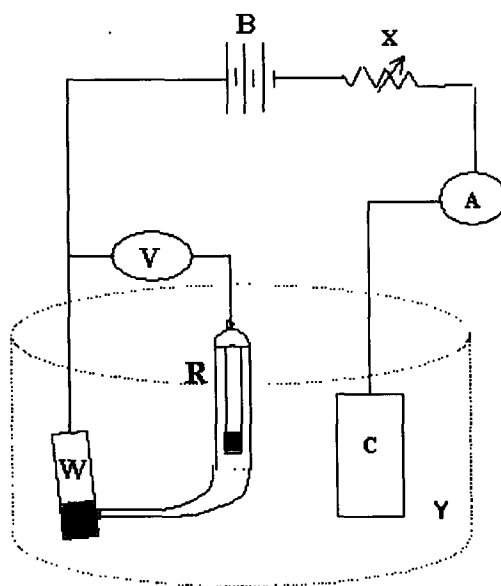


**Fig 5.14 Experimental set up for Tafel measurements**

**B** – Battery or AC supply

**X** – Variable Resistance

**A** – Ammeter

**V** – Voltmeter

**W** – Working electrode

**R** – Reference Electrode

(SCE with lugging capillary)

**C** – Counter Electrode (Pt foil)

**Y** – Cell containing 2.5 M H<sub>2</sub>SO<sub>4</sub> + 1M MeOH

## 5.2 .8 Results and Discussion

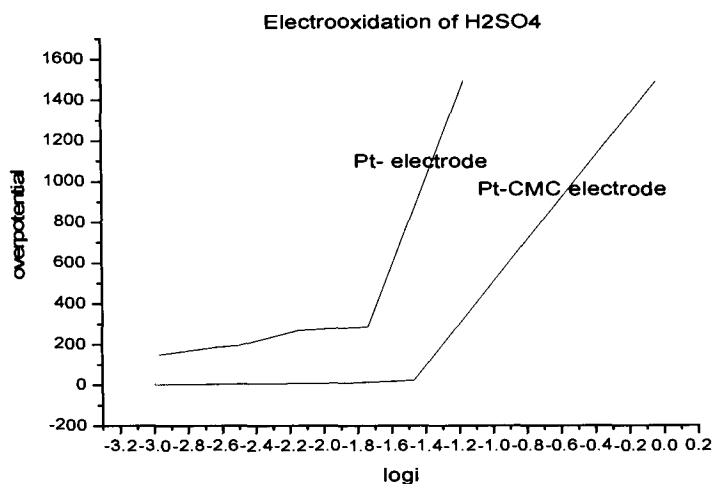
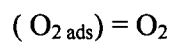
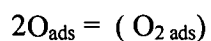
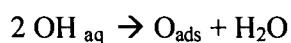
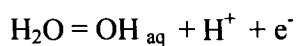


**Fig 5.15 Tafel plot of electrooxidation of sulphuric acid acidified water.**

It was found that the use of Pt/C electrode resulted in higher evolution of oxygen as compared to Pt at the same overpotential.

The proposed mechanism for oxygen evolution could be as postulated [91] on glassy carbon



CMC N carbon has high porosity and surface functional groups which facilitated oxygen adsorption and evolution on its surface.

## 5.3 CATALYTIC REACTIONS OF CARBONS AND MnO<sub>2</sub>/C

### 5.3.1 Introduction

Activated carbons are known to be good catalysts and have been used to catalyze several reactions. They have also been used as supports for other catalyst. The catalytic activity can be enhanced by impregnating the carbon with the substance specific catalyst.

*Table 5.3 Gives the list of the impregnated chemical and the application of the impregnated carbon.*

Impregnation of carbon	
Chemicals	Examples for application
Sulfuric acid	Ammonia, amine, mercury
Phosphoric acid	Ammonia, amine
Potassium Carbonate	Acid gases (HCL, HF, SO <sub>2</sub> ,) H <sub>2</sub> S, mercaptan.
Iron Oxide	H <sub>2</sub> S, mercaptan.
Potassium iodide	H <sub>2</sub> S, PH <sub>3</sub> , Hg, AsH <sub>3</sub> , Radioactive Gases/radioactive methyl iodide
Triethylene Diamine (TEDA)	Radioactive Gases/radioactive methyl iodide
Sulfur	Mercury
Potassium Permanganate	H <sub>2</sub> S from oxygen-lacking gases
Manganese IV Oxide	Aldehyde

Silver	Phosphine, arsine, domestic drinking water  Filters
Zinc oxide	Hydrogen cyanide
Chromium Copper-silver Salts	Civil and military gas protection  Phosgene, chlorine, arsine
Mercury II Chloride	Vinyl chloride synthesis  Vinyl fluoride synthesis
Zinc acetate	Vinyl acetate synthesis
Noble metals (palladium, platinum)	Organic synthesis,  Hydrogenation.

**Table 5.3 List of the impregnating chemical and the application of the impregnated carbon[92]**

### 5.3.2 Decomposition of potassium chlorate

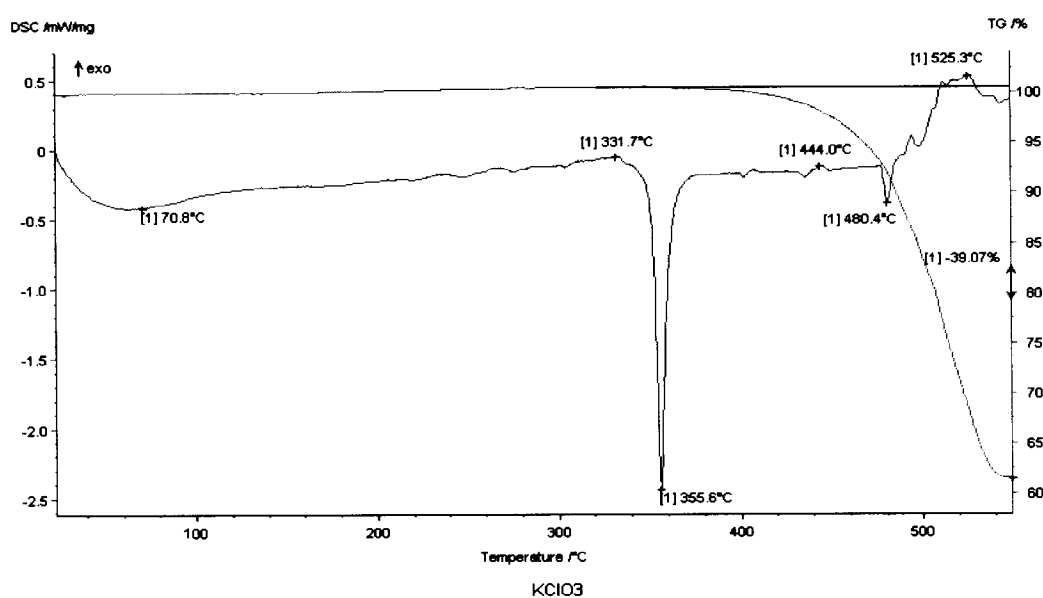


**Fig 5.16 Thermogravimetric analysis of potassium chlorate**

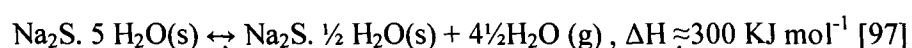
It is well known that potassium chlorate decomposes at a higher temperature to give potassium chloride and oxygen. It melts at 355<sup>0</sup>C and decomposes at 480<sup>0</sup>C.

Potassium chlorate is used as an oxidizing agent and source of oxygen for many chemical reactions. It is an important component in the making of explosives. To reduce the decomposition temperature, manganese dioxide is the standard catalyst. The search for more efficient and cheap catalyst is on. Carbon as well as impregnated ones are researched upon as a viable alternative catalyst.

### *5.3.3 Phase change of sodium sulphide*

In recent years much effort has been put into the development of heat driven solid sorption chemical heat pumps and heat transformers [93] for heating as well as cooling purposes. The working principle of this apparatus is based on the exothermic absorption and endothermic desorption of vapour in solids, e.g. water in silica or zeolites [94], ammonia in metal salts [95] or in carbon [96]. The thermal effects and thus the attainable energy densities are much larger, about one order of magnitude, in the case of chemisorption, e.g. hydration of metal salts, than in the case of physisorption of e.g. water in silica.

The structural, thermodynamic and phase properties of the Na<sub>2</sub>S-H<sub>2</sub>O system are important in a waste heat driven solid-vapour absorption heat pump for cooling purposes in buildings and industrial processes. The heat pump operation is based on the following equilibrium reaction:



The present concern about themes like greenhouse effect, pollution, renewable energy and durable society has incited researchers to find better ways of using the limited energy resources at our disposal. This resulted in the development of fuel cells, solar cells and heat pumps, to mention only a few. At the same time energy efficiency has a huge potential for reduction of energy consumption and CO<sub>2</sub> reduction.

Sulphur impregnated carbons are used for mercury elimination which has toxic properties, causes environmental hazards or poisons catalytic industrial processes. More than ninety percent removal has been achieved for this carbon. Sodium sulfide is a potential chemical for producing sulphur impregnated carbons.

#### *5.3.4 Catalytic gasification of carbon*

While carbon acts as a catalyst and catalyst support for many reactions, its gasification temperature becomes significant. The carbon oxidation rate is greatly enhanced by catalytic agents, which are often the inorganic impurities that are commonly found in the sample. The gasification of carbons in the presence of catalytic agents is loosely referred to as “catalytic gasification”. The implications of catalytic gasification has practical importance in the conversion of coal by reaction with H<sub>2</sub>O (steam) or CO<sub>2</sub> to gaseous fuels or chemical feedstocks. A recent review by Wood and Sancier [67] provides an excellent survey of papers published since 1979 on the catalytic gasification of carbon.

The catalytic effect of Carbon and MnO<sub>2</sub>/C in the decomposition reaction of potassium chlorate and phase change of sodium sulphide is the subject of investigation as well as the catalytic effect of these compounds on carbon gasification.

### 5.3.5 Experimental

The following samples were used for Thermo gravimetric analysis using the Shimadu instrument.

1. C1: activated carbons obtained from SD Fines Chemicals Ltd
2. CMC: activated carbon synthesized from CMC
3.  $\text{MnO}_2/\text{C1}$ : manganese dioxide supported on C1 by calcining manganese nitrate.
4.  $\text{MnO}_2$ : synthesized by calcining manganese nitrate.
5.  $\text{KClO}_3$ : obtained from Loba Chemicals
6. MK: prepared by mixing  $\text{KClO}_3 + \text{MnO}_2$  in the ratio 1:1
7. C1K: prepared by mixing C1 and  $\text{KClO}_3$
8. CMCK: prepared by mixing CMC and  $\text{KClO}_3$
9. MC1K: prepared by mixing  $\text{MnO}_2/\text{C1}$  and  $\text{KClO}_3$
10. NS: fused sodium sulphide obtained from Loba Chemie
11. C1NS: prepared by mixing C1 and fused sodium sulphide.
12. CMC NS: prepared by mixing CMC and  $\text{Na}_2\text{S}$
13. MC1NS: prepared by mixing  $\text{MnO}_2/\text{C1}$  and  $\text{Na}_2\text{S}$
14. C1KNS: prepared by mixing C1,  $\text{KClO}_3$ ,  $\text{Na}_2\text{S}$
15. CMCKNS: prepared by mixing CMC,  $\text{KClO}_3$ ,  $\text{Na}_2\text{S}$

### 5.3.6 Results and Discussions

Manganese dioxide is a known catalyst used in the in the preparation of oxygen, to reduce the decomposition temperature of potassium chlorate. Fig 5.17 profiles the decomposition temperature of  $KClO_3$ ,  $MnO_2$ ,  $KClO_3+MnO_2$ ,

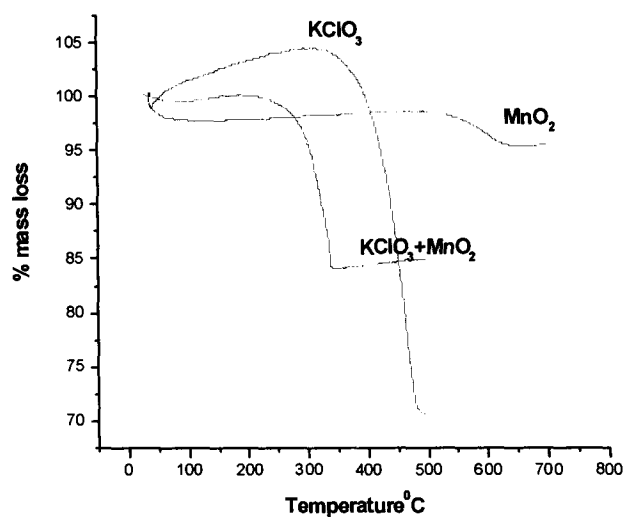


**Fig 5.17 TG of  $KClO_3$ ,  $MnO_2$  and  $KClO_3+MnO_2$  in argon atmosphere.**

<b>catalyst</b>	<b><math>KClO_3</math></b>	<b><math>MnO_2</math></b>	<b><math>KClO_3+MnO_2</math></b>
Decomposition temp	480 °C	520 °C	350 °C

**Table 5.4 List of the Decomposition temperature of  $KClO_3$ ,  $MnO_2$  and  $KClO_3+MnO_2$**

The decomposition temperature of  $KClO_3$  decreased from 480 °C to 350 °C indicating the catalytic role played by manganese dioxide.

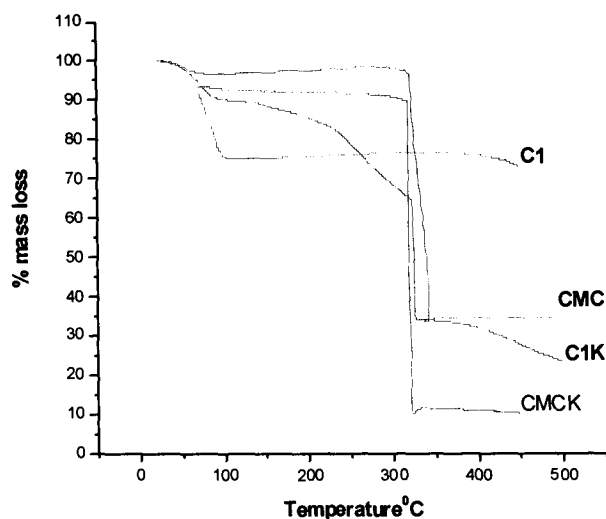


***Fig 5.18 TG of C1 and CMC in oxygen atmosphere and TG of C1K and CMCK in argon atmosphere.***

Fig 5.18 indicates very clearly that the carbons were instrumental in decreasing the decomposition temperature of  $\text{KClO}_3$ .

In an atmosphere of oxygen, C1 oxidized at  $425^\circ\text{C}$  whereas CMC got oxidized at  $340^\circ\text{C}$ . The decomposition temperature of  $\text{KClO}_3$  came down to  $325^\circ\text{C}$  from  $480^\circ\text{C}$  which is much lower than manganese dioxide catalysed reaction temperature of  $350^\circ\text{C}$ .

C1 gets oxidized at  $425^\circ\text{C}$  indicated by the weight loss due to the formation of carbon dioxide whereas the weight loss indicated by C1K is at  $325^\circ\text{C}$ . The weight loss can be attributed to the formation of carbon dioxide when C1 reacts with the oxygen obtained by the decomposition of potassium chlorate in an atmosphere of argon.

The weight loss indicated by the TG of C1K at 100 °C is due to the moisture and the subsequent weight loss indicated by the gradual downward graph is due to the decomposition of potassium chlorate. At 325 °C a sharp decline in weight loss is seen. This is due to the oxidation of the carbon.

It is a known fact that alkali metals acts as catalyst in the gasification of carbons. In this instance potassium chlorate catalyzed the oxidation the oxidation of C1 which otherwise oxidised at 425 °C.

C1 thus is an effective catalyst for the decomposition of potassium chlorate in the temperature range of 250 °C to 300 °C. Potassium chlorate is good catalyst for the oxidation of C1.

CMC also acts as a catalyst for potassium chlorate decomposition as is indicated by the sharp weight loss at 325 °C. The decomposition of potassium chlorate provides the oxygen for oxidation of CMC. The oxidation of CMC in oxygen takes place at 340 °C whereas with potassium chlorate it takes place at 325 °C in an inert atmosphere.

Though CMC catalyses the decomposition of potassium chlorate, its oxidation temperature is close to the decomposition temperature of  $\text{KClO}_3$ . Hence, it can only be used in reactions where the oxidation temperature of CMC is increased.

Comparatively, the efficiency of C1 is much better. Potassium chlorate acts as good catalyst for the oxidation of CMC as well similar to C1.

The efficacy of catalyst can further be enhanced by supporting  $MnO_2$  on carbon as shown by the TG profiles in Fig 5.19.

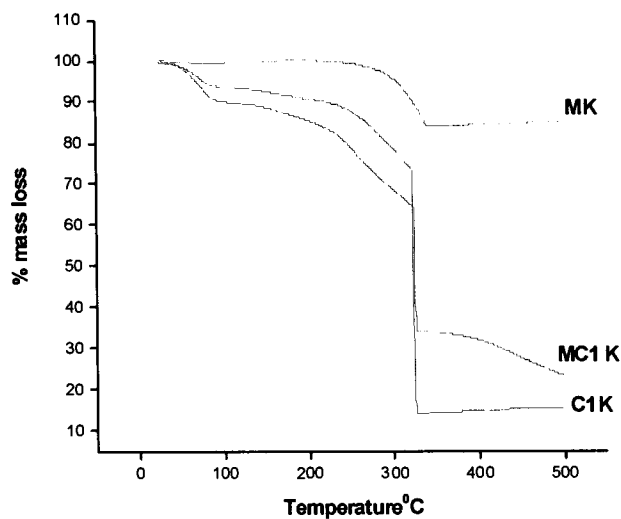


**Fig 5.19 TG profiles of mixtures of  $MnO_2 + KClO_3$ ,  $MnO_2/C1 + KClO_3$ ,  $C1 + KClO_3$  in argon atmosphere.**

The decomposition of potassium chlorate is much more for manganese dioxide on carbon (MC1K) as compared to just carbon (C1) as well as for manganese dioxide as catalyst (MK). However, in case where carbon is one of the components, the weight loss is sharp and more because of the oxidation of carbon catalysed by potassium salts.

When sodium sulphide was added to a mixture of C1K and CMCK separately, the oxidation of carbons took place at a much lower temperature of  $225^{\circ}C$  and  $275^{\circ}C$  respectively as evident from TG profiles in Fig 5.20

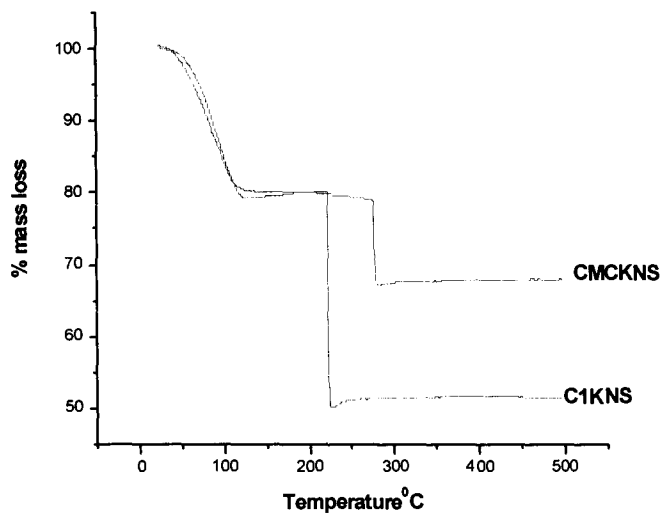


*Fig 5.20 TG profiles of mixtures of CMC + KClO<sub>3</sub> + Na<sub>2</sub>S and C1 + KClO<sub>3</sub> + Na<sub>2</sub>S in argon atmosphere.*

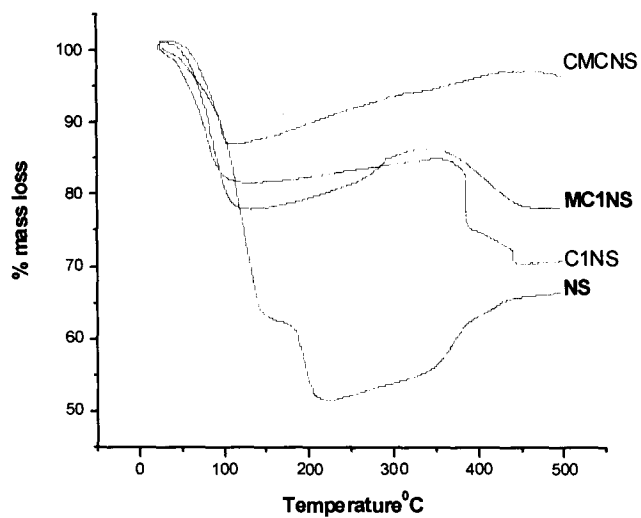


*Fig 5.21 TG profiles of CMC + Na<sub>2</sub>S, MnO<sub>2</sub>/C1 + Na<sub>2</sub>S, C1 + Na<sub>2</sub>S, Na<sub>2</sub>S in argon atmosphere.*

With the addition of catalyst the melting temperature has been delayed.

Andersson [100] and Mereiter [105] considered the structure of  $\text{Na}_2\text{S}\cdot 5\text{H}_2\text{O}$  to consist of alternating layers of sodium, water and sulphur, represented by  $\cdots\text{—S—H}_2\text{O—Na—H}_2\text{O—S—}\cdots$ . This structure leads to a high mobility of 4 out of 5 water molecules. The transformation of  $\text{Na}_2\text{S}\cdot 5\text{H}_2\text{O}$  to  $\text{Na}_2\text{S}\cdot 2\text{H}_2\text{O}$  was assumed to be a topotactic process, in which 3 out of 5 water molecules can be removed from the crystal, followed by a shift in the crystallographic position of some of the sodium atoms and the remaining water molecules. This gives a new structure, the  $\text{Na}_2\text{S}\cdot 2\text{H}_2\text{O}$  phase. Dehydration of this compound to the anhydrous  $\text{Na}_2\text{S}$  phase was also assumed to occur in a topotactic process.

The melting temperature of  $\text{Na}_2\text{S}\cdot 9\text{H}_2\text{O}$  and mixtures of  $\text{Na}_2\text{S}\cdot 5\text{H}_2\text{O}$  with  $\text{Na}_2\text{S}\cdot 2\text{H}_2\text{O}$  and of  $\text{Na}_2\text{S}\cdot 2\text{H}_2\text{O}$  with  $\text{Na}_2\text{S}$  increases with decrease in hydration as per reported work on the crystallographic, physical and thermochemical properties of the  $\text{Na}_2\text{S—H}_2\text{O}$  system [97-105].

Furthermore it is seen that the presence of  $\text{Na}_2\text{S}\cdot 2\text{H}_2\text{O}$  phase does not lead to significant changes in the melting temperature for samples with compositions between  $\text{Na}_2\text{S}\cdot 5\text{H}_2\text{O}$  and  $\text{Na}_2\text{S}\cdot \frac{1}{2}\text{H}_2\text{O}$

The rising proportion of the profiles in Fig 5.3.5 is believed to be due to the catalytic oxidation of  $\text{S}^{2-}$  to neutral sulphur, followed by formation of polysulphide clusters or  $\text{S}_x$  agglomerates.

It is therefore concluded that the manganese oxide supported on carbon C1 is more effective in Na<sub>2</sub>S oxidation as evident from TG profiles.

#### 5.3.7 Conclusions

- It was observed that the maximum current of  $2.5 \times 10^{-3}$  A was produced for CMC N carbon without OMS-2.
- The current density increased on addition of OMS-2 for all carbons but decreased for CMC N and was maximum for carbon C2 .
- Pt/C electrode resulted in higher evolution of oxygen as compared to Pt at the same overpotential.
- CMC N and C1 carbons decreased the decomposition temperature of KClO<sub>3</sub>.
- KClO<sub>3</sub> catalysed the gasification of carbons.
- Manganese oxide supported on carbon C1 is more effective in Na<sub>2</sub>S oxidation

## REFERENCES

1. K. Kinoshita, Carbon Electrochemical and Physiochemical properties, A Willey Interscience Publication (1987).
2. E.I Shoben, M. L. Deveney and T.M. O'Grady, Eds.( ACS Symposium 21), Washington D. C. (1976) 91.
3. A. Burke, J. Power Sources, 91 (2000) 37.
4. B. Kotz, M. Carlen, Electrochim. Acta, 45 (2000) 2483.
5. B E Conway, Electrochemical Supercapacitors, Kluwer Academic Publishers, New York (1999) 12.
6. G. Gutmann, J Power Sources, 84 (1999) 275.
7. L. P. Jarvis, T. B. Atwater, P. J. Cygan, J Power Sources, 79 (1999) 60.
8. R. A. Huggins, Solid State Ionics, 134 (2000) 179.
9. A. J. Bard, L. R. Faulkner, Electrochemical Methods, Fundamentals and Applications, John Wiley & Sons, Inc.( 2001).
10. C. C. Hu, Y. H. Huang, J Electrochem. Soc, 146 (1999) 2465.
11. C. C. Hu, K. H. Chang, Electrochim. Acta, 45 (2000) 2685.
12. C. C. Hu, K. H. Chu. J Electroanal. Chem, 503 (2001) 105.
13. E. Faggioli, P Rena, V Danel, X. Andrieu, R. Mallant, H. Kahlen, J. Power Sources, 84 (1999) 261.
14. W. R. Smith Encyclopedia of Chemical Technology, 2<sup>nd</sup> ed, Interscience New York, 4 (1964) 243.
15. E. M. Dannenberg in Kirk Othmer Encyclopedia of Chemical Technology, 3<sup>rd</sup> ed, Wiley New York, 4 (1978) 631.
16. H.G. Golding, Research development, 46 (1973).
17. M. Bregazzi, Electrochem Technol, 5 (1967) 507.

18. C. L. Mantel, Carbon and Graphite hand book, Interscience, New York (1968) 76.
19. K. V. Kordesch, BNL 51418, Brookhaven National Laboratory (1979).
20. J. H. Je and J. Y. Lee, Carbon, 22 (1984) 318.
21. J. E. Lewis, J. D. Bacha, J. W. Newman and J. L. White, Eds (ACS symposium Series, 303) Washington DC (1986) 269.
22. J. Lahaye and G. Prado, P.L.Walker and P. A. Throver, Eds, Dekker, New York (1979) 167.
23. L. Mackles, R. A. Heindl, I.E. Mong, J. Am. Ceram Soc, 36 (1953) 266.
24. T. Ishikawa and T. Nagaoki, Eds, Recent Carbon Technology, JEC press, Inc, (1983) 70.
25. W.E. Chambers, Mech Eng, 37 (1975).
26. S. Otani, Y. Kokubo and T. Koi Tabashi, Bull chem. Soc Jpn, 43 (1970) 3291.
27. K. Kawamura and G. M Jenkins, J Mat Sc, 7, (1972) 1099.
28. S. Yamada and M Yamamoto, Carbon, 6 (1968) 741.
29. C. M. Krutechen, D. G. Flom, 11<sup>th</sup> Biennial Conference on Carbon, Gutlimberg, Tennessee, June 4-8 (1973).
30. Y.R. Nian, H. Teng, J Electrochem Soc, 149 (2002) 1008-1014.
31. C.T. Hsieh, H Teng, Carbon, 40 (2002) 667-674.
32. T. Momma, X.J Liu, T. Osaka, Y. Ushio, Y. Sawada, J Power Sources, 60 (1996) 249-253.
33. M. J. Bleda-Martinez, E Morallon, D. Cazorla-Amoros, Electrochimica Acta 52 (2007) 4962-4968.
34. D.Y. Qu, H. Shi, J Power Sources, 74 (1998): 99-107.
35. H. Shi, Electrochim Acta, 41 (1996) 1633-1639.

36. I. Tanahashi, A. Yoshida, A. Nishino, *J Electrochem Soc*, 137 (1990) 3052-3057.
37. D. Lozano-Castello, D. Cazorla-Amoros, A. Linares-Solano, S. Shiraishi, S. Kurihara, H. Oya, *Carbon*, 41 (2003) 1765-1775.
38. O. Tanaike, H. I. Hatori, Y. Yamada, S. Shiraishi, A. Oya, *Carbon*, 41 (2003) 759-1764.
39. R. O Grisdale, *J.Appl.Physics*, 24 (1953) 1288.
40. G. R. Henning, *Proceedings of the fifth Conference on carbon*, Pergamon Press, New York, 1 (1962) 143.
41. F. J. Vastola, P. L. Walker, *Proceeding of the fifth Conference on Carbon*, Vol 2, Pergamon Press, New York (1963) 211.
42. R. O. Lussow, F. J. Vastola, P. L. Walker, *Carbon*, 5 (1967) 591.
43. P. J. Hart, F. J. Vastola, P.L. Walker, *Carbon*, 5 (1967) 363.
44. R. C. Bansal, F. J. Vastola, P. L. Walker, *Carbon*, 8 (1970) 443.
45. R.C. Bansal, F. J. Vastola, P. L. Walker, *J Coll Sc*, 32 (1970) 187.
46. P. L. Walker and J. Janov, *J Coll Sc*, 28 (1968) 449.
47. W. R. Smith and M. H. Polley, *J Phys Chem*, 60 (1956) 689.
48. F. Rodriguez-Reiniso and P. A. Thrower, *Carbon*, 12 (1974) 269.
49. W. M. Qiao, Y. Korai, I. Mochida, Y Hori, T Maeda, *Carbon*, 40 (2002) 351-358.
50. H. Oda, A. Yamashita, S. Minoura, M. Okamotoa, T Morimoto, *J Power Sources*, 158 (2006) 1510-1516.
51. B. Z. Fang, L. Binder, *J Phys Chem*, 110 (2006) 7877-7882.

52. B. Z Fang, Y. Z Wei, K. Suzuki, M Kumagai, *Electrochimica Acta* , 50 (2005) 3616-3621.
53. A.Swiatkowski, M. Pakula, S. Biniak, M Walczyk, *Carbon*, 42 (2004) 3057-3069.
54. A. Burke, *I. Power Sources*, 91 (2000) 37.
55. B. Kotz, M. Carlen, *Electrochim. Acta*, 45 (2000) 2483.
56. B. E. Conway, *Electrochemical Supercapacitors*, Kluwer Academic Publishers, New York (1999) 12.
57. C. C. Hu, Y. H. Huang, *J Electrochem. Soc*, 146 (1999) 2465.
58. C. C. Hu, K. H. Chang, *Electrochim. Acta*, 45 (2000) 2685.
59. C. C. Hu, K. H. Chu, *J Electroanal. Chem*, 503 (2001) 105.
60. E. Faggioli, P. Rena, V Danel, X.Andrieu, R Mallant, H. Kahlen, *J. Power Sources*, 84 (1999) 261.
61. C. Lin, J. A. Ritter, D. B. N. Popov, *J. Electrochem Soc*, 145 (1998) 4097.
62. V. Srinivasan, J. W. Weidner, *J. Electrochem. Sec*, 144 (1997) 210.
63. H.Y. Lee, S. W. Kim, H. Y. Lee, *Electrochem. Solid State Lett*, 4 (2001) 19.
64. S. C. Pang, M. A. Anderson, T. W. Chapman, *J Electrochem. Soc*, 147 (2000) 444.
65. H. Y. Lee, J. B. Goodenough, *J. Solid State Chem*, 144 (1999) 220.
66. H. Y. Lee, J. B. Goodenough, *J. Solid State Chem*, 148 (1999) 81.
67. C. C. Hu, C. Y. Cheng, *Electrochem. Solid State Lett*. 5 (2002) 43.
68. C. C. Hu, T.W. Tsou. *Electrochem. Commun*, 4 (2002) 105.
69. M. Pourbaix, *Atlas of Electrochemical Equilibria in Aqueous Solutions*, National Association of Corrosion Engineers, Houston, T. X (1966).286.

70. M. M. Doeff, A. Anapolsky, L. Edman, T. J. Richardson, L. C. De Jonghe, J Electrochem. Soc, 148 (2001) 230.
71. L. I. Hill, R Portal, A. Le Gal La Salle, A Verbaere, D. Guyomard, Electrochem. Solid State Lett, 4 (2001) 1.
72. C.C. Hu, T. W. Tsou, Electrochim. Acta, 47 (2002) 3523.
73. J. Jiang, A. Kucernak, Electrochim. Acta, 47 (2002) 2381.
74. R. Patrice, B. Gerand, J. B. Leriche, L. Seguin, E. Wang, R. Moses, K. Brandt, J M. Tarascon, J Electrochem. Soc, 148 (2001) 448.
75. S. Rodrigues, N. Munichandraiah, A. K. Shukla, J Appl Electrochem, 28 (1998) 1235.
76. G. E. P. Box, W. G. Hunter, J S Hunter, Statistics for Experiments, Wiley, New York (1978) 374.
77. J. Chmiola, G. Yushin, R. K. Dasch, Y. Gogotsi, J of Power sources, 158 (2006) 765-772.
78. P. V. Samant, M. F. R. Pereira, J. L. Figueiredo, Catalysis 102- 103 (2005) 183-188.
79. J. S. Rebelló, P. Samant, J .L. Figueiredo, J. B. Fernandes, Journal of Power Sources, 153 (2006) 36-40.
80. P. Kissinger, W. R. Heineman, J of Chemical Education, 60 (1983) 9
81. K. Nakato, S. Takabayashi, A. Imanishi, K. Murakoshi, Y. Nakato, Solar Energy Materials and Solar cells,83 (2004) 323-330.
82. Q. L. Zhuang, T. Kyotani, A. Tomita, Carbon 32 (1994) 539-540.
83. M. A. P. Sherwood, J Electron Spectrosc Relat Phenom, 81 (1996) 319-342.
84. J. Zawadzki, P. A. Thrower, Ed.; Marcel Dekker: New York, 28 (1988) 147-386.

85. C. C. Hu, T. W. Tsou, *Electrochem. Commun*, 4 (2002) 105.
86. J. D. M. Bockris and D. M. Drazic, *Electrochemical Science*, (1972).
87. D. Laser and M. Ariel, 52,291, *J Electrochemical Chem*, 64, 1974.
88. N. Roses and H.Sokol, *J. of Electrochem*,131 (1984) 1742.
89. E. Nasc Mulli and E. Gulcadi, *J. Appl Electrochem*, 12 (1984) 73.
90. D. Tryk, et al, *The Electrochemical Pennington Society*, N J (1984) 192.
91. D. R. Crow, *Principles and Applications of Electrochemistry*, 4<sup>th</sup> Edn, Blackies, Academics & Professional, (1994).
92. J.O'M. Bockris, A. K. Reddy & M. de Gamboa-Aldeco, *Modern Electrochemistry*, Plenum Publishers, 2A (2000).
93. C. Schweigler, S. Summerer, H.M. Hellmann, F. Ziegler, *International Sorption Heat Pump Conference*, Munich, Germany, March 24-26 (1999).
94. G. Restuccia, J. A. Arnoud, R. Quagliata, *International Journal of Energy Research*, 12.1(1988) 101.
95. U. Rockenfeller, L. D. Kirol, *US Patent* 5548971, (1996).
96. J. A. Carp, P. W. Bach, *European Heat Waste Potential*, Energy Research Centre of Nethrlands, (2000)
97. N. I Kopylov, *Russian Journal of Inorganic Chemistry*, 132 (1968) 276.
98. N. I. Kopylov, V. Yu, Kaminski, *Russian Journal of Inorganic Chemistry*, 442 (1999) 261.
99. J. Y. Andersson, J. de Pablo, M. Azoulay, *Thermochimica Acta*, 91 (1985) 223.
100. J. Y. Andersson, M. Azoulay: *J. Chem Soc. Dalton trans*, (1986) 469.
101. *Crystallographic database, JCPDS-ICDD Powder Diffraction* (1997).

102. International Centre for Diffraction Data, Newtown Square, PA 19073-3273 USA, (1997).
103. D. Bedlivy, A. Preisinger, *Zeitschrift für Kristallografie*, 121:2-4 (1965) 114.
104. D. Bedlivy, A. Preisinger, *Zeitschrift für Kristallografie*, 121:2-4 (1965) 135.
105. K. Mereiter, A. Preisinger, A. Zellner, W. Mikenda, H. Steidl, *J. Chem. Soc. Dalton Trans*, (1984) 1275.

## SUMMARY AND CONCLUSIONS

- Activated carbon has been synthesized from sodium salt of carboxy methyl cellulose by low temperature physical activation.
- The activated carbon from CMC has high surface area comparable to commercial carbons.
- It has both acidic and basic sites; hence it is amphoteric in nature.
- It has less, but strong acidic sites.
- The solution of CMC N carbon is basic.
- High porosity and surface functional groups makes it an ideal adsorbent.
- The paramagnetic nature of the carbon makes it a potential material for electrochemical applications.
- Its surface chemistry can be utilized to catalyse reactions.
- Its porosity provides large surface area to support catalyst.
- Surface functional groups were altered on treatment with nitric acid.
- Due to the increased acidity on carbons decomposition of hydrogen peroxide decreased. CMC N showed no significant change.
- It was observed that the equilibration time increased for functionalized C1 and C2 but decreased for functionalized CP and CMC N carbons.
- It was observed that there was no adsorption of Mn ions by the treated and untreated carbons except for CMC N carbon.

- In case of Cu ions adsorption it was observed that there was a marginal increase in case of C1 and slightly more in case of C2.
- TiO<sub>2</sub> /C was used to test photocatalytic degradation of methylene blue dye. It was found that the insitu preparation of TiO<sub>2</sub> /C showed better photocatalytic activity as compared to mechanically mixed sample TiO<sub>2</sub> +C .
- C2 showed better adsorption of methylene blue in the dark but decreased in the light. TiO<sub>2</sub> /C showed better photodegradation of the dye in the light as compared to carbon.
- Photocatalytic activity was also tested for the anatase and rutile phase of TiO<sub>2</sub>. It was observed that the carbon supported anatase phase gave better photodegradation.
- C2 was a better support for TiO<sub>2</sub> as compared to SiO<sub>2</sub>. TiO<sub>2</sub>/SiO<sub>2</sub> did not show any significant decomposition of methylene blue.
- Effect of percentage loading of TiO<sub>2</sub> on carbon was studied. It was observed that 10% loading showed better photocatalytic activity as compared to 5% and 30% loading.
- It was observed that the maximum current of  $2.5 \times 10^{-3}$  A was produced for CMC N carbon without OMS-2.
- The current density increased on addition of OMS-2 for all carbons but decreased for CMC N and was maximum for carbon C2.
- Pt/C electrode resulted in higher evolution of oxygen as compared to Pt at the same overpotential.
- CMC N and C1 carbons decreased the decomposition temperature of KClO<sub>3</sub>.
- KClO<sub>3</sub> catalysed the gasification of carbons.
- Manganese oxide supported on carbon C1 is more effective in Na<sub>2</sub>S oxidation

## ACHIEVEMENT

*A high surface area activated carbon has been synthesized from sodium salt of carboxyl methyl cellulose by low temperature physical activation.*

### *Research Paper communicated*

*A simple method to prepare high surface area activated carbon from carboxyl methyl cellulose by low temperature physical activation method.*

### *Research Papers under preparation.*

- 1. Adsorption of metal ions  $\text{Cu}^{2+}$  and  $\text{Mn}^{2+}$  by activated carbons prepared from carboxyl methyl cellulose*
- 2. Catalytic activity of activated carbons prepared from carboxyl methyl cellulose.*

### *Presentations*

*Sabina Martins* - Photocatalysis on Carbon supported  $\text{TiO}_2$  catalysts presented at 'Advances in Catalysis and Nanostructured Materials' seminar at Goa University, December 2003.

*Sabina Martins, Aditi R. Gandhe, Julio B. Fernandes* – Enhanced photocatalytic activity on carbon supported  $\text{TiO}_2$ , at 4<sup>th</sup> National Symposium and Conference on Solid State Chemistry and Allied Areas organized jointly by Indian Association of Solid State Chemists and Allied Scientists and Goa University, Goa, December 2005.

